

University of Windsor

Scholarship at UWindor

Electronic Theses and Dissertations

Theses, Dissertations, and Major Papers

7-1-2007

Titanium complexes of phosphinimide ligands with pendant hemilabile donars.

Krishan Yadav
University of Windsor

Follow this and additional works at: <https://scholar.uwindsor.ca/etd>

Recommended Citation

Yadav, Krishan, "Titanium complexes of phosphinimide ligands with pendant hemilabile donars." (2007). *Electronic Theses and Dissertations*. 6977.
<https://scholar.uwindsor.ca/etd/6977>

This online database contains the full-text of PhD dissertations and Masters' theses of University of Windsor students from 1954 forward. These documents are made available for personal study and research purposes only, in accordance with the Canadian Copyright Act and the Creative Commons license—CC BY-NC-ND (Attribution, Non-Commercial, No Derivative Works). Under this license, works must always be attributed to the copyright holder (original author), cannot be used for any commercial purposes, and may not be altered. Any other use would require the permission of the copyright holder. Students may inquire about withdrawing their dissertation and/or thesis from this database. For additional inquiries, please contact the repository administrator via email (scholarship@uwindsor.ca) or by telephone at 519-253-3000ext. 3208.

**Titanium Complexes of Phosphinimide Ligands with Pendant
Hemilabile Donors**

by

Krishan Yadav

A Thesis

Submitted to the Faculty of Graduate Studies and Research
Through the Department of Chemistry and Biochemistry
In Partial Fulfillment of the Requirements for
The Degree of Master of Science at the
University of Windsor

Windsor, Ontario, Canada

July 2007

© 2007 Krishan Yadav



Library and
Archives Canada

Bibliothèque et
Archives Canada

Published Heritage
Branch

Direction du
Patrimoine de l'édition

395 Wellington Street
Ottawa ON K1A 0N4
Canada

395, rue Wellington
Ottawa ON K1A 0N4
Canada

Your file *Votre référence*
ISBN: 978-0-494-35002-7
Our file *Notre référence*
ISBN: 978-0-494-35002-7

NOTICE:

The author has granted a non-exclusive license allowing Library and Archives Canada to reproduce, publish, archive, preserve, conserve, communicate to the public by telecommunication or on the Internet, loan, distribute and sell theses worldwide, for commercial or non-commercial purposes, in microform, paper, electronic and/or any other formats.

The author retains copyright ownership and moral rights in this thesis. Neither the thesis nor substantial extracts from it may be printed or otherwise reproduced without the author's permission.

AVIS:

L'auteur a accordé une licence non exclusive permettant à la Bibliothèque et Archives Canada de reproduire, publier, archiver, sauvegarder, conserver, transmettre au public par télécommunication ou par l'Internet, prêter, distribuer et vendre des thèses partout dans le monde, à des fins commerciales ou autres, sur support microforme, papier, électronique et/ou autres formats.

L'auteur conserve la propriété du droit d'auteur et des droits moraux qui protègent cette thèse. Ni la thèse ni des extraits substantiels de celle-ci ne doivent être imprimés ou autrement reproduits sans son autorisation.

In compliance with the Canadian Privacy Act some supporting forms may have been removed from this thesis.

Conformément à la loi canadienne sur la protection de la vie privée, quelques formulaires secondaires ont été enlevés de cette thèse.

While these forms may be included in the document page count, their removal does not represent any loss of content from the thesis.

Bien que ces formulaires aient inclus dans la pagination, il n'y aura aucun contenu manquant.


Canada

Abstract

A series of new phosphinimine compounds have been synthesized to investigate the effects of a pendant heteroatom donor in the ligand framework on the reactivity of the resulting cyclopentadienyl-titanium complexes. The phosphinimine ligands (L) of the type $\text{NP}(\text{}^t\text{Bu}_2)\{(\text{CH}_2)_3\text{XBn}\}$ ($X = \text{O}, \text{S}$) were incorporated into the metal complexes CpTiCl_2L and $\text{Cp}^*\text{TiCl}_2\text{L}$. The methyl abstraction of the corresponding dialkyl precursors resulted in the first example of stable cationic titanium phosphinimide complexes in solution without the need for an external stabilizing reagent.

Using a reliable polymerization testing protocol, the titanium pre-catalysts were tested for ethylene polymerization. While the dihalide precursors showed moderate activity with MAO as the co-catalyst, the dialkyl precursors showed good to excellent activity with the co-catalysts $\text{B}(\text{C}_6\text{F}_5)_3$ and $[\text{Ph}_3\text{C}]^+[\text{B}(\text{C}_6\text{F}_5)_4]^-$, with polymerization activities ranging from 40 to 4900 $\text{g mmol}^{-1} \text{h}^{-1} \text{atm}^{-1}$. Of the dimethyl pre-catalysts tested, the complex featuring a pendant thioether and the bulkier Cp^* ancillary ligand, was the most active catalyst upon activation with 2 equivalents of $[\text{Ph}_3\text{C}]^+[\text{B}(\text{C}_6\text{F}_5)_4]^-$.

Preliminary polymerization testing of the dialkyl precursors with 2 equivalents of $[\text{Ph}_3\text{C}]^+[\text{B}(\text{C}_6\text{F}_5)_4]^-$ showed markedly higher activities at 60 °C. These results show promise for thermal stability of hemilabile phosphinimide systems provided by an interaction between the pendant donor and the reactive cationic titanium centre. The presence of a pendant heteroatom donor may stabilize the reactive metal centre at elevated temperatures. Indeed, these systems are the first variants of the simple titanium phosphinimide catalysts, $\text{CpTiMe}_2[\text{NP}(\text{}^t\text{Bu})_3]$, to show good to excellent activities under

laboratory conditions. The potential of the pendant donor derivatives has been demonstrated and evaluation for commercial use is underway.

Dedication

This work is dedicated to my wife-to-be, Jaishica, and my best friend, Roberto.

Acknowledgments

There are several people who have helped me tremendously along the way and with whom I've made lasting friendships with. First and foremost, I would like to thank Jenny McCahill for her wealth of information, helpfulness, tremendous experience and willingness to give me a hand when I needed it. Without Jenny, this project would have been impossible, and any success from this work is a result of her time and efforts as well as mine. I would also like to thank Meghan Dureen, Osamah Alhomaidan, and Greg Welch for their useful discussions and insight about all things chemistry. Meghan – hope you find a new drinking partner. Osamah – watch out for the Arsenal next season! Greg – please leave Terry alone.

I would also like to personally thank Dr. Preston Chase (Mr. Bruce Chemistry) for his invaluable wealth of information and excellent and constructive criticism of my work. Without your willingness to help, I would certainly be at a loss! Also thanks to Steve (Culture Shock) Geier, who has always been helpful and is always a good laugh. Big thanks to Anjan for morning coffees and aimless discussions about chemistry. Thanks to Sharonna, especially for teaching me basic lab skills when I first began. My gratitude to the rest of the Stephan group: Shamola, Ian, Raj, Alberto, Guangcai, Matthias, and anyone else whom I may have forgotten to mention.

A big thank you to Dr. Doug Stephan, who has been a very supportive influence in my life for the past two years. He has been an inspiration during the bleakest of times and shows his passion for chemistry on a daily basis. Thanks to Nilesh Kaka and Neeta Kaki for inspiring me to achieve success. Last but not least, massive thanks to my incredible parents and brother for their support without which I would certainly be lost.

Table of Contents

Abstract	iii	
Dedication	v	
Acknowledgments	vi	
List of Tables	x	
List of Figures	xi	
List of Schemes	xiv	
List of Abbreviations, Nomenclature and Symbols	xv	
Chapter		
1	A Brief History of α-Olefin Polymerization	
1.1	The Origin of α -Polyolefins	1
1.2	Homogeneous α -Olefin Polymerization Catalysts	2
1.3	Group IV Olefin Polymerization Phosphinimide Catalysts	8
1.4	Hemilabile Ligands in Coordination Chemistry	11
	1.4.1 Olefin Oligomerization	15
1.5	Scope of This Work	19

2	Hemilabile Ligand Design and Reactivity of Selected Ti(IV) Phosphinimide Complexes	
2.1	Introduction: Synthesis of phosphinimines and Ti(IV) phosphinimide complexes	22
2.1.1	Results and Discussion: Complex Synthesis	24
2.2	Introduction: Reactivity of Ti(IV) phosphinimide complexes with $B(C_6F_5)$ and $[Ph_3C]^+[B(C_6F_5)_4]^-$	31
2.2.1	Results and Discussion: Activation of Dialkyl Precursors	34
2.3	Conclusions	41
3	Reactivity of Hemilabile Phosphinimide Titanium Complexes in the Presence of Ethylene	
3.1	Introduction	43
3.2	Polymerization Mechanism Involving Group IV Metals	43
3.3	General Considerations	46
3.4	Polymerization Protocol	49
3.5	Results and Discussion	51
3.5.1	Polymerizations with MAO as the Co-catalyst	54
3.5.2	Polymerizations with $B(C_6F_5)_3$ as the Co-catalyst	56
3.5.3	Polymerizations with $[Ph_3C]^+[B(C_6F_5)_4]^-$ as the Co-catalyst	60
3.5.4	Polymerization Testing at Elevated Temperatures	62
3.6	Conclusions	64

4	Experimental	
4.1	General Considerations	66
4.2	Phosphines	67
4.3	Phosphinimines	68
4.4	Titanium Complexes	70
4.5	Activated Complexes	75
4.6	Ethylene Polymerization Technique	77
	References	79
Appendix A	Supplementary X-Ray Data	83
Vita Auctoris		84

List of Tables

Table 2.1	Selected NMR spectral data for 2.15-2.18 (X = O 2.15, 2.16 ; X = S 2.17, 2.18)	38
Table 2.2	Selected NMR spectral data for 2.19-2.22 (X = O 2.19, 2.20 ; X = S 2.21, 2.22)	39
Table 3.1	Rating of the effectiveness of a catalyst based on its activity	47
Table 3.2	Polymerization Conditions	52
Table 3.3	Polymerization results with MAO as co-catalyst	54
Table 3.4	Polymerization results with $B(C_6F_5)_3$ as co-catalyst	57
Table 3.5	Polymerization results with $[Ph_3C]^+[B(C_6F_5)_4]^-$ as co-catalyst	61
Table 3.6	Effect of temperature on catalyst activities	63

List of Figures

Figure 1.1	Activation of Cp_2MCl_2 with MAO	4
Figure 1.2	Formation of isotactic propylene using the stereoselective <i>ansa</i> -metallocene [<i>rac</i> -Et-[Ind] ₂]ZrCl ₂ pre-catalyst and MAO co-catalyst	5
Figure 1.3	Structure of a generic Constrained Geometry Catalyst	6
Figure 1.4	McConville Bis-amide Catalysts	7
Figure 1.5	FI catalysts	8
Figure 1.6	Steric similarity between Cp, tritox and phosphinimide ligands	9
Figure 1.7	Preferred bonding mode of phosphinimine ligand compared to Cp as proposed by Dehnicke	10
Figure 1.8	Group IV phosphinimide olefin polymerization pre-catalysts	11
Figure 1.9	General action of a hemilabile ligand	12
Figure 1.10	Types of hemilabile reactions	13
Figure 1.11	Selected transition metal complexes featuring P-O ligands	15
Figure 1.12	Pendant donor-metal interaction to stabilize cationic metal centre	17
Figure 1.13	Pendant arene coordination in titanium-phosphinimide complexes	20
Figure 2.1	(a) Reduction of $\text{Cp}'(\text{}^t\text{Bu}_2(2\text{-C}_6\text{H}_4\text{Ph})\text{PN})\text{TiCl}_2$ to give $\text{Cp}'(\text{}^t\text{Bu}_2(2\text{-C}_6\text{H}_4\text{Ph})\text{PN})\text{Ti}$. (b) Formation of cationic species $[\text{}^t\text{Bu}_2(2\text{-C}_6\text{H}_4\text{Ph})\text{PNTiMe}_2]^+[\text{RB}(\text{C}_6\text{F}_5)_3]^-$.	23
Figure 2.2	Synthetic route to titanium-phosphinimides	26

Figure 2.3	ORTEP drawing of 2.7 with labeling scheme. Thermal ellipsoids are drawn at the 30% probability level	27
Figure 2.4	ORTEP drawing of 2.8 with labeling scheme. Thermal ellipsoids are drawn at the 30% probability level	28
Figure 2.5	Synthetic route to titanium-phosphinimide derivatives	29
Figure 2.6	^1H NMR spectrum for complex 2.11	30
Figure 2.7	Equilibrium between pre-catalyst, activator, and ion pair	32
Figure 2.8	Activation of 2.11-2.14 with $\text{B}(\text{C}_6\text{F}_5)_3$	35
Figure 2.9	^1H NMR spectrum of (a) the neutral dimethyl complex 2.11 , (b) the activated complex 2.15 , (c) the addition of THF to 2.15 displaces the pendant ether-titanium interaction	36
Figure 2.10	Activation of 2.11-2.14 with $[\text{Ph}_3\text{C}]^+[\text{B}(\text{C}_6\text{F}_5)_4]^-$	38
Figure 2.11	Portion of the VT ^1H NMR showing the temperature-dependent second order coupling of the benzylic methylene proton resonances for complex 2.17	41
Figure 3.1	Cossee-Arlman mechanism	44
Figure 3.2	Modified Cossee-Arlman mechanism with counterion considerations	45
Figure 3.3	Common chain termination pathways	45
Figure 3.4	Catalysts tested for polymerization	53
Figure 3.5	Decomposition pathways in the reaction of AlMe_3 and $\text{TiMe}_2[\text{NP}(\text{tBu}_3)]_2$	55

- Figure 3.6** Suggested formation of the dication
 $[(\text{Cp})(\text{tBu}_3\text{NP})\text{Ti}(\mu\text{-MeB}(\text{C}_6\text{F}_5)_3)_2]^{2+}$ 59
- Figure 3.7** Order of polymerization activity of titanium complexes with
a pendant hard or soft ligand 59

List of Schemes

Scheme 1.1	Proposed trimerization cycle	19
Scheme 2.1	Synthetic route to ether- and thioether-phosphinimine ligands	25
Scheme 3.1	Possible interaction between [Me-MAO] ⁻ and the pendant donor	55

List of Abbreviations, Nomenclature and Symbols

Å	Ångstrom
°	degrees
α	alpha
β	beta
Bn	benzyl
σ	sigma
δ	chemical shift in parts per million
η	hapticity
atm	atmosphere (pressure)
C	Celsius
CGC	Constrained Geometry Catalyst
Cl	chloride
Cp	cyclopentadienyl
DFT	Density Functional Theory
Et	ethyl
FI	<i>Fenokishi-Imin</i>
ΔG^\ddagger	Gibbs free energy of activation
GC	gas chromatography
g	grams
ΔH^\ddagger	enthalpy of activation
h	hour
Hz	Hertz

HDPE	high density polyethylene
ΔH_{ips}	ion pair separation energy
ICI	Imperial Chemical Industries
In	indenyl
ⁱ Pr	<i>iso</i> -propyl
$ J_{X-Y} $	coupling constant between atoms X and Y
K	Kelvin
kg	kilogram
LAO	linear <i>alpha</i> -olefins
LDPE	low density polyethylene
LLDPE	linear low density polyethylene
<i>m</i>	<i>meta</i>
MAO	methylalumoxane
Me	methyl
mL	milliliter
mmol	millimole
mol	mole
NMR	nuclear magnetic resonance
<i>o</i>	<i>ortho</i>
<i>p</i>	<i>para</i>
Ph	phenyl
ppm	parts per million
ΔS^\ddagger	entropy of activation

THF

tetrahydrofuran

'Bu

tert-butyl

Chapter 1

A Brief History of α -Olefin Polymerization

1.1 The Origin of α -Polyolefins

Thermoplastics remain an integral part of modern society and have a variety of applications including thin film packaging, photographic and magnetic tape, beverage and trash containers, wire and cable insulation, and a variety of automotive parts and upholstery.¹ One important class of thermoplastics is the polyolefins, which include polyethylene, polystyrene and polypropylene. The feedstock petrochemical ethylene can be polymerized using a variety of techniques to give a diverse array of products ranging from low-density polyethylene (LDPE) to high-density polyethylene (HDPE), each of which offers distinct polymer properties.

LDPE is a highly branched polymer with molecular weights typically in the range of 6000 – 40000. LDPE was the first commercially produced polyolefin, and was developed in 1939 by Imperial Chemicals Industries (ICI) in England. The process to make LDPE involves free-radical polymerization using traces of oxygen or peroxide as the initiator. A drawback to this approach was the necessity for extreme conditions (250 °C, 3000 atm).¹ The high degree of branching in LDPE reduces the crystallinity of the polymer, giving rise to low density and a low crystalline-melting temperature. Branching in the free-radical polymerization process may be reduced through increasing the pressure. For example, nearly linear polyethylene may be produced at pressures approaching 5000 atm. Obviously, there was a need to produce linear polyethylene (HDPE) without the requirement of extraordinarily high temperatures and pressures.

Fifteen years after the discovery at ICI, a new way to make HDPE using transition metal catalysts was developed. This breakthrough came independently through the work of Ziegler and Natta, which led to the development of heterogeneous system capable of producing HDPE.^{2,3} The Ziegler-Natta catalysts consist of a mixture of an early transition metal complex with a trialkylaluminum reagent. The best known system, $\text{TiCl}_3/\text{Et}_2\text{AlCl}$,⁴ is highly active at 25°C and 1000 atm. This lies in stark contrast to extreme conditions required for earlier radical polymerization methods. These catalyst systems, for which Ziegler and Natta won the Nobel Prize in 1963, and modern variations still account for more than 15 million tons of polyethylene and polypropylene annually.⁵ Nonetheless, such heterogeneous mixtures do have distinct disadvantages. These catalysts operate with multiple active sites, making rational catalyst modification for control of the polymer properties arduous at best. The lack of convenient spectroscopic or physical techniques, such as NMR or mass spectrometry, to examine the surfaces under catalytic conditions also exacerbates the problems of design modification.⁶ Finally, due to the heterogeneity of the system, only the exposed surfaces are reactive, leaving the bulk of the catalyst buried and inactive. In this respect, the development of homogeneous catalysts with a well-defined active site would certainly circumvent these drawbacks.

1.2 Homogeneous α -Olefin Polymerization Catalysts

In general terms, a homogeneous olefin polymerization catalyst may be generated using a pre-catalyst and a co-catalyst. The pre-catalyst is often a neutral transition metal complex of the form $\text{L}_n\text{MRR}'$ ($\text{R}, \text{R}' = \text{alkyl group}$). The co-catalyst is commonly a Lewis acid that is capable of activating the pre-catalyst by abstracting an alkyl group (R') to

give the cationic transition metal complex $[L_nMR]^+$. Examples of common activators include methylalumoxane (MAO), $B(C_6F_5)_3$, and $[Ph_3C]^+[B(C_6F_5)_4]^-$. Once the cationic transition metal has been formed, the anion (i.e. $[MeMAO]^-$, $[MeB(C_6F_5)_3]^-$, $[B(C_6F_5)_4]^-$) plays an important role in the polymerization process by serving as the counterion to stabilize the metal complex.⁷ Furthermore, greater ion pair separations can result in higher activities for olefin polymerization, although with typically reduced stability of the catalyst.⁸ It is important to recognize that a transition metal-based homogeneous olefin polymerization catalyst is comprised of the ion pair between the cationic metal complex and the counterion.

Well-defined homogeneous systems provide key advantages over traditional heterogeneous Ziegler-Natta catalysts. For example, mechanistic studies would be greatly facilitated with a soluble catalyst of known composition and a more uniform molecular weight distribution would be obtained from a single site catalyst.⁹ Biscyclopentadienyl titanium dichloride-alkylaluminum metallocene complexes, developed in the 1950's, were the first reported examples of homogeneous catalysts upon activation with alkylaluminum reagents.^{9,10} In their investigation of the zirconocene Cp_2ZrCl_2 activated with an alkylaluminum co-catalyst, Sinn and Kaminsky found that the addition of water led to catalyst activities rivaling that of the Ziegler-Natta catalysts.¹¹ Water was found to react with the alkylaluminum reagent to form MAO, which was the cause of the dramatic improvement in activity. A typical metallocene pre-catalyst is a Group IV metal (Ti, Zr, Hf) dichloride complex with two aromatic ligands (Cp, indenyl, fluorenyl). Co-catalysts for these systems are organoalumoxanes such as MAO, which acts to alkylate the

dichloride metallocene followed by abstraction of a methyl anion to give the metallocene monomethyl cation (**Figure 1.1**).

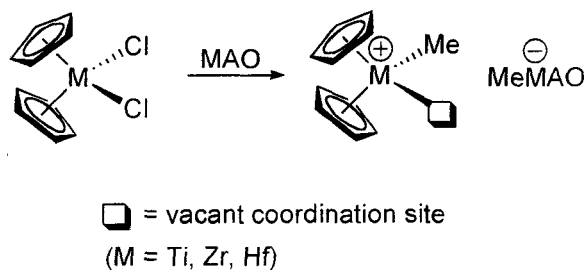


Figure 1.1 Activation of Cp_2MCl_2 with MAO

Overall, metallocene catalysts can be a hundred times more active than conventional Ziegler-Natta catalysts. For example, the *ansa* bis(fluorenyl) complex $(\text{C}_{13}\text{H}_8\text{-C}_2\text{H}_4\text{-C}_{13}\text{H}_8)\text{ZrCl}_2$ produces 300 tonnes of PE/g of Zr-h after activation with a cocatalyst.¹² A further attractive point is the ability of metallocenes to act as ‘single-site’ catalysts to produce polymers with narrow molecular weight distributions. An advantage to metallocenes is that the nature of the active site is clearer than heterogeneous Ziegler-Natta catalysts and simple modification of the ancillary ligands can tailor these systems for maximum activity or tailoring polymer properties. For example, introducing alkyl groups on Cp ligands have a positive effect on catalyst activity. Presumably, the increased steric bulk on the ancillary ligand results in a better separation between the cation and $[\text{MeMAO}]^-$ to give improved activities.¹³ Bridging the aromatic ligands to give *ansa*-metallocenes can have dramatic effects on the type of polymer produced. For example, the ethylene-bridged $[\text{rac-Et-}[\text{Ind}]_2]\text{TiCl}_2$ and $[\text{rac-Et-}[\text{Ind}]_2]\text{ZrCl}_2$ (Ind = indenyl) activated with MAO gave the first homogeneous catalysts capable of producing isotactic polypropylene (**Figure 1.2**).^{14,15}

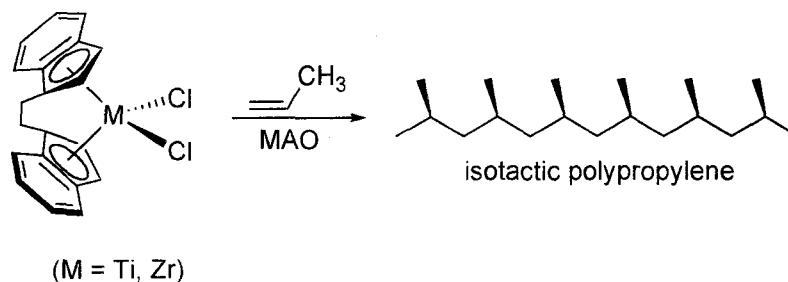
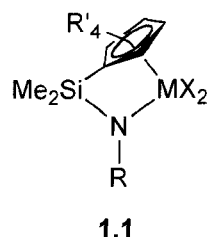


Figure 1.2 Formation of isotactic propylene using the stereoselective *ansa*-metallocene [*rac*-Et-[Ind]₂]ZrCl₂ pre-catalyst and MAO co-catalyst

Based upon the success of metallocene chemistry, more recent efforts have been made to develop new catalysts that feature non-Cp ligands about Group IV metals. Part of this drive has been fuelled by a desire to avoid the ever-growing patent sphere encompassing Group IV metallocenes. Although there has been an increase in the number of publications for Group VIII and Group X metals, nonmetallocene systems based on Group IV metals are far more predominant.^{16,17}

The ‘constrained geometry catalysts’ (CGC) were the first examples of nonmetallocene catalysts utilized on a commercial scale. The CGC ligands were first introduced by Bercaw and coworkers, who developed organoscandium olefin polymerization catalysts.¹⁸ The CGC ‘half sandwich’ ligand incorporates a bulky amide group linked to a cyclopentadienyl unit. Shortly after the introduction of these ligands, patents for Group IV CGC systems (**Figure 1.3**) were awarded to Dow Chemical Company^{19,20} and the Exxon-Mobil Corporation.²¹⁻²³



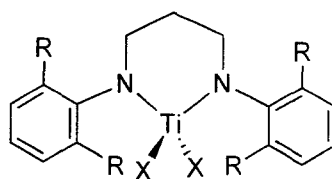
(M = Ti, Zr; R = alkyl, aryl; R' = H, Me; X = Cl, Me)

Figure 1.3 Structure of a generic Constrained Geometry Catalyst

One of the key design features of these catalysts is the open nature of the active site which allows them to incorporate other bulkier olefins such as 1-hexene into the polymer.²⁴ The steric strain imparted by the CGC ligand allows for the copolymerization of ethylene with larger α -olefins ranging in size from 1-decene to 1-octadecene. Through variation of the Cp unit, the bridge, and the amido groups of the ligand, a variety of materials may be accessed, ranging from high-density polyethylene (HDPE) to linear low-density polyethylene (LLDPE).²⁴

Metal complexes featuring chelates, such as the CGC catalysts, have shown much promise in the polymerization of olefins. A very significant advance in this respect came in the mid 1990's, when McConville and coworkers reported that bulky bis-amide chelate complexes serve as highly active catalysts for polymerization of 1-hexene.²⁵⁻²⁷ A general structure of the chelating bis-amide catalyst is shown in **Figure 1.4**. Activities as high as 350 kg of poly(1-hexene) $\text{mmol}^{-1} \text{hr}^{-1}$ were obtained (X = Me, R = 2,6-ⁱPr₂-C₆H₃).²⁶ Furthermore, these systems were the first example of the living polymerization of an aliphatic α -olefin at room temperature.²⁵ These bis-amide catalysts were the first examples of highly effective fully nonmetallocene complexes for olefin polymerization.

Modifications of these chelate complexes by other groups have been recently reviewed by Gibson and coworkers.¹⁶

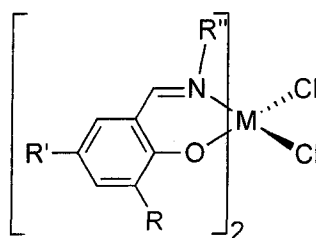


1.2

(X = Me, Cl; R = Me, ⁱPr)

Figure 1.4 McConville Bis-amide Catalysts

Another example of nonmetallocene catalysts with exceptionally high activities and molecular weights are the FI catalysts (**Figure 1.5**).²⁸⁻³¹ These systems incorporate two phenoxy-imine ligands (the acronym FI is derived from the Japanese pronunciation *Fenokishi-Imin Haiishi*). There are several impressive aspects to these catalysts. Both the extremely high activity (519 kg PE/mmol cat•h) of the FI-Zr complex (**1.3**; R = ^tBu, R' = H, R'' = Ph) and the exceptionally high molecular weight obtained when activated with [Ph₃C][B(C₆F₅)₄]^tBu₃Al (M_v = 505 × 10⁴) are among the highest values obtained for homogeneous polymerization catalysts.²⁸ Furthermore, Ti-based FI catalysts are shown to be highly active, and have one of the highest reported turnover frequencies (TOF = 20000 min⁻¹ atm⁻¹) for the living polymerization of ethylene.³¹



1.3

(M = Ti, Zr; R = H, Me, ⁱPr, ^tBu, adamantyl, cumyl, 1,1-diphenylethyl;
R' = H, Me; R'' = Ph, Cy, C₆F_{6-n}H_n)

Figure 1.5 FI catalysts

1.3 Group IV Olefin Polymerization Phosphinimide Catalysts

Another exciting field of the ‘post-metallocene revolution’ are Group IV metal complexes featuring sterically demanding phosphinimide ligands.³² A suitable approach in the design of new nonmetallocene catalysts is to incorporate ligands that mimic Cp units sterically and electronically. Given the large degree of success experienced by nitrogen-based ligand systems, phosphinimide chemistry has shown real promise in early-transition-metal olefin polymerization catalysis.³² The work of Wolczanski and coworkers highlighted the steric analogy between Cp ligands and tri-*tert*-butyl methoxide (tritox).³³ As shown in **Figure 1.6**, the phosphinimide ligand also follows this concept due to its structure. Stephan and coworkers reported that the cone angle for the phosphinimide ligand, ^tBu₃PN was found to be 87°, which is similar to the cone angle for a metal-bound Cp ligand (83°).³⁴ This serves as further evidence that both types of ligand create similar steric environments about titanium. One key difference is that the steric bulk of the phosphinimide ligand is considerably removed from the titanium centre, as the Ti-P and Ti-Cp-centroid distances were found to be 3.0 and 2.2 Å, respectively.³⁴

Given the large degree of success experienced by nitrogen-based ligand systems, such as the McConville and FI catalysts, phosphinimide chemistry should show real promise in early-transition-metal olefin polymerization catalysis. Indeed, titanium complexes incorporating the tri-*tert*-butylphosphinimide ligand ($\text{NP}(\text{tBu})_3$) are remarkably active catalysts upon activation, rivaling the metallocenes in this respect.³⁵

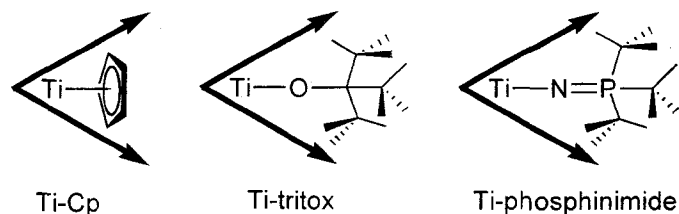


Figure 1.6 Steric similarity between Cp, tritox and phosphinimide ligands

In terms of electronics, a reasonable analogy between Cp and phosphinimide ligands was established by Dehnicke and coworkers.^{36,37} In his review of phosphinimine ligands with transition metals, Dehnicke suggests a $(\sigma, 2\pi)$ set of orbitals for the metal-nitrogen triple bond (**Figure 1.7**); comparable to the 6 electrons donated by a Cp ligand.³⁷ In this model, the σ -bonding network between phosphorus, nitrogen and the metal, is comprised of the overlap of the sp^3 orbitals of phosphorus with the sp orbitals of nitrogen and the d orbitals of appropriate symmetry on the metal. The unused metal d and nitrogen p orbitals make up the metal-nitrogen π -bond. The remaining p orbital on nitrogen and the d_{z^2} orbital on phosphorus are involved in the nitrogen-phosphorus π -bond. The NPR_3^- and Cp^- ligands both have one formal negative charge, and the structural and bonding features of the ligands to the same transition metal should be closely related.

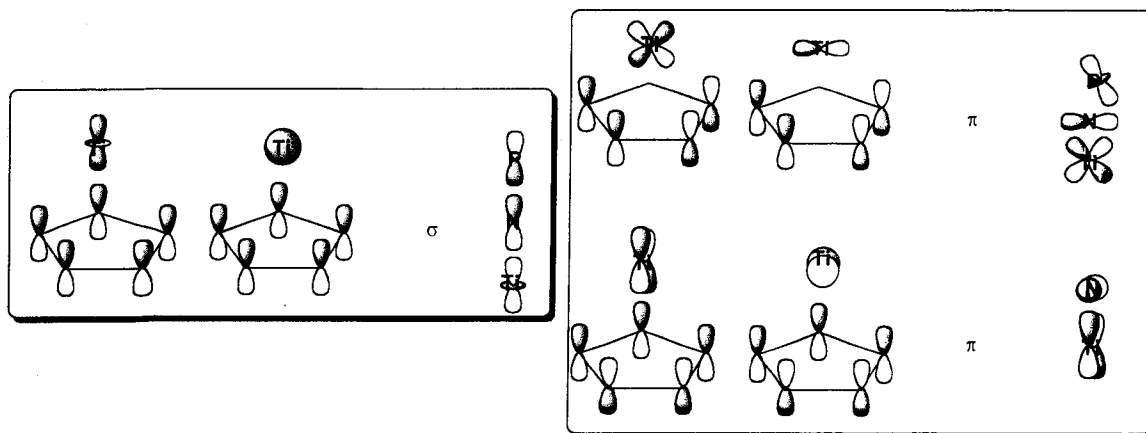


Figure 1.7 Preferred bonding mode of phosphinimine ligand compared to Cp as proposed by Dehnicke

However, based on simple electron-counting and structural data of titanium-phosphinimide complexes, Stephan and coworkers suggested that in some cases, phosphinimide ligands are more similar to a sterically demanding, four-electron-donating, “imide”.³⁸ For example, the Ti-N distance in the solid-state for $(\eta^1\text{-Cp})(\eta^5\text{-Cp})_2\text{Ti}(\text{NP}^t\text{Bu}_3)$ was 1.844(2) Å.³⁸ The dramatic lengthening of the Ti-N bond (compared to, for example, $(\eta^5\text{-Cp})(\eta^1\text{-Ind})_2\text{Ti}(\text{NP}^t\text{Bu}_3)$; Ti-N distance of 1.77 Å) is not consistent with a Ti-N triple bond. This suggests that there are examples in which a formally 18-electron assignment of the complex with the phosphinimide acting as a 4-electron donor to the metal is more appropriate.

This consideration of sterics and electronics in catalyst design proved to be fruitful in the pursuit of new olefin polymerization catalysts. A series of phosphinimide systems reported by Stephan and coworkers in 1999 provided polymerization activities that were 2-3 times those of the metallocenes under similar conditions.³⁹ In further support of these findings, Density Functional Theory (DFT) calculations performed by

Ziegler and coworkers showed that the $[(NPR_3)_2TiMe]^+$ system had the lowest separation energy (compared to $[(1,2-Me_2Cp)_2ZrMe]^+$, $[(Cp)(NCR_2)TiMe]^+$, $[(CpSiR_2NMe)TiMe]^+$, and $[(Cp)(OSiR_3)TiMe]^+$) with a series of anions ($[B(C_6F_5)_4]^-$, $[Me(C_6F_5)_3]^-$, $[Me-MAO]$).⁴⁰ Despite the remarkable activity of these particular titanium systems, the zirconium analogues are not as active for olefin polymerization. This may be attributed to the significantly larger ionic radius of zirconium, which facilitates deactivation pathways over chain propagation.⁴¹ Selected phosphinimide derivatives reported by the Stephan group are shown in **Figure 1.8**.^{35,39,41-44}

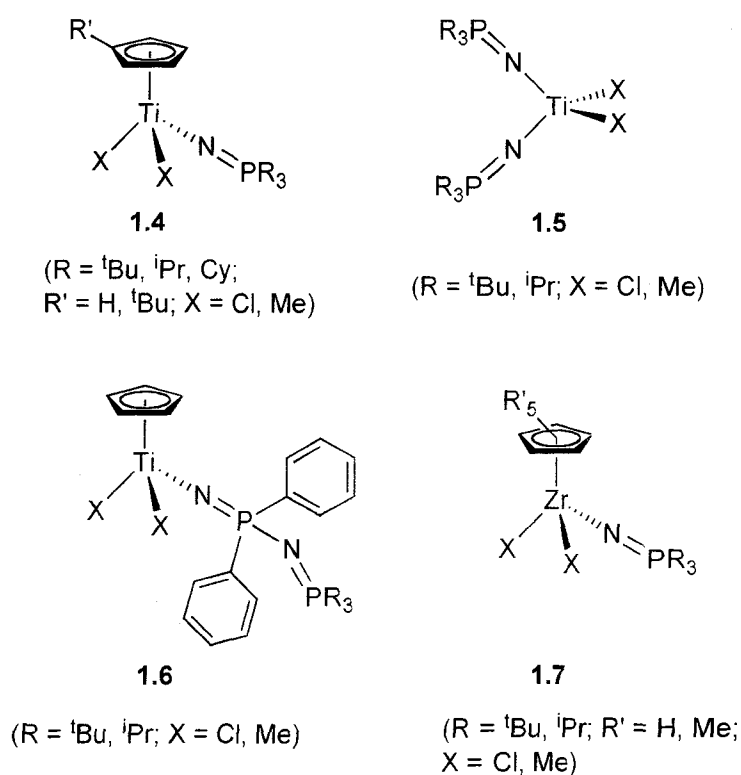


Figure 1.8 Group IV phosphinimide olefin polymerization pre-catalysts

1.4 Hemilabile Ligands in Coordination Chemistry

The key component of a Group IV olefin polymerization catalyst is the highly reactive cationic transition metal centre. However, catalyst stability issues have been

identified as one important problem to be addressed in future systems. Hemilabile ligands provide promise in this respect due to the potential of a pendant donor in the ligand framework to stabilize the metal by coordination but transiently dissociate to provide an active site and retain reactivity. Hemilabile ligands are polydentate chelates that feature at least two different groups capable of bonding. By definition, this ligand class has two important features: a substitutionally inert portion (X) which anchors the ligand to the metal and a labile section (Y) that can intermittently dissociate from the metal (**Figure 1.9**). The coordination/dissociation of the labile portion is a reversible process that is dependant on the presence of coordinating ligands, substrates or solvent molecules (Z).⁴⁵

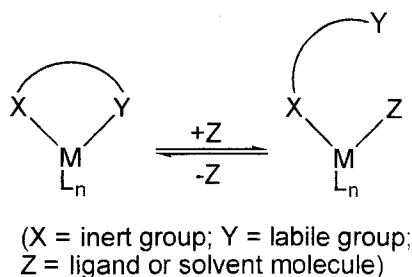


Figure 1.9 General action of a hemilabile ligand

Mechanistically, a number of different hemilabile processes have been identified, including a ‘wind screen wiper’ reaction, ‘tick-tock’ mechanism, ligand ‘interchange’ process, or a ligand displacement mechanism (**Figure 1.10**).⁴⁵ The phrase ‘hemilabile’ was first coined in 1979 by Jeffrey and Rauchfuss in their investigation of the bidentate ligand *o*-(diphenylphosphino)anisole, which participates in a fluxional ‘wind screen wiper’ process (**Figure 1.10(a)**).⁴⁶ Of course, this type of behavior is not limited to bidentate systems.

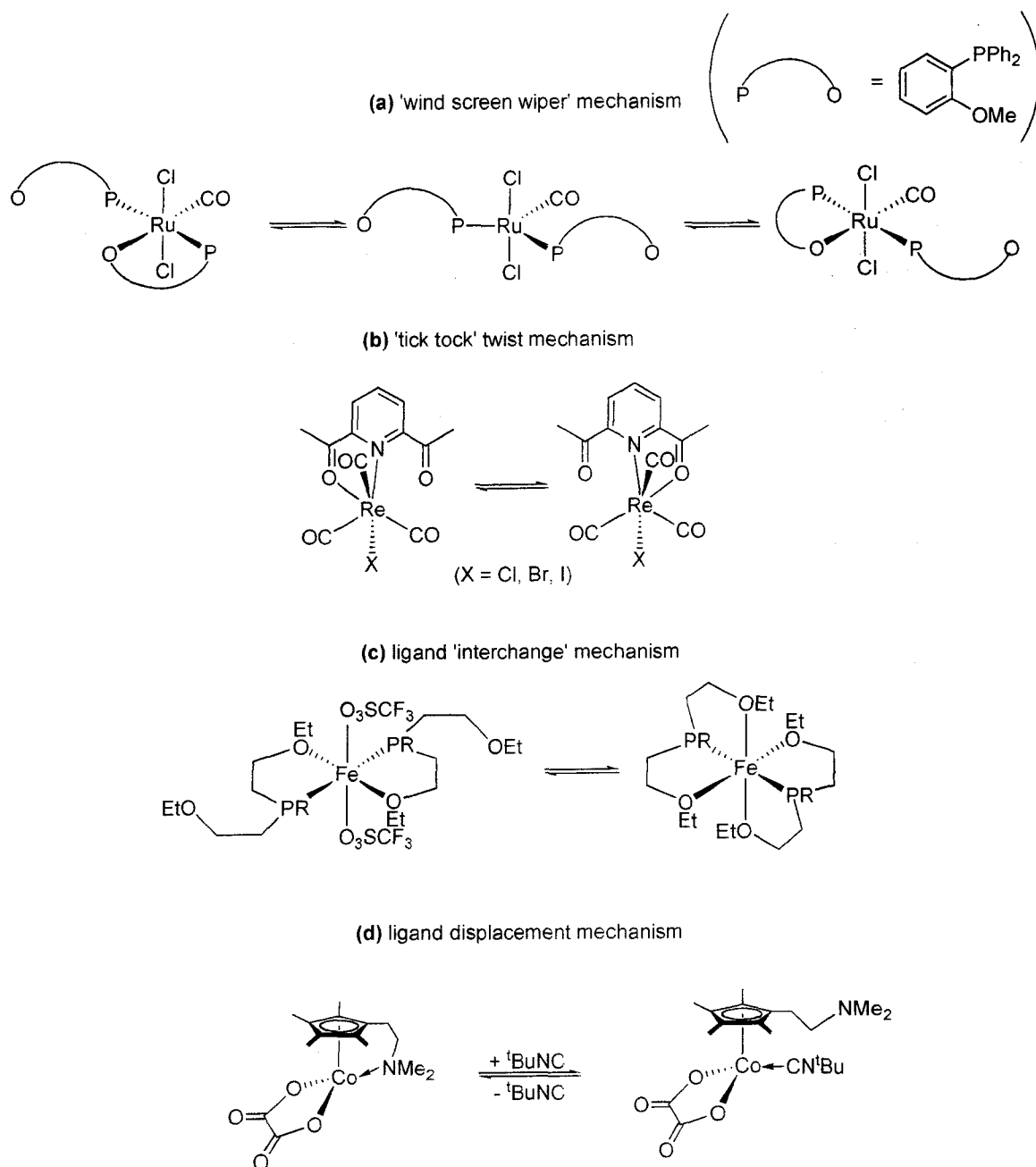


Figure 1.10 Types of hemilabile reactions

Polydentate ligands can show similar effects, as reported by Orell and coworkers in 1995.⁴⁷ In this case, a 'tick-tock' twist mechanism occurred with the making/breaking of two Re—O bonds for the tridentate pyridine-Re system (**Figure 1.10(b)**). The strongly

bound pyridine group acts as an inert ‘anchor’ to rhenium, while weakly bonding ketone groups rapidly exchange in a fluxional manner. Another type of hemilabile behavior reported in the literature has been ligand ‘interchange’ reactions in which coordinating counterions are in equilibrium with the labile portion of the hemilabile ligand. As seen in **Figure 1.10(c)**, Chadwell and coworkers report such phenomena in an iron(II) system where rapid interchange occurs between the polydentate ether-phosphine and two triflate counterions.⁴⁸

The final process, ligand displacement, is of particular interest for catalytic applications. Jutzi and coworkers found that in the case of the dimethylaminoethyl-cyclopentadienyl ligand, the weakly coordinating pendant amino group could be easily and reversibly displaced from cobalt by *tert*-butylisocyanide (**Figure 1.10(d)**).⁴⁹ Hemilabile ligand displacement is important to researchers for two major reasons. First, the ability of the ‘weak-donor’ portion of the ligand to occupy an empty coordination site of a reactive transition metal centre would be very useful for homogenous catalysis. In olefin polymerization, for example, the active catalyst for metallocene and nonmetallocene systems is a very reactive cationic transition metal centre. Clearly, the incorporation of a hemilabile ligand would, in theory, provide stability in such a case. The second attractive feature to this ligand class is the *reversibility* of the hemilabile activity. Not only can these ligands provide stability to reactive transition metal centers, but they are also capable of dissociating to allow a more strongly coordinating ligand, substrate, or solvent molecule, to take its place. The inert portion of the ligand serves as an anchor to keep it tethered to the metal; the labile portion is in turn available for recoordination if there is an empty coordination site.

A vast number of transition metal compounds featuring hemilabile phosphorus-oxygen (P,O) ligands were reported in the literature and subsequently reviewed by Lindner and Bader in 1991 (**Figure 1.11**).⁵⁰ A number of other examples of this ligand class are based on carbon, nitrogen and arsenic.⁴⁵ However, bidentate ligands with phosphorus as the inert group are the most well studied class of hemilabile ligands. The major advantage to using P,O ligands is their ability to increase the electron density at the metal centre via a metal-oxygen interaction. In light of this, oxidative addition of a substrate as well as the reductive elimination of the product is facilitated.⁵⁰

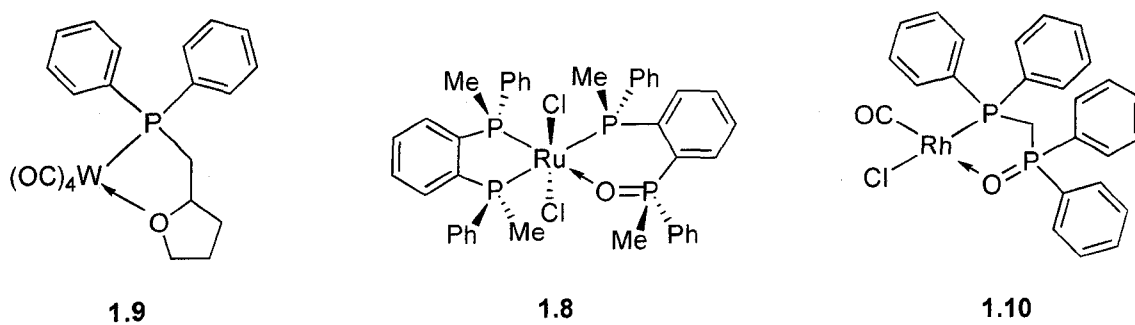


Figure 1.11 Selected transition metal complexes featuring P-O ligands

1.4.1 Olefin Oligomerization

New reactions affording a C-C linkage to selectively form new organic materials are highly sought after for industrial purposes. In this light, there is an ever-increasing demand for polymerization and oligomerization products from linear alpha olefin (LAO) monomers. LAOs are useful intermediates for the production of detergents, plasticizers, synthetic lubricants and copolymers. The three largest full range producers of LAOs are Shell, BP-Amoco and Chevron-Phillips.⁵¹ Specifically, 1-hexene and 1-octene are of particular interest as they serve as comonomers to produce LLDPE. The average molecular weights of the products are determined by the relative rates of the chain

propagation and termination steps. Early transition metals (Groups IV-VI) tend to favor chain propagation, which leads to polymer formation. However, in the case of Group VIII metals, chain termination (via β -elimination) is often favored to give oligomeric products.⁵⁰ In a similar vein, homogeneous nickel(II) catalysts discovered by Keim⁵² have been found to give a mixture of oligomeric products via the Shell Higher Olefins Process (SHOP). Nickel(II) complexes containing P,O chelates are good catalyst choices because the resultant square planar systems favor olefin coordination. Indeed, the P,O chelate in the nickel catalyst for the SHOP process is thought to be responsible for the high selectivity.⁵² However, it is important to note that there is no evidence of any hemilabile activity for these catalysts.

Following the success of late metal systems for production of low molecular weight oligomers, a number of mid and early transition metal complexes have been found to be selective for ethylene trimerization. Chromium catalysts have largely dominated this area. These catalysts are typically chromium(III) salts (usually carboxylates) with a Lewis basic donor (typically pyrroles or 1,2-diethoxyethane). A vast number of such systems have been published in the literature and subsequently reviewed.⁵¹ The inherent disadvantage to these catalysts is that the nature of the active species is unknown, making it difficult to modify the catalyst to control performance.

In a recent significant finding, Hessen and coworkers were able to develop the first highly active and selective non chromium-based ethylene trimerization catalyst.⁵³⁻⁵⁵ The key to this truly remarkable study was the finding that toluene, the solvent, can act to stabilize the active titanium(II) trimerization catalyst for the $\text{Cp}^*\text{TiMe}_3/\text{B}(\text{C}_6\text{F}_5)_3$ system.⁵⁶ The observation by Pellecchia and coworkers that a minor product for this

catalyst system was 1-hexene clearly indicated the presence of a titanium(II) intermediate. Hessen and coworkers reasoned that if toluene could serve (quite poorly) as a weak donor to stabilize a cationic titanium(II) intermediate, then introducing a pendant arene onto the ancillary cyclopentadienyl ligand could mimic the solvent stabilization mode, but with greater effect.

The monocyclopentadienyl titanium hydrocarbyl species with an intramolecularly coordinated aromatic group proved to be a poor catalyst (lower activities and molecular weights) for styrene and propylene polymerization. However, this system was highly selective for ethylene trimerization. The activity of these titanium catalysts rival the best chromium catalysts with respect to activity and selectivity.⁵¹ The major advantage is that the active site appears to be well-defined in comparison to the chromium systems. The activation of the pre-catalyst with a Lewis acid is shown in **Figure 1.12**. The intramolecular interaction between the pendant arene and the metal centre was clearly established by ¹H and ¹³C{¹H} NMR spectroscopy.⁵⁵

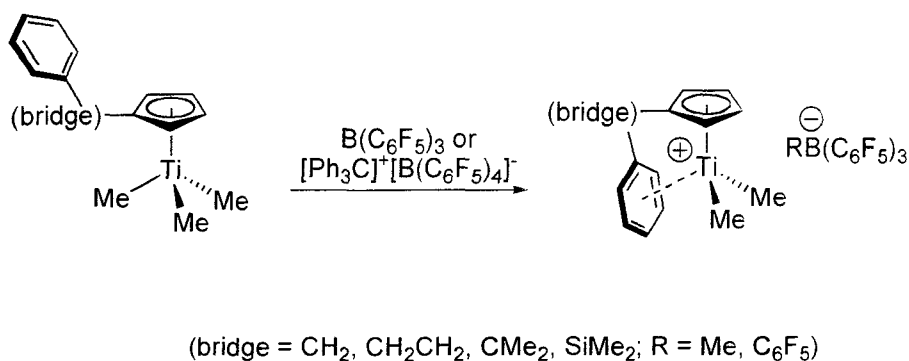


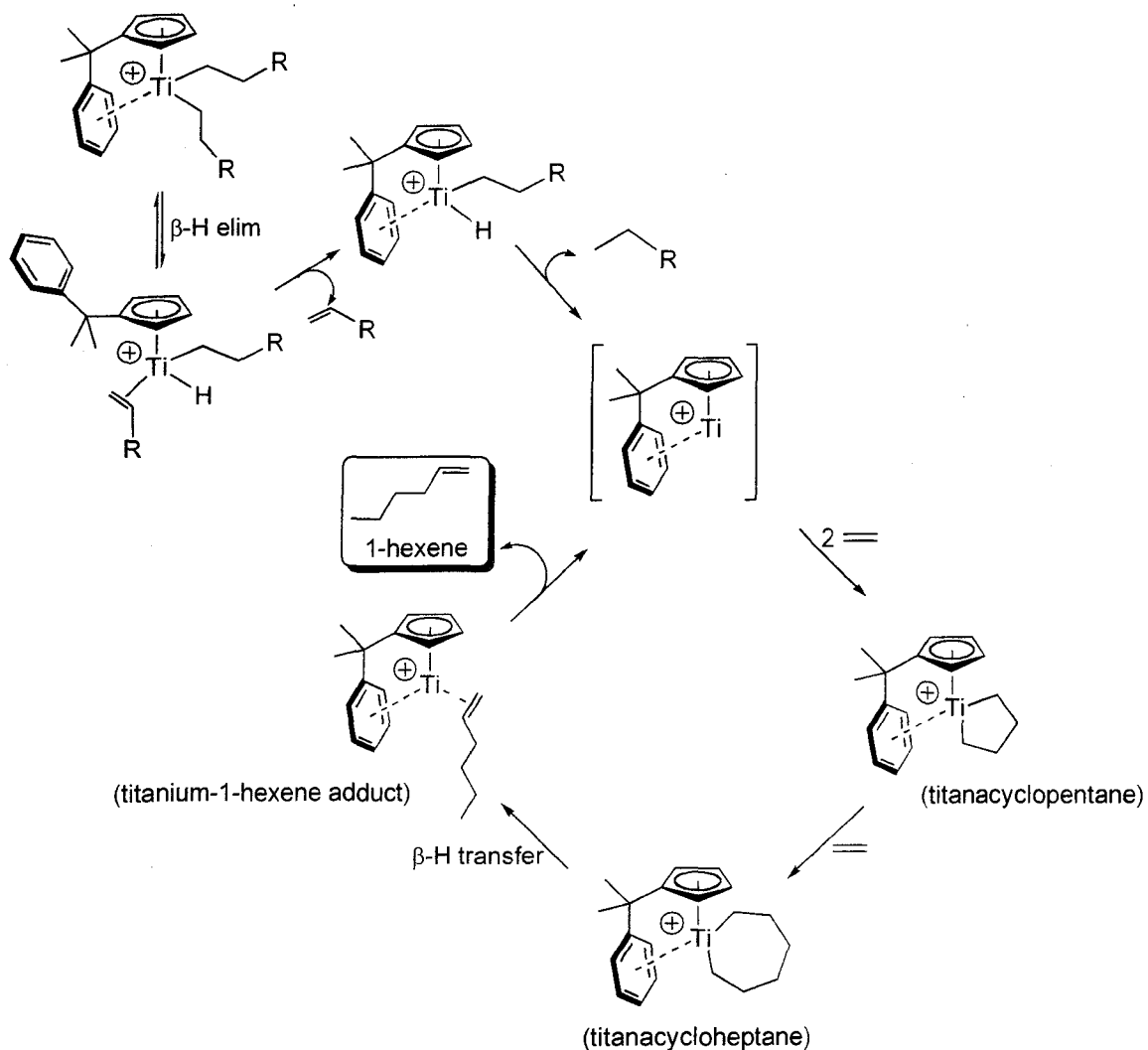
Figure 1.12 Pendant donor-metal interaction to stabilize cationic metal centre

When the catalyst (C₅H₄CMe₂Ph)TiCl₃ was activated with MAO, the major products were C₆ (83 wt %) and C₁₀ (14 wt %) with a very small amount of polyethylene.

The production of a C₁₀ fragment was attributed to co-trimerization of 1-hexene with two ethylene units.⁵⁵ Conversely, the pendant-free (C₅H₄CMe₃)TiCl₃/MAO system produced polyethylene as the major product. This clearly indicates that the pendant arene is of utmost importance to switching the selectivity of the catalyst from polymerization to trimerization. Another important aspect of the catalyst design is the nature of the bridging group (**Figure 1.12**). The use of a C₂ ethylene bridge produced a highly selective catalyst but with poor activity. In this case, the coordination of the arene to titanium is too strong. The use of a dimethyl silyl group as a bridge results in an unstable complex when activated. However, CMe₂ as a bridge gave the highest activity and selectivity.⁵⁵ Therefore it is clear that the bridging unit also plays a crucial role in terms of the steric strain induced, strength of the metal-arene interaction, and the orientation of the arene moiety.

This work is a fantastic example of a catalyst that can be dramatically affected by the incorporation of a hemilabile ligand to afford selectivity and stability. The mechanism of the oligomerization process was elucidated by Blok and coworkers.⁵⁷ Based on DFT calculations they suggested that the oligomerization process occurs through metallacyclic intermediates (**Scheme 1.1**). The key step is the formation of a titanium(II) species when the alkyl-hydride complex undergoes reductive elimination. The titanium(II) species coordinates two ethylene molecules to generate a titana(IV)cyclopentane. A further insertion of a third ethylene monomer gives rise to a titana(IV)cycloheptane. For the titanium catalyst featuring the hemilabile pendant arene ligand, direct C_β to C_α H transfer occurs to give a 1-hexene adduct. However, for the 'naked' system without a pendant donor, this process is endothermic and thus further

insertion of ethylene monomers is favored to give polymer.⁵⁷ Direct C_{β} to C_{α} hydrogen transfer is exothermic when a pendant donor is featured, and thus the arene donor plays a large role in the chemistry at the metal centre.



Scheme 1.1 Proposed trimerization cycle⁵⁷

1.5 Scope of This Work

It is apparent that hemilabile ligands in coordination chemistry have shown much promise towards preparing highly selective olefin oligomerization catalysts.⁵³⁻⁵⁵

Furthermore, the incorporation of a hemilabile donor in the ligand framework has the potential of stabilizing reactive transition metal centers that are suitable for olefin polymerization, and thus improving the thermal stability of potential catalysts. Group IV catalysts featuring phosphinimide ligands have proven to be highly active polymerization catalysts due to the steric and electronic similarities shared between phosphinimide and Cp ligands.³² Recent results in the Stephan group have shown promise in terms of developing hemilabile phosphinimide systems. Titanium complexes featuring di-*tert*-butylbiphenylphosphinimide ligands with a potentially hemilabile arene (**Figure 1.13**) have been synthesized, and an interaction between the pendant arene and Ti(II) and Ti(IV) metal centers has been observed.^{43,44}

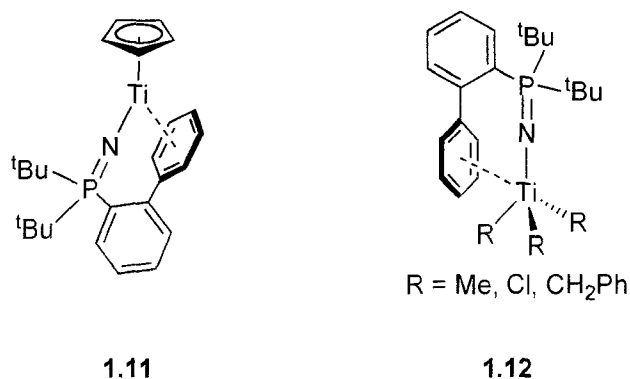


Figure 1.13 Pendant arene coordination in titanium-phosphinimide complexes

In this thesis, the goal is to develop new hemilabile phosphinimide ligands featuring a tethered heteroatom donor. The first part of this work will highlight the synthesis of these S- and O-donor versions of these ligands and the preparation of selected titanium complexes. The reactivity of Lewis acids with the titanium dialkyl species, and the role of the pendant donor in the activated complex, will also be discussed. Finally, the second portion of this thesis will examine the titanium pre-

catalysts for their potential as polymerization or oligomerization catalysts upon activation with a series of co-catalysts.

Chapter 2

Hemilabile Ligand Design and Reactivity of Selected Ti(IV)

Phosphinimide Complexes

2.1 Introduction: Synthesis of phosphinimines and Ti(IV) phosphinimide complexes

Hemilabile ligands are of interest to organometallic researchers based on their ability to transiently provide open coordination sites at the metal during reaction that are “masked” in the ground-state structure and to stabilize reactive intermediates.⁵⁸ This is especially important in the area of homogeneous α -olefin polymerization catalysis since the active species is a highly reactive cationic transition metal complex. The recent discovery of a titanium complex, which incorporates a hemilabile arene ligand, by Hessen and coworkers remains the only example of a well-defined, *highly active* catalyst selective for ethylene trimerization.⁵³ Huang and coworkers reported half-sandwich titanium complexes bearing a pendant ether group, $\text{CH}_3\text{OCH}_2\text{CH}_2\text{CpTiCl}_3$ and $\text{CH}_3\text{OCH}(\text{CH}_3)\text{CH}_2\text{CpTiCl}_3$, that are highly selective for ethylene trimerization but have moderate activity upon activation with MAO.⁵⁹

Previous attempts in the Stephan group have been successful in the synthesis of titanium phosphinimide catalysts with a hemilabile function. Graham and coworkers⁴³ reported titanium complexes incorporating the di-*tert*-butylbiphenylphosphinimine ligand (**Figure 2.1**). The sterically crowded environment provided by the ancillary Cp' (Cp' = C_5H_5 or C_5Me_5) ligand on titanium inhibited free rotation of the biphenyl substituent, where the pendant arene faces away from the metal centre. Reduction of these complexes

with magnesium led to a transient Ti(II) species, which subsequently reduced the arene moiety and concomitantly reoxidized the metal (**Figure 2.1a**). This work lent credence to the possibility that the di-*tert*-butylbiphenylphosphinimine ligand could possess hemilabile character under a more sterically open situation. Ghesner and coworkers⁴⁴ prepared a series of LMR₃ complexes (M = Ti, Zr) featuring the aforementioned phosphinimine but without a sterically encumbering Cp' (Cp' = C₅H₅ or C₅Me₅) ancillary ligand. Complexes were isolated in which the pendant arene was shown to favor an orientation proximal to titanium. Furthermore, cationic complexes in which the metal centre was stabilized by the pendant arene were prepared through reaction with the bulky Lewis acid B(C₆F₅)₃ (**Figure 2.1b**).

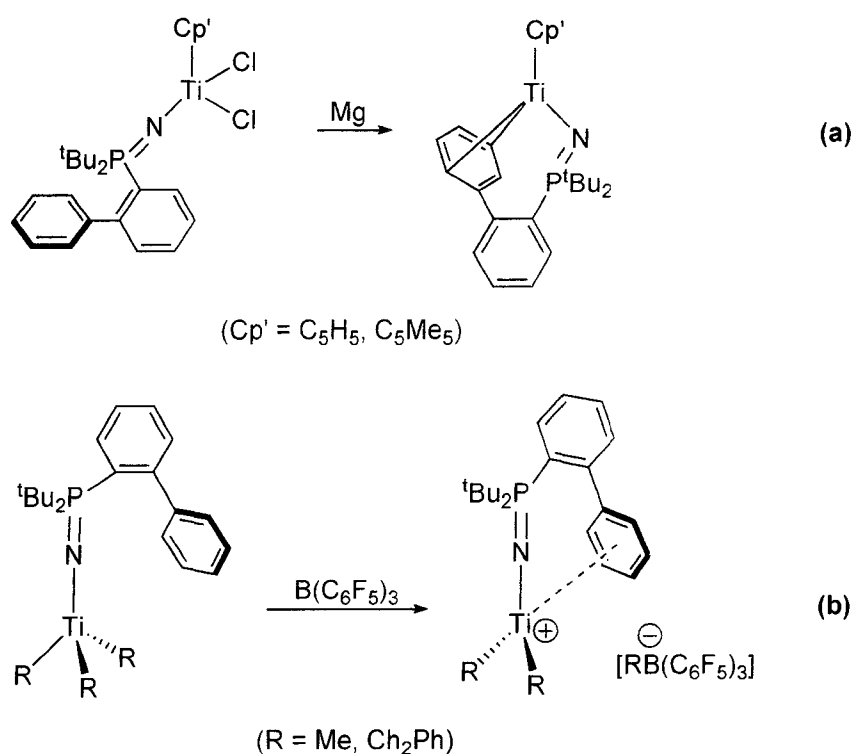


Figure 2.1 (a) Reduction of Cp'(^tBu₂(2-C₆H₄Ph)PN)TiCl₂ to give Cp'(^tBu₂(2-C₆H₄Ph)PN)Ti. (b) Formation of cationic species [Cp'(^tBu₂(2-C₆H₄Ph)PN)TiMe₂]⁺[RB(C₆F₅)₃]⁻.

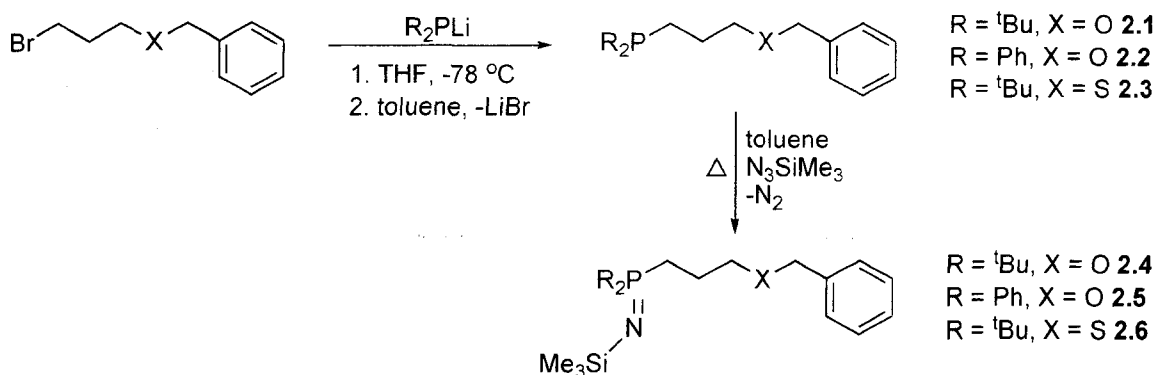
While these systems did not show any catalytic activity for olefin polymerization, the development of phosphinimide ligands with a pendant arene that interacts with titanium is a promising result. Using different pendant donors on the phosphinimide ligand may provide new catalysts for olefin polymerization while maintaining stability at the electrophilic metal centre. In this chapter, synthetic routes were developed to prepare a series of new phosphinimine ligands bearing a pendant ether or thioether group. Selected titanium complexes featuring pendant ether and thioether phosphinimide ligands were subsequently prepared. The potential of either hard (oxygen) or soft (sulfur) donors to stabilize the highly reactive titanium metal centre was probed by investigating their reactivity in solution with boron-based Lewis acids.

2.1.1 Results and Discussion: Complex Synthesis

New phosphines and the corresponding phosphinimine ligands were prepared in high yield using short and simple synthetic routes. The synthesis of the ether-phosphine $R_2P(CH_2)_3OBn$, $R = ^iBu$ **2.1**, Ph **2.2**, was carried out via nucleophilic attack of the lithium phosphide salt R_2PLi ($R = ^iBu, Ph$) on the commercially available benzyl 3-bromopropyl ether in THF. This reaction is highly exothermic and so must be carried out at low temperature ($-35\text{ }^\circ\text{C}$). Formation of the phosphine is almost immediate with a change in color from yellow to colorless. Removal of THF *in vacuo* and addition of toluene precipitated LiBr, which was removed via filtration over Celite. Subsequent removal of toluene *in vacuo* gave a viscous oil as the pale yellow phosphine product. The $^{31}\text{P}\{^1\text{H}\}$ NMR spectrum showed a single resonance peak (-15.7 ppm **2.1**, 27.0 ppm **2.2**) indicating formation of a single product with no further purification necessary. To make the

analogous thioether phosphine ${}^t\text{Bu}_2\text{P}(\text{CH}_2)_3\text{SBn}$ **2.3**, benzyl 3-bromopropylthioether was first prepared in high yield (93% yield) using a previously published method.⁶⁰ While reaction at $-35\text{ }^\circ\text{C}$ gave multiple products, lowering the reaction temperature to $-78\text{ }^\circ\text{C}$ allowed for formation of a single, pure species. A single peak in the ${}^{31}\text{P}\{^1\text{H}\}$ NMR spectrum (27.4 ppm) indicated the formation of **2.3**.

The synthesis of the corresponding phosphinimines $\text{Me}_3\text{Si-N}=\text{P}(\text{R}_2)[(\text{CH}_2)_3\text{XBn}]$, $\text{R} = {}^t\text{Bu}$, $\text{X} = \text{O}$ **2.4**; $\text{R} = \text{Ph}$, $\text{X} = \text{O}$ **2.5**; $\text{R} = {}^t\text{Bu}$, $\text{X} = \text{S}$ **2.6**, was carried out by azide oxidation of the phosphine ligands (Staudinger reaction⁶¹) in toluene. Refluxing the mixture for 12 hours and removal of toluene *in vacuo* afforded a viscous pale yellow oil. The formation of phosphinimines where $\text{R} = \text{Ph}$ was confirmed by a downfield shift in the ${}^{31}\text{P}\{^1\text{H}\}$ NMR spectrum (1.56 ppm). Interestingly, when $\text{R} = {}^t\text{Bu}$, the downfield shift was far less dramatic (27.1 ppm; $\Delta = < 1\text{ ppm}$). Further evidence was provided by the presence of a TMS singlet in the ${}^1\text{H}$ NMR spectra (0.31 ppm **2.4**, 0.49 ppm **2.5**). The synthetic route is outlined in **Scheme 2.1**.



Scheme 2.1 Synthetic route to ether- and thioether-phosphinimine ligands

Previous findings in the Stephan group have shown that there is a strong correlation between the polymerization activity of titanium catalysts and the substituents

on phosphorus. For example, catalysts derived from $\text{CpTi}(\text{NPCy}_3)\text{Cl}_2$ and $\text{CpTi}(\text{NP}^i\text{Pr}_3)\text{Cl}_2$ exhibit relatively low ethylene polymerization activity when activated with MAO. This lies in stark contrast to the more sterically demanding *tert*-butyl substituents, which have shown the highest olefin polymerization activity for the phosphinimide systems of this type.^{34,39} In light of these findings, prepared titanium complexes featuring pendant ether and thioether groups presented in this work feature *tert*-butyl substituents on phosphorus. Substitution of these ligands on titanium was achieved in high yield via Me_3SiCl elimination, as shown in **Figure 2.2**.

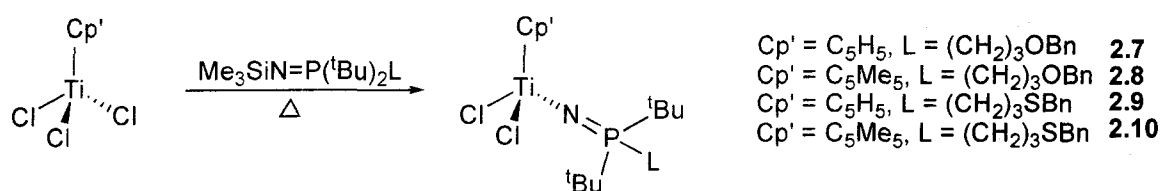


Figure 2.2 Synthetic route to titanium-phosphinimides

Addition of a toluene solution of **2.4** to an orange solution of CpTiCl_3 in toluene at room temperature gave a dark orange mixture. Refluxing overnight and removal of solvent *in vacuo* afforded a dark orange oil. Subsequent washing with hexanes gave a yellow solid (73.2% yield). A downfield shift for the Cp resonance (6.46 ppm) and absence of the TMS signal in the ^1H NMR spectrum indicated formation of the product $\text{CpTiCl}_2[\text{NP}^i\text{Bu}_2(\text{CH}_2)_3\text{OBn}]$ **2.7**. Ligand substitution onto Cp^*TiCl_3 was accomplished using the same process to give the orange solid product $\text{Cp}^*\text{TiCl}_2[\text{NP}^i\text{Bu}_2(\text{CH}_2)_3\text{OBn}]$ **2.8** (81.3% yield). The same trends were seen in the ^1H NMR data for **2.8**. In both cases, $^{31}\text{P}\{^1\text{H}\}$ NMR spectroscopy showed a downfield shift for the product resonances of the metal complexes (39.9 ppm **2.7**, 38.5 ppm **2.8**). The benzylic methylene protons were

equivalent in the ^1H NMR spectrum, which unsurprisingly suggested no titanium-oxygen interaction in the neutral species. X-ray quality crystals of **2.7** were grown through evaporation of a dilute solution in hexanes (**Figure 2.3**).

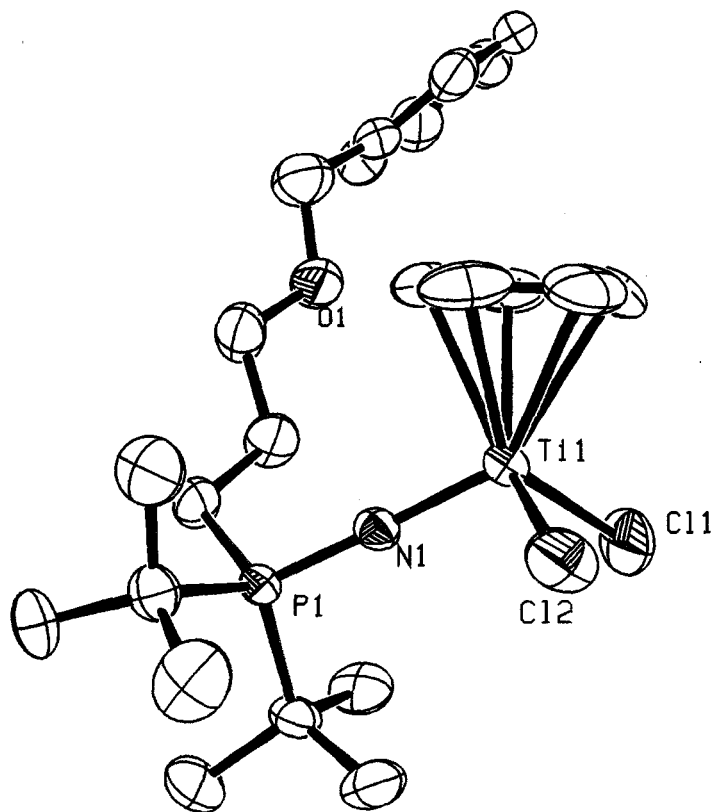


Figure 2.3 ORTEP drawing of **2.7**; 30% ellipsoids are shown, hydrogen atoms have been omitted for clarity. Selected bond distances and angles: Ti1-N1 1.754(3) Å, N1-P1 1.601(3) Å, Ti1-C11 2.2981(15) Å, Ti1-C12 2.2977(15) Å, Ti1-N1-P1 179.5(2)°, C11-Ti1-C12 101.26°.

The Ti-O distance of 5.296 Å confirms no interaction between titanium and oxygen in the solid state. The pseudo-tetrahedral geometry about titanium was similar to

other titanium phosphinimide complexes. The almost perfect linearity of the Ti-N-P angle [$179.5(2)^\circ$] was indicative of some multiple bond character in the Ti-N bond. Additionally, the N-P distance of $1.601(3) \text{ \AA}$ was similar to previously reported titanium phosphinimide complexes.^{62,63} The molecular structure of **2.8** was also confirmed crystallographically (**Figure 2.4**). A Ti-O distance of 5.204 \AA again reveals no interaction between oxygen and the metal centre. The overall structure was similar to **2.7**.

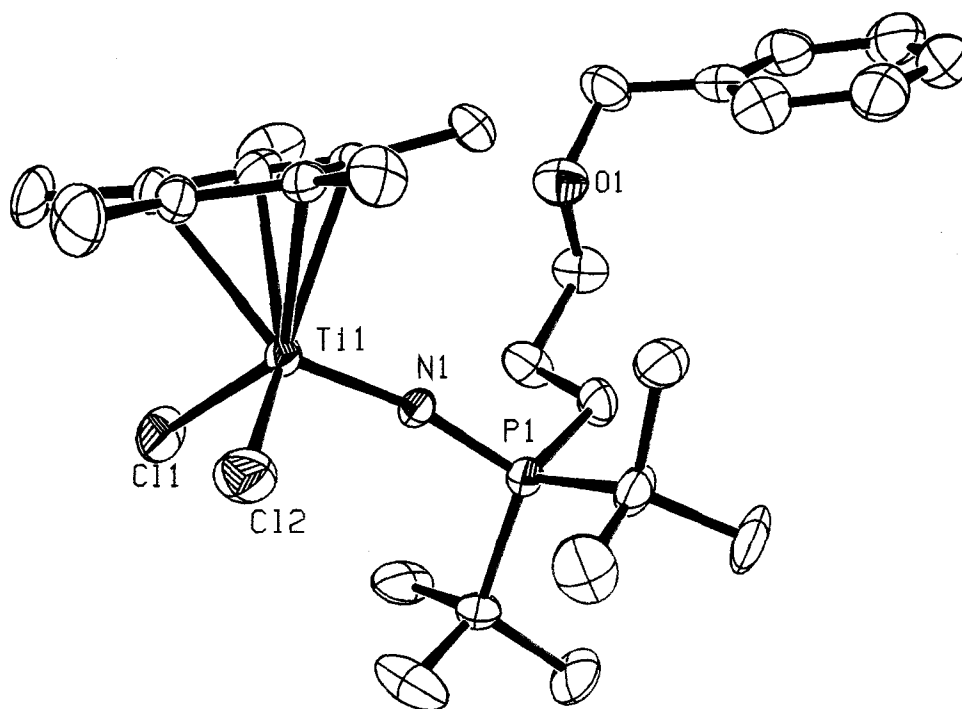


Figure 2.4 ORTEP drawing of **2.8**; 30% ellipsoids are shown, hydrogen atoms have been omitted for clarity. Selected bond distances and angles: Ti1-N1 $1.766(3) \text{ \AA}$, N1-P1 $1.604(3) \text{ \AA}$, Ti1-C11 $2.3047(14) \text{ \AA}$, Ti1-C12 $2.3176(16) \text{ \AA}$, Ti1-N1-P1 $168.7(2)^\circ$, C11-Ti1-C12 $101.43(6)^\circ$.

Thioether-containing titanium complexes $\text{CpTiCl}_2[\text{NP}(\text{tBu})_2(\text{CH}_2)_3\text{SBn}]$ **2.9**, and $\text{Cp}^*\text{TiCl}_2[\text{NP}(\text{tBu})_2(\text{CH}_2)_3\text{SBn}]$ **2.10**, were also prepared in relatively good yield (76.7% **2.9**, 61.3%, **2.10**). There were clear differences in the ^1H NMR spectra compared to **2.7** and **2.8**, respectively. Both the benzylic and methylene protons *alpha* to sulfur were shifted upfield when compared to the corresponding oxygen systems. The benzylic protons were equivalent, again suggesting no titanium-sulfur interaction for the neutral species.

The dialkyl titanium species $\text{CpTiMe}_2[\text{NP}(\text{tBu})_2(\text{CH}_2)_3\text{OCH}_2\text{Ph}]$ **2.11**, $\text{Cp}^*\text{TiMe}_2[\text{NP}(\text{tBu})_2(\text{CH}_2)_3\text{OCH}_2\text{Ph}]$ **2.12**, $\text{CpTiMe}_2[\text{NP}(\text{tBu})_2(\text{CH}_2)_3\text{SCH}_2\text{Ph}]$ **2.13** and $\text{Cp}^*\text{TiMe}_2[\text{NP}(\text{tBu})_2(\text{CH}_2)_3\text{SCH}_2\text{Ph}]$ **2.14** were prepared in moderate to excellent yields (77% **2.11**, 81.7% **2.12**, 46% **2.13**, 91.9% **2.14**) by reaction of the dichloride derivatives with either alkyllithium (MeLi) or Grignard reagents (MeMgBr) in benzene and ether, respectively (**Figure 2.5**).

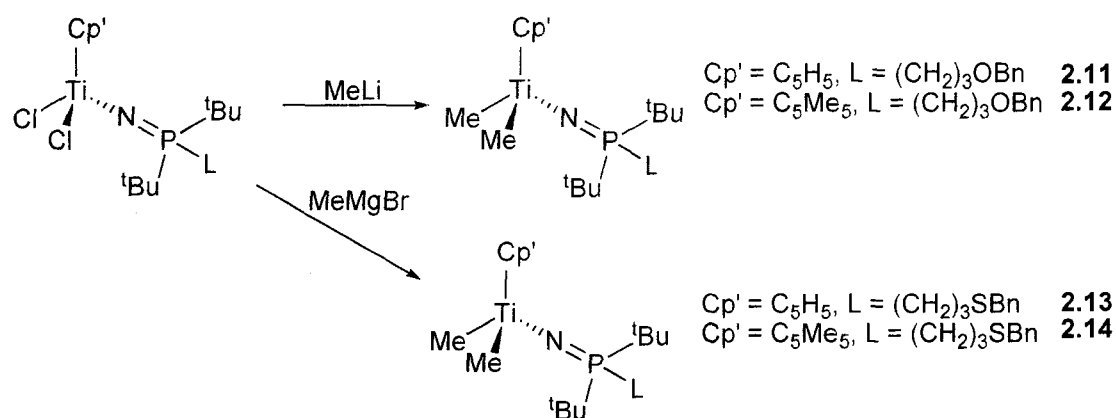


Figure 2.5 Synthetic route to titanium-phosphinimide derivatives

The ^1H NMR spectrum for **2.11** is shown in **Figure 2.6**. In the case of the Cp^* systems **2.12** and **2.14**, the dialkyl products were isolated as solids following extraction.

cooling and filtration of the reaction mixture with hexanes. However, the Cp-dialkyl products **2.11** and **2.13** could only be isolated as waxy oils. Presumably, less steric bulk with the unsubstituted Cp complexes and the long pendant alkyl chain were the likely reason these dialkyl species could not be isolated as crystalline solids. Expected upfield shifts in the $^{31}\text{P}\{^1\text{H}\}$ NMR spectra upon alkylation of the metal complexes was observed in all cases. ^1H NMR chemical shifts for the methyl groups ranged from 0.63 ppm for **2.11** to 0.40 ppm for **2.14**, comparable to those reported for similar titanium-phosphinimide complexes.³⁵

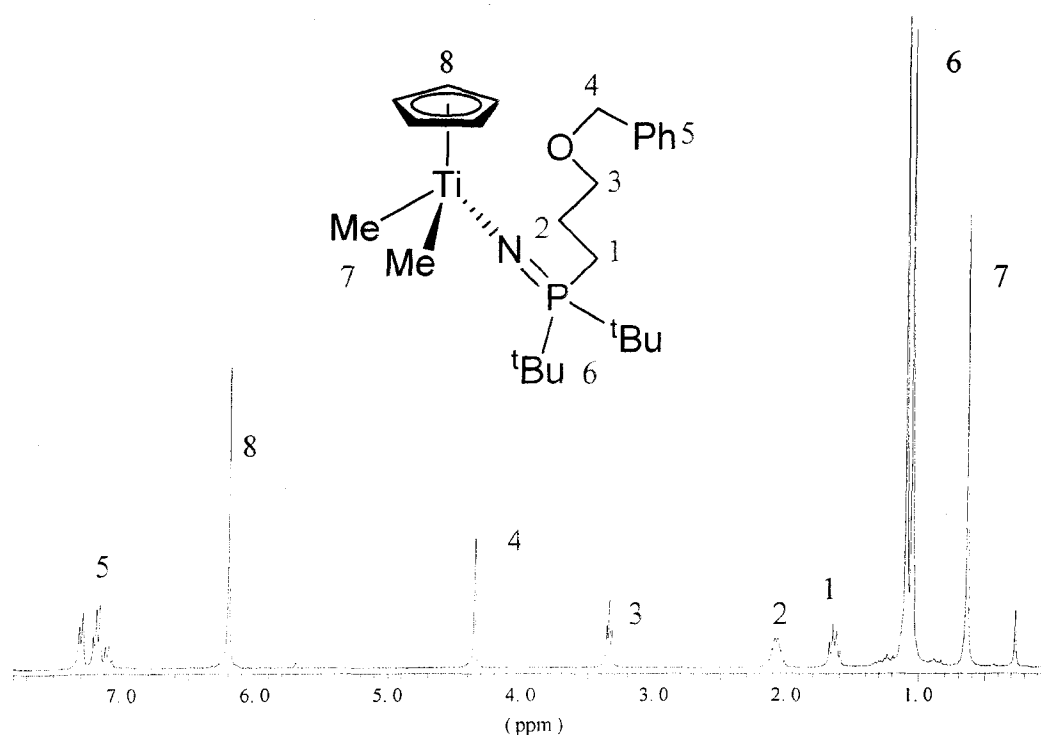


Figure 2.6 ^1H NMR spectrum for complex **2.11**

2.2 Introduction: Reactivity of Ti(IV) phosphinimide complexes with $B(C_6F_5)_3$ and $[Ph_3C]^+[B(C_6F_5)_4]^-$

The previous section discussed the design of hemilabile phosphinimide ligands and their incorporation into Ti(IV) complexes. It has been established that early transition metal phosphinimide systems catalytically polymerize olefins.³² Incorporation of a heteroatom donor into the ligand framework should impart unique reactivity for this new class of Ti-phosphinimide systems. Before testing catalyst precursors for polymerization purposes, it is important to investigate the reactivity of the pre-catalyst with commonly used activators. NMR spectroscopy is a powerful tool for determining if stable ion pairs are being generated in solution. This section focuses on the activation of the dialkyl titanium systems with the Lewis acids methylalumoxane (MAO), tris(pentafluorophenyl)borane, $B(C_6F_5)_3$, and trityl borate, $[Ph_3C]^+[B(C_6F_5)_4]^-$.

Single-site homogeneous olefin polymerization catalysts are often comprised of two ligands (L, L') and two alkyl groups (R, R') bound to a group(IV) transition metal centre. These neutral species are not effective catalysts and require activation by a co-catalyst. Hence the choice of co-catalysts often bears a large influence on the performance of olefin polymerization catalysts.⁷ Lewis acids such as $B(C_6F_5)_3$, $[Ph_3C]^+[B(C_6F_5)_4]^-$ and MAO are commonly used to abstract an alkyl group R^- to give the active catalyst $[LL'MR']^+$. There are two major considerations concerning the co-catalyst. First, the catalytic precursors should rapidly and cleanly transform to the active catalyst. Second, the anionic portion of the catalyst is a crucial part of the catalytically active ion pair and is capable of exerting significant influence on both the polymerization

process and the polymer produced.^{7,64} **Figure 2.7** depicts the formation of the active catalyst from the pre-catalyst and co-catalyst in metal-catalyzed olefin polymerization.

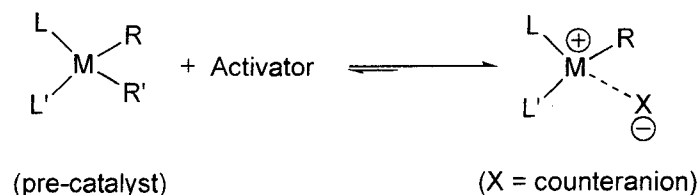


Figure 2.7 Equilibrium between pre-catalyst, activator, and ion pair

The importance and understanding of boron-based activators, in particular, has been well developed over the last 20 years. In the early 1990s, Marks^{65,66} and Ewen⁶⁷ first reported the utility of the strong Lewis acid $\text{B}(\text{C}_6\text{F}_5)_3$ as a promoter of highly efficient olefin polymerization in conjunction with Group IV metallocene dialkyls. The bulky fluoroaryl groups are strongly electron withdrawing, which provides sufficient Lewis acidity at the boron centre to affect methyl abstraction of a dialkyl catalyst precursor. Furthermore, $\text{B}(\text{C}_6\text{F}_5)_3$ has good solubility in nonpolar, noncoordinating solvents and the boron centre is surrounded by highly electronegative functional groups that are resistant to electrophilic attack.⁶⁶

Another common co-catalyst is $[\text{Ph}_3\text{C}]^+[\text{B}(\text{C}_6\text{F}_5)_4]^-$.⁶⁸ The trityl borate co-catalyst (among other $[\text{B}(\text{C}_6\text{F}_5)_4]^-$ -based activators) has been shown to be highly active for olefin polymerization.⁶⁹ The trityl ionic activator is a powerful alkyl- and hydride-abstracting oxidizing reagent. However, $[\text{B}(\text{C}_6\text{F}_5)_4]^-$ -based activators suffer from poor thermal stability, which results in very short catalytic lifetimes.⁷⁰

Group IV metallocenes have also been shown to be highly active in the polymerization of α -olefins when combined with MAO.¹⁵ This oligomeric activator is

prepared through the controlled hydrolysis of AlMe_3 to give $[-\text{Al}(\text{Me})-\text{O}]_n$, where $n \approx 5$ -20. MAO acts to alkylate dihalide catalyst precursors and subsequently abstract a methyl group to produce a catalytically active species. A disadvantage is that the exact structure of MAO is not well understood. Furthermore, depending on the nature of the H_2O source used in its synthesis, MAO-activated metallocenes may exhibit widely differing activities in olefin polymerization.⁷

Cp titanium-phosphinimide dialkyl pre-catalysts have shown higher activity when using C_6F_5 -boron-based activators as opposed to the analogous dihalide precursors in conjunction with MAO.^{34,35} Modeling studies with AlMe_3 suggest C-H bond activation as a possible degradation pathway for phosphinimide catalysts in the presence of MAO.^{35,71} Alternately, interaction between an aluminum centre and the phosphinimide ligand may suppress catalytic activity. High activities have also been seen with the bis-phosphinimide titanium complex $\text{TiMe}_2[\text{NP}(\text{tBu})_3]_2$ with both $\text{B}(\text{C}_6\text{F}_5)_3$ and $[\text{Ph}_3\text{C}]^+[\text{B}(\text{C}_6\text{F}_5)_4]^-$.³⁵ Markedly lower activities were observed with the corresponding dihalide systems and MAO.

In terms of polymerization, monomer uptake and insertion into the M-C bond are the crucial steps for polymer chain propagation. Ziegler and coworkers highlighted the importance of the counterions ($[\text{MeB}(\text{C}_6\text{F}_5)_3]^-$, $[\text{B}(\text{C}_6\text{F}_5)_4]^-$, $[\text{TMA-MAOMe}]^-$ and $[\text{MAOMe}]^-$) in a theoretical study.⁴⁰ The uptake and insertion of monomer are likely influenced by the mobility and coordination of the counterion, respectively. The ion-pair separation energy (ΔH_{ips}), which is an indicator of counterion mobility, was found to be lowest for $[\text{B}(\text{C}_6\text{F}_5)_4]^-$ and thus the weakest interactions with all of the studied cations ($[(\text{NPR}_3)_2\text{TiMe}]^+$, $[(\text{Cp})(\text{NCR}_2)\text{TiMe}]^+$, $[(\text{CpSiR}_2\text{NR}')\text{TiMe}]^+$, $[(\text{Cp})\text{OSiR}_3\text{TiMe}]^+$,

$[(\text{Cp})\text{NPR}_3\text{TiMe}]^+$, $[(1,2\text{-Me}_2\text{Cp})_2\text{ZrMe}]^+$). The relative coordinative ability of the typical anions is in the order of $\text{MAOMe}^- > \text{TMA-MAOMe}^- > \text{MeB}(\text{C}_6\text{F}_5)_3^- > [\text{B}(\text{C}_6\text{F}_5)_4]^-$. The conclusion can be drawn that greater mobility of the counteranion in turn leads to higher olefin polymerization activities.

2.2.1 Results and Discussion: Activation of Dialkyl Precursors

In contrast to MAO, activation of catalyst precursors with the well-defined species $\text{B}(\text{C}_6\text{F}_5)_3$ or $[\text{Ph}_3\text{C}]^+[\text{B}(\text{C}_6\text{F}_5)_4]^-$ can be conveniently studied using NMR spectroscopy. $^{31}\text{P}\{^1\text{H}\}$ and ^1H NMR variable-temperature (VT) NMR spectroscopy is useful for investigating the stability of the cationic species generated following alkyl abstraction. ^{19}F and ^{11}B NMR experiments are ideal for determining the formation of a stable anionic species. This is particularly relevant for $\text{B}(\text{C}_6\text{F}_5)_3$, where clear changes in the NMR spectra indicate the formation of an anionic alkyl borate. The difference in chemical shift of the *meta* and *para* fluorines ($\Delta\delta$ (m,p- ^{19}F NMR)) is a good qualitative probe for the mode of coordination of $[\text{RB}(\text{C}_6\text{F}_5)_3]^-$ (R = Me, CH_2Ph) to, for example, cationic d^0 metals. Values of 3-6 ppm indicates coordination to give contact ion pairs; <3 ppm indicates solvent-separated ion pairs.^{72,73}

Previous work in the Stephan group has shown activation of species analogous to **2.11-2.14** with both $\text{B}(\text{C}_6\text{F}_5)_3$ and $[\text{Ph}_3\text{C}]^+[\text{B}(\text{C}_6\text{F}_5)_4]^-$.³⁹ With this knowledge in hand, investigations were undertaken to examine the activation of the dialkyl precursors. If the activations are done in toluene, clathrate-like oils are formed that are unsuitable for NMR analysis. Therefore, a deuterated haloarene solvent ($\text{C}_6\text{D}_5\text{Br}$) was used to ensure solubility.⁷⁴ Initial efforts to activate the dialkyl precursor **2.11** with either of the

aforementioned Lewis acids at room temperature resulted in a mixture of products, as evidenced by $^{31}\text{P}\{^1\text{H}\}$ NMR spectroscopy. However, when the reaction was repeated at $-35\text{ }^\circ\text{C}$ by slowly adding a cooled solution of the activator to a solution of **2.11**, followed by warming to room temperature, this resulted in the clean formation of the cationic species $[\text{CpTiMe}(\text{N}=\text{P}(\text{tBu})_2(\text{CH}_2)_3\text{OBn})]^+[\text{MeB}(\text{C}_6\text{F}_5)_3]^-$ **2.15**.

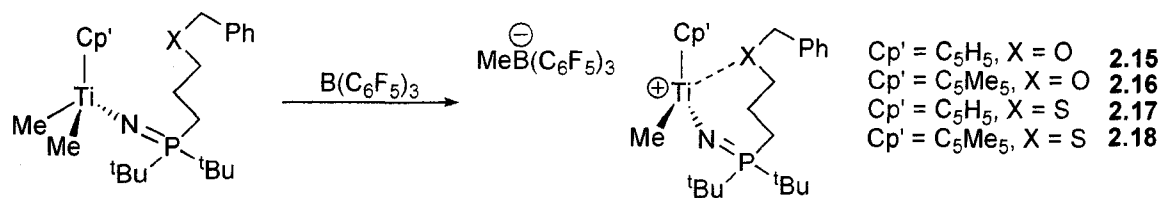


Figure 2.8 Activation of **2.11-2.14** with $\text{B}(\text{C}_6\text{F}_5)_3$

The $^{31}\text{P}\{^1\text{H}\}$ NMR spectrum displayed a singlet at 45.4 ppm, which signified formation of a single product. A singlet at -15.0 ppm in the ^{11}B NMR spectrum confirmed the generation of an anionic borate. Furthermore, the ^{19}F NMR spectrum showed a $\Delta\delta$ (m,p) value of 2.38, clearly indicating that the methyl borate anion was not tightly bound to the metal centre.^{72,73} Interestingly, the ^1H NMR spectrum (**Figure 2.9(b)**) at $-35\text{ }^\circ\text{C}$ showed that both the methylene protons *alpha* to oxygen and the benzylic methylene protons were diastereotopic. This was most clearly seen with the benzylic methylene protons, which were clearly resolved as two doublets (4.96 ppm, $|J_{\text{H-H}}| = 12$ Hz; 4.61 ppm, $|J_{\text{H-H}}| = 12$ Hz). The methylene protons *alpha* to oxygen were clearly two different sets of signals, although they were broad and poorly resolved. Additionally, the *tert*-butyl resonances were two overlapping doublets (1.24 and 1.19 ppm), indicating that they were now inequivalent. The Cp (6.72 ppm) and $\text{MeB}(\text{C}_6\text{F}_5)_3$

0.58 ppm) resonances were sharp and broad singlets, respectively. The remaining methylene protons were obscured by the broad Ti-Me peak (1.47 ppm).

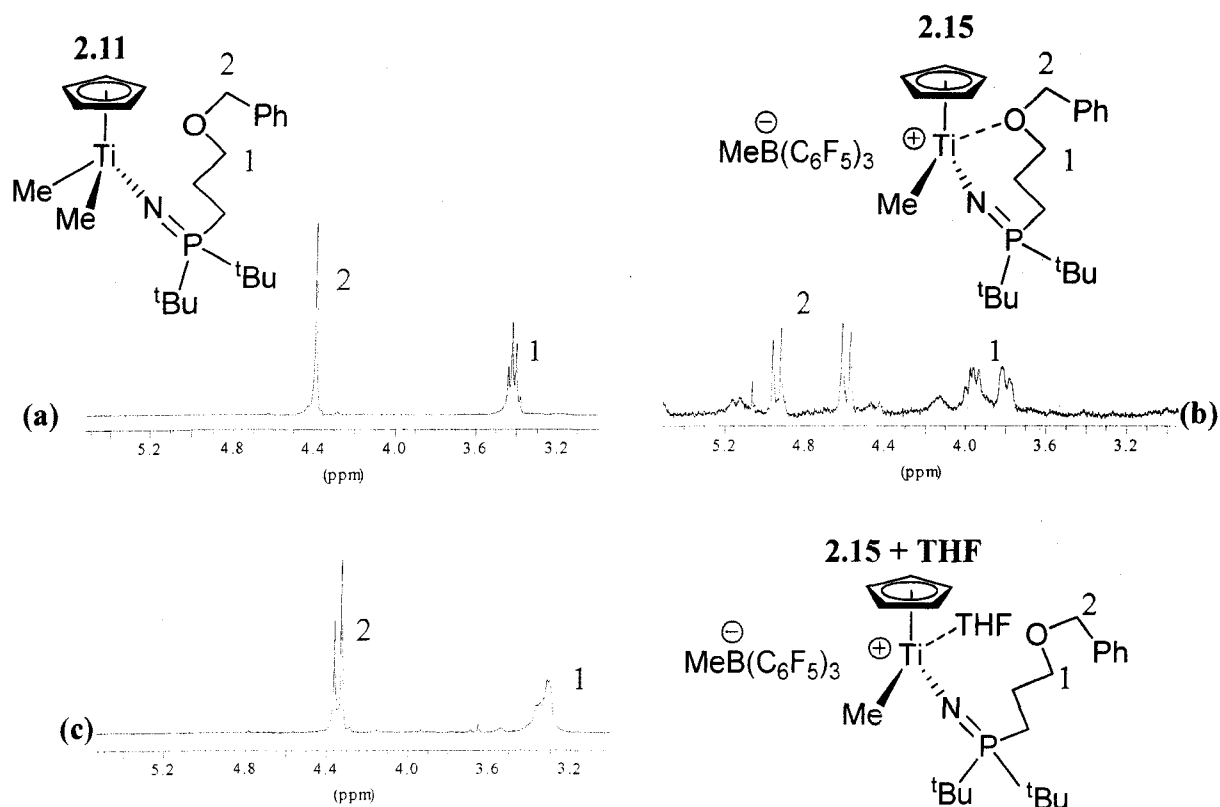


Figure 2.9 ^1H NMR spectrum of (a) the neutral dimethyl complex **2.11**, (b) the activated complex **2.15**, (c) the addition of THF to **2.15** displaces the pendant ether-titanium interaction

To further establish the presence of an oxygen-titanium interaction, **2.15** was treated with a stoichiometric amount of THF. The ^1H NMR spectrum (**Figure 2.9(c)**) revealed that the benzylic methylene protons and methylene protons *alpha* to oxygen each resolved into single resonances. This showed that the pendant ether interaction with the metal centre had been displaced by the addition of a stronger donor. These findings

confirmed that upon treatment of **2.11** with $B(C_6F_5)_3$, species **2.15** was formed in which: (i) a methyl group had been cleanly abstracted from the titanium centre resulting in a *solvent separated ion pair* and (ii) the inequivalency of the benzylic methylene protons, the methylene protons *alpha* to oxygen, and the *tert*-butyl groups suggested the formation of a hard-hard interaction between the oxygen donor and titanium. The presence of a heteroatom donor in the pendant ligand was favorable towards forming a donor-stabilized ion pair in solution.

Similar reactions with **2.12-2.14** gave the stable ion pairs $[Cp'TiMe(N=P(tBu)_2(CH_2)_3XBn)]^+[MeB(C_6F_5)_3]^-$ ($Cp' = C_5Me_5$, $X = O$ **2.16**; $Cp' = C_5H_5$, $X = S$ **2.17**; $Cp' = C_5H_5$, $X = S$ **2.18**). Low temperature ($-35\text{ }^\circ\text{C}$) ^1H NMR spectra for these activated complexes showed similar trends to **2.15**. In all cases, confirmation of a solvent separated anionic methyl borate was also evident by ^{11}B and ^{19}F NMR spectroscopy. Furthermore, the pendant donor was found to coordinate to the metal centre as evidenced by the diastereotopic benzylic methylene protons and the methylene protons *alpha* to X ($X = O, S$). **Table 2.1** shows the relevant NMR data for complexes **2.15-2.18**.

Table 2.1 Selected NMR spectral data for **2.15-2.18** (X = O **2.15, 2.16**; X = S **2.17, 2.18**)

	<i>Complex</i>	2.15	2.16	2.17	2.18
¹⁹F	$\Delta \delta(m,p)$	2.38	2.37	2.33	2.30
¹¹B		-15.0 (s)	-15.0 (s)	-14.7 (s)	-14.6 (s)
³¹P		45.4 (s)	43.0 (s)	45.7 (s)	44.4 (s)
¹H	CHH-X-CHHBz	4.96 (d)	4.08 (d)	3.18 (d)	3.22 (d)
	CHH-X-CHHBz	4.61 (d)	3.99 (d)	2.99 (d)	2.77 (d)
	$ J_{H-H} $	12 Hz	7 Hz	12 Hz	14 Hz

Low temperature (-35°C) reactions of complexes **2.11-2.14** with $[\text{Ph}_3\text{C}]^+[\text{B}(\text{C}_6\text{F}_5)_4]^-$ afforded the ion pair complexes $[\text{Cp}'\text{TiMe}(\text{N}=\text{P}(\text{tBu})_2(\text{CH}_2)_3\text{XBn})]^+[\text{B}(\text{C}_6\text{F}_5)_4]^-$ ($\text{Cp}' = \text{C}_5\text{H}_5$, X = O **2.19**; $\text{Cp}' = \text{C}_5\text{Me}_5$, X = O **2.20**; $\text{Cp}' = \text{C}_5\text{H}_5$, X = S **2.21**; $\text{Cp}' = \text{C}_5\text{Me}_5$, X = S **2.22**) (**Figure 2.10**).

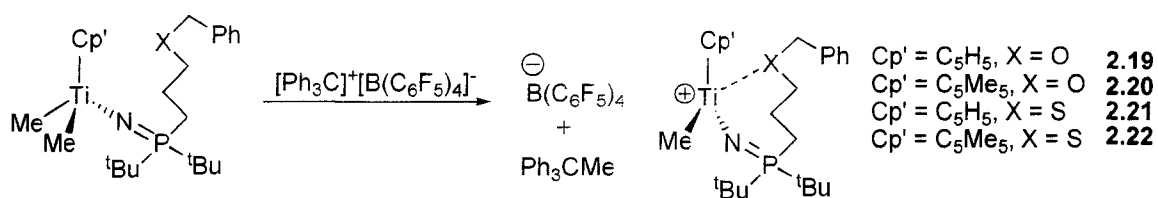


Figure 2.10 Activation of **2.11-2.14** with $[\text{Ph}_3\text{C}]^+[\text{B}(\text{C}_6\text{F}_5)_4]^-$

Coordination of the heteroatom donor to titanium was also observed for the activated species **2.19-2.22**. ^1H NMR spectroscopy showed that the benzylic methylene protons and the methylene protons *alpha* to X (X = S, O) were diastereotopic. Again,

only the benzylic methylene protons were clearly resolved as two doublets. Table 2.2 highlights the relevant NMR data for complexes **2.19-2.22**. The benzylic methylene protons for complex **2.19** were surprisingly observed as a broad singlet, which can be attributed to second order coupling. The methylene protons *alpha* to oxygen were inequivalent, indicating that the titanium-oxygen interaction was still intact.

Table 2.2 Selected NMR spectral data for **2.19-2.22** (X = O **2.19, 2.20**; X = S **2.21, 2.22**)

Complex	2.19	2.20	2.21	2.22	
Nucleus					
³¹P	45.1 (s)	43.0 (s)	45.4 (s)	44.3 (s)	
¹H	CHH-X-CHHBz	3.99 (br s)	4.08 (d)	3.28 (d)	3.24 (d)
	CHH-X-CHHBz		4.02 (d)	3.13 (d)	2.77 (d)
	$ J_{H-H} $		7 Hz	13 Hz	14 Hz

A variety of donor-stabilized cationic Ti-phosphinimide complexes of the type $[\text{Cp}(\text{NP}^t\text{Bu}_3)\text{TiMe}(\text{L})][\text{RB}(\text{C}_6\text{F}_5)_3]$ (R = Me, C₆F₅; L = Py, 4-EtPy, NC₅H₄NMe₂, PMe₃, PⁿBu₃, PPh₃, P(*p*-MeC₆H₄)₃) have been previously reported⁷⁵. However, complexes **2.15-2.22** represent the first example of cationic titanium-phosphinimide complexes which do not require the introduction of an external donor (L) to induce stability.

VT NMR experiments were conducted to investigate both the thermal stability and coordinative strength of the donor atoms to titanium. Data was collected in 5 °C increments from -30 °C to 60 °C. It is important to note that in all cases (**2.15-2.22**),

increasing the temperature did not cause dissociation of the pendant donor from the electron poor metal centre on the NMR timescale. This conclusion was drawn based on the observation that the methylene protons *alpha* to X (X= O, S) remained inequivalent up to the 60 °C temperature limit. Displacement of the pendant ether or thioether moiety was not observed on the NMR timescale at elevated temperatures, presumably due to the electrophilicity of the metal centre.

In the case of the pendant ether complexes (**2.15**, **2.16**, **2.19**, **2.20**), no change in the ¹H NMR spectra was observed over the entire temperature range. However, the pendant thioether complexes exhibited temperature-dependent second order coupling of the benzylic methylene proton resonances for the systems bearing the less bulky Cp ancillary ligand (**2.17**, **2.21**). No changes were observed in the ¹H NMR spectra over the entire temperature range for the thioether complexes bearing the bulkier Cp* ancillary ligand (**2.18**, **2.22**). As shown in **Figure 2.11**, at elevated temperatures one set of doublets shifts downfield until at approximately 303 K, the chemical shifts become so similar that they overlap. It is thought that the second order nature of the benzylic resonances and the observed chemical shift temperature dependence is an interesting artifact but that the complexes persists as a donor stabilized cation in solution.

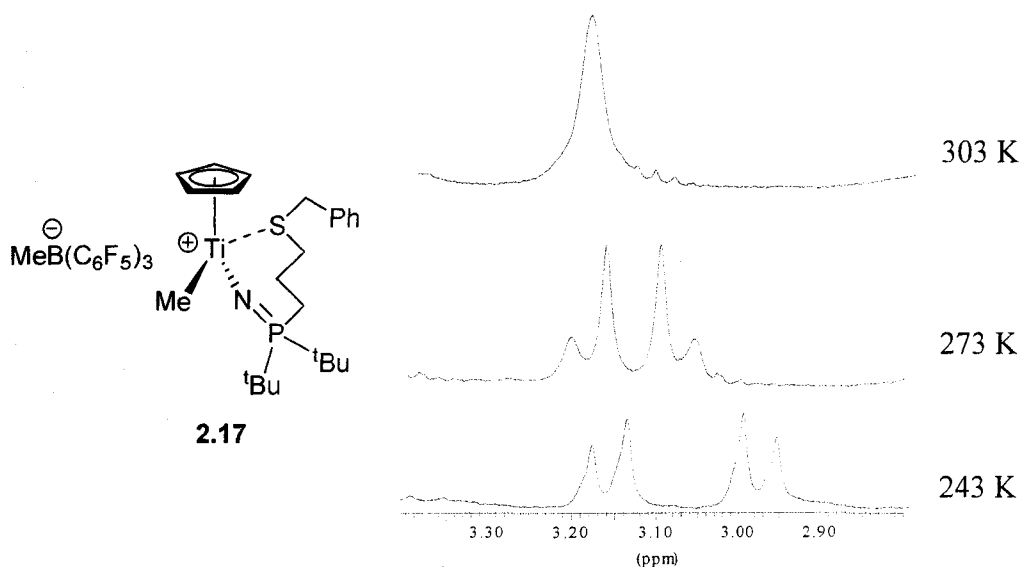


Figure 2.11 Portion of the VT ^1H NMR showing the temperature-dependent second order coupling of the benzylic methylene proton resonances for complex **2.17**

2.3 Conclusions

New phosphinimine ligands featuring a pendant ether or thioether moiety have been prepared. Substitution onto a titanium centre was achieved in good to high yields via Me_3SiCl elimination. Solid-state structures of some of these complexes show a near linear Ti-N-P bond angle and multiple bond-like Ti-N distances. Dialkyl derivatives of these complexes were readily prepared in moderate to good yields. The presence of the pendant ether or thioether ‘arm’ is of considerable interest as a potential hemilabile system that could catalyze the polymerization or oligomerization of ethylene. These complexes are of particular interest due to the presence of a hard (oxygen) or soft (sulfur) heteroatom donor that could potentially provide stable cationic species upon alkyl abstraction with a Lewis acid.

Stable ion pairs in solution have been prepared using dialkyl titanium catalyst precursors **2.11-2.14** and the appropriate activator. Activated complexes **2.15-2.22** represent the first example of cationic titanium-phosphinimide complexes which do not require the introduction of an external donor (L) to induce stability. These systems are unique in that the donor is intrinsically built into the phosphinimide ligand fragment.

In all cases, the pendant ether or thioether coordination to titanium persisted in the absence of other donors even at elevated temperatures. This is due to the very electron-poor titanium centre. However, temperature-dependent second order coupling was observed for complexes **2.17** and **2.21**.

It is important to note that the intramolecular interaction can be disrupted by the introduction of an external base, such as THF, showing that the Ti-O or -S interaction is labile in the presence of donors, which bodes well for reactivity with olefins. The contrast between using either a hard (oxygen) or soft (sulfur) donor to stabilize the cationic Ti-phosphinimide species should provide unique reactivity in the presence of ethylene. Polymerization studies are discussed in the next chapter.

Chapter 3

Reactivity of Hemilabile Phosphinimide Titanium Complexes in the Presence of Ethylene

3.1 Introduction

The previous section discussed the design of hemilabile phosphinimide ligands and their incorporation into Ti(IV) complexes. Furthermore, the reactivity of these complexes with the discrete activators $B(C_6F_5)_3$ and $[Ph_3C]^+[B(C_6F_5)_4]^-$ gave heightened stability of cationic titanium-phosphinimides in solution without the addition of an external base. Stability of these complexes was shown to be due to the coordination of a hard (oxygen) or soft (sulfur) donor in the pendant ligand. It has been established that early transition metal phosphinimide systems catalytically polymerize olefins.³² Incorporation of a pendant donor should impart unique reactivity for these new titanium-phosphinimide systems. This chapter describes the polymerization testing methods and reactivity of hemilabile titanium-phosphinimide complexes in the presence of ethylene.

3.2 Polymerization Mechanism Involving Group IV Metals

Homogeneous α -olefin polymerization catalyzed by Group IV catalysts entails activation, propagation, and chain termination.⁷⁶ Activation of catalyst precursors with a Lewis acid has been discussed in the previous chapter. The catalytically active species is a coordinatively unsaturated cationic alkyl complex. Once the active catalyst has been generated in solution, the first step of the propagation cycle is the binding of the olefin to the vacant coordination site at the metal.^{77,78} Unlike d^8 Ni(II) and Pd(II) catalysts, Ti(IV)

and Zr(IV) catalysts have d^0 metal centers and thus sigma donation from the olefin to the empty metal orbital occurs but the metal cannot participate in back-bonding. Therefore, the bonding between the olefin and a Group IV d^0 metal must consist entirely of electrostatics, van der Waals interactions, and charge transfer.⁷⁶ The dominant interaction is charge transfer from the olefin to the metal. The next step in the propagation cycle is the insertion of the olefin into a metal-carbon bond. The metal-carbon σ -bond pair interacts with the carbon-carbon π -bond pair of the olefin. This propagation mechanism, as proposed by Cossee and Arlman^{77,78}, is shown in **Figure 3.1**.

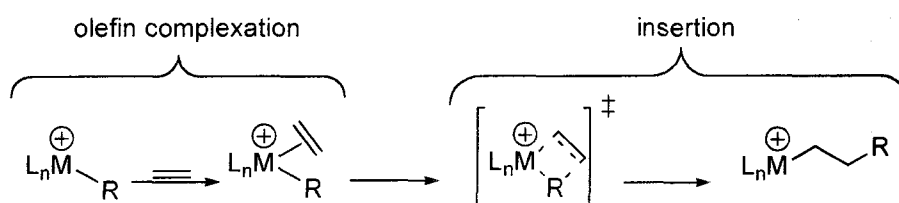


Figure 3.1 Cossee-Arlman mechanism

The influence of the counteranion in the propagation mechanism has been shown to be significant through experimental^{7,66} and theoretical^{40,79,80} studies. For example, when the insertion of ethylene into $[Cp_2ZrEt]^+[MeB(C_6F_5)]^-$ was modeled using computational methods, the authors reported that the most favorable approach of the olefin to the metal centre was from the opposite side of where the anion was coordinated.⁸⁰ This in turn causes a concomitant increase of the zirconium-methyl distance. Consideration of the anion into the Cossee-Arlman mechanism is shown in **Figure 3.2**.

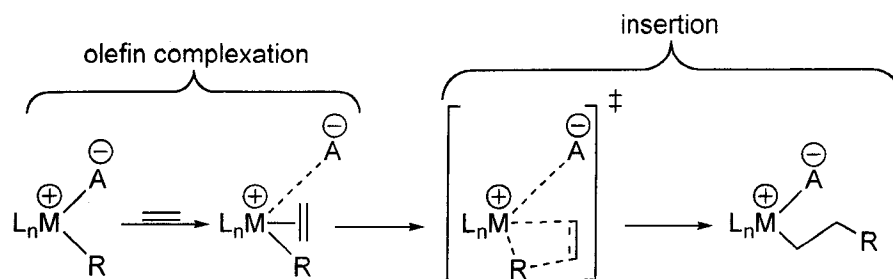


Figure 3.2 Modified Cossee-Arman mechanism with counterion considerations

Chain termination may occur through β -hydride elimination (**Figure 3.3 (a)**), β -hydride transfer to monomer (**Figure 3.3 (b)**), chain transfer to the counterion (**Figure 3.3 (c)**), or by irreversible deactivation of the catalyst.⁷⁶

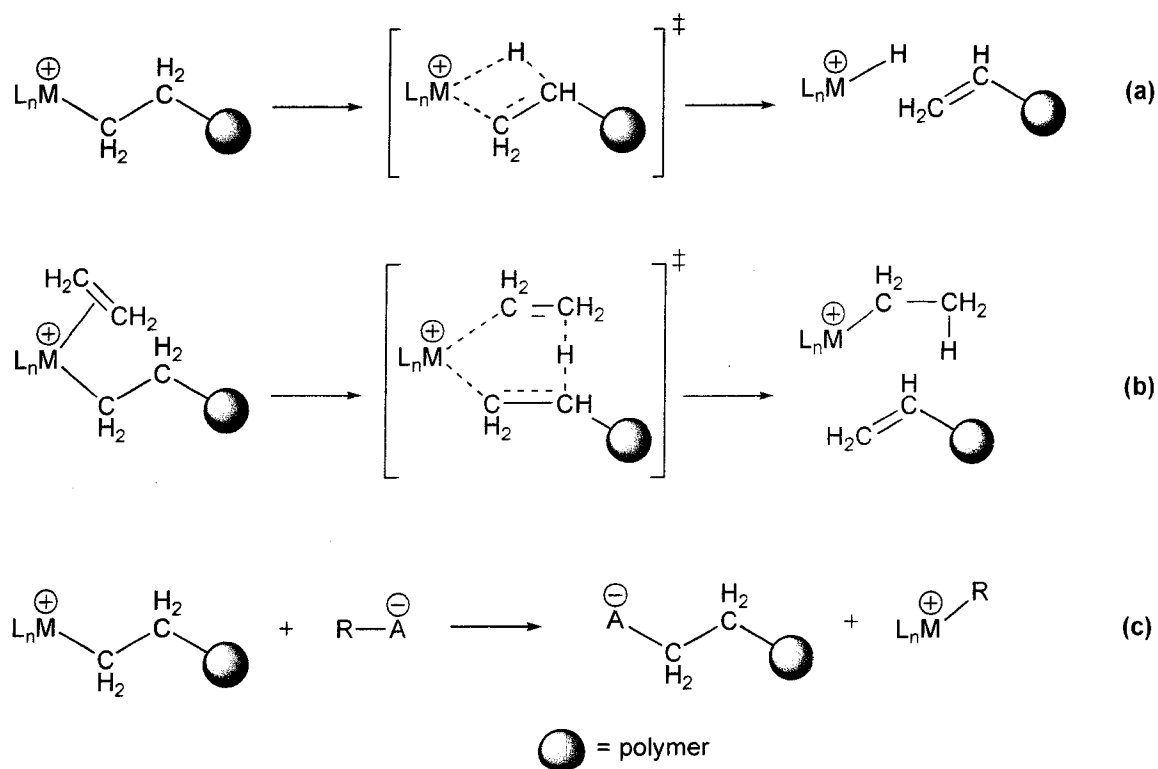


Figure 3.3 Common chain termination pathways

3.3 General Considerations

Catalyst activity, molecular weight distribution of the polymer, thermal stability and patent position are the four main criteria that must be considered in the design of new catalysts for olefin polymerization. In terms of catalyst performance, the amount of polymer production and the molecular weight distributions are the important factors. Catalyst activity is used to evaluate the amount of polymer produced over a period of time (**Equation 3.1**). Literature convention is to describe activity of a catalyst in the units $\text{g mmol}^{-1} \text{h}^{-1} \text{bar}^{-1}$ or $\text{g mmol}^{-1} \text{h}^{-1} \text{atm}^{-1}$.

$$\text{Activity} = \frac{\text{polymer mass (g)}}{\text{amount of catalyst (mmol)} \times \text{time (h)} \times \text{pressure (atm or bar)}} \quad (3.1)$$

Experimentally determined activities are heavily influenced by the polymerization testing conditions and reactor setup. Often, little or no information is often provided about catalyst lifetimes in the literature, and consequently activities for the same catalyst can vary widely when reported by different research groups.⁸¹ For example, a short polymerization run for a catalyst that is only active for 30 seconds will have an inflated activity compared to the same run over a one hour period. To aid in the comparison of catalyst activities to other systems, Gibson and coworkers designed a scale of merit ranging from very low to very high, as shown in **Table 3.1**.⁸¹

Table 3.1 Rating of the effectiveness of a catalyst based on its activity^a

Rating	Activity [g mmol ⁻¹ h ⁻¹ bar ⁻¹]
Very low	< 1
Low	1 – 10
Moderate	10 – 100
High	100 – 1000
Very high	> 1000

^a Data borrowed from Gibson and coworkers – see Reference 81

Information on the molecular weight distribution of polymer samples is commonly determined via gel permeation chromatography (GPC). This technique is able to provide molecular-weight averages that are important in determining polymer properties: the number average \overline{M}_n (Equation 3.2), the weight average \overline{M}_w (Equation 3.3), and the polydispersity index (PDI) of the polymer (Equation 3.4).¹

$$\overline{M}_n = \frac{\sum_{i=1}^N N_i M_i}{\sum_{i=1}^N N_i} \quad (3.2) \quad \overline{M}_w = \frac{\sum_{i=1}^N N_i M_i^2}{\sum_{i=1}^N N_i M_i} \quad (3.3) \quad PDI = \frac{\overline{M}_w}{\overline{M}_n} \quad (3.4)$$

N_i is the total number of molecules with a molecular weight of M_i .

Thermal stability of the catalyst during polymerization is of critical importance since commercial olefin polymerization is typically performed in the temperature range of 70 – 160 °C.³² High temperatures are required to keep the polymer in solution in order to maintain a constant monomer flow and prevent reactor fouling. Pre-catalysts with

strong metal-ligand bonds afford more resistance to thermal degradation. The incorporation of hemilabile ligands into transition metal pre-catalysts can provide an additional facet of stability. Previous attempts to 'trap' cationic titanium phosphinimide complexes have only been successful with the introduction of an external base such as THF.⁷⁵ Presumably, during polymerization the ethylene monomer acts to stabilize the metal centre. The incorporation of a pendant donor in the ligand framework can stabilize the highly reactive metal centre, excluding the need for an external reagent. This additional stability from the pendant ether or thioether should in theory protect the metal centre and provide improved stability under thermal duress. Of course, temperature stability cannot be properly investigated without testing catalysts for polymerization at elevated temperatures. The aim of titanium systems with a hemilabile ligand is to establish thermal stability well beyond that of conventional catalysts.

A final aspect to consider is that the ever-growing sphere of patents that cover olefin polymerization catalysts is a serious limitation. A new pre-catalyst is not commercially attractive unless it falls outside the current patents for olefin polymerization. With this in mind, the phosphinimide ligands discussed in **Chapter 2** are unique in that a pendant heteroatom donor has been built into the ligand framework. The resulting titanium complexes **2.7-2.14** are the first examples of transition metal complexes incorporating a hemilabile phosphinimide ligand where the pendant moiety is an ether or thioether group. Efforts to design commercially viable highly active, thermally stable olefin polymerization or oligomerization catalysts are fruitless if patent position is not carefully considered.

3.4 Polymerization Protocol

Thorough reactor cleaning is essential to ensure no moisture or other contaminants are present in the reactor vessel.⁸² Prior to reactor assembly, any residual polymer was removed and the vessel was washed with toluene and acetone. Following assembly, the reactor vessel and solvent storage unit were refilled with nitrogen with 4 refill/evacuation cycles over at least 90 minutes.

Approximately 600 mL of toluene was transferred to the solvent storage container from a purification column. The solvent was purged with dry nitrogen for 20 minutes and then transferred to the reactor vessel by differential pressure. The solvent was stirred at 1500 ± 10 RPM and the temperature was kept constant at 30 ± 2 °C. The system was then exposed to ethylene via five vent/refill cycles. Once the ethylene flow meter read 0.000, the reactor was ready for injection of the $\text{Al}(\text{}^i\text{Bu})_3$ (TiBAI), a solvent scrubber that removes the final traces of water (if applicable), pre-catalyst, and co-catalyst.

Once the reactor had been readied for injection, the pre-catalyst, co-catalyst and solvent scrubber stock solutions were prepared in an inert atmosphere glovebox. The stock solutions were loaded into syringes and transferred to the reactor for injection immediately to avoid contamination or sample decomposition. TiBAI scrubber was used as a solvent scrubber only for polymerizations using either $\text{B}(\text{C}_6\text{F}_5)_3$ or $[\text{Ph}_3\text{C}]^+[\text{B}(\text{C}_6\text{F}_5)_4]^-$ as the co-catalyst. When testing the dichloride precursors, MAO served as both the activator and solvent scrubber. The following is an example of a polymerization experiment using $\text{CpTi}(\text{NP}^i\text{Bu}_3)\text{Me}_2$ as the catalyst, $\text{B}(\text{C}_6\text{F}_5)_3$ as the co-catalyst, and TiBAI as the solvent scrubber.

Pre-Catalyst Stock Solution: $\text{CpTi}(\text{NP}^t\text{Bu}_3)\text{Me}_2$ (11 mg, 0.031 mmol) was weighed into a vial. Toluene (5.00 mL) was added to dissolve the catalyst (6.12 mmol $\text{CpTi}(\text{NP}^t\text{Bu}_3)\text{Me}_2$ /L). 1.0 mL of the solution (0.0060 mmol $\text{CpTi}(\text{NP}^t\text{Bu}_3)\text{Me}_2$) was transferred into a syringe for injection into the reactor.

Co-Catalyst Stock Solution: $\text{B}(\text{C}_6\text{F}_5)_3$ (17 mg, 0.035 mmol) was weighed into a vial. Toluene (9.00 mL) was added to dissolve the co-catalyst (3.91 mmol $\text{B}(\text{C}_6\text{F}_5)_3$ /L). 1.5 mL of the solution (0.0060 mmol) was transferred into a syringe for injection into the reactor.

Solvent Scrubber Stock Solution: 0.66 mL of a 25.2 weight % solution of TiBAI in heptanes (density = 0.710 g/mL, 0.595 mmol TiBAI) was diluted with toluene (14.33 mL) to give a clear, colorless solution (41.5 mmol TiBAI /L). 3.0 mL of the solution (0.120 mmol, 20.0 equivalents) was transferred into a syringe for injection into the reactor.

Injection Sequence: The 3.0 mL of TiBAI solution (0.125 mmol, 20.8 equivalents) was injected into the reactor via the catalyst injection inlet. The solvent scrubber was allowed to stir for 5 minutes. Next, the 1.0 mL pre-catalyst solution of $\text{CpTi}(\text{NP}^t\text{Bu}_3)\text{Me}_2$ (0.0060 mmol) was injected. Immediately afterwards, the 1.5 mL solution of $\text{B}(\text{C}_6\text{F}_5)_3$ (0.0060 mmol) was injected. When testing the dichloride precursors, MAO was injected and the solution was allowed to stir for 5 minutes. The dichloride pre-catalyst was then injected.

Polymerization and Polymer Collection: The reactor was allowed to stir (1500 ± 10 RPM) for 5 minutes at 30 ± 2 °C at 2 atm of ethylene. Following the 5 minute reaction time, the polymerization was halted by closing off the ethylene inlet valve and venting

the reactor. Stirring was stopped and the reactor was disassembled. The reactor contents were then transferred to a 4 L beaker containing approximately 100 mL of 10% HCl (v/v) in MeOH to help precipitate any polymer remaining in solution. The polymer was then collected via filtration, washed with toluene, and dried overnight. The following day, the polymer was weighed and the catalyst activity was calculated using **Equation 3.1**.

3.5 Results and Discussion

The variability of reported activities in the literature poses a significant challenge to researchers to directly compare results. The sensitivity of the catalyst activity depends primarily on reactor size, choice of solvent, choice of co-catalyst and scavengers, quality of stirring, the order of addition, temperature, pressure, and time.¹⁶ Researchers typically employ either Schlenk line techniques or a polymerization reactor to evaluate the performance of olefin polymerization catalysts. Using the Büchi polymerization reactor in this study holds several advantages including better control over reaction conditions such as temperature, stirring rate and ethylene pressure. Certain variables were kept constant to ensure reproducibility during the polymerization reactions, which are summarized in **Table 3.2**.

Table 3.2 Polymerization Conditions

Temperature^a	30 °C
Ethylene Pressure	2 atm
Stirring rate	1500 rpm
Amount of co-catalyst^a	0.0060 mmol
Catalyst concentration^a	10 μmol/L
Solvent	Toluene
Solvent Volume	600 mL
Equivalents of TiBAI	20

^aAmount of co-catalyst and [catalyst] were halved when performing high temperature runs (60 °C)

Using a standard was important to gain a relative measure of the activity of the new catalysts. The highly active titanium-phosphinimide catalyst $\text{CpTi}(\text{NP}^t\text{Bu}_3)\text{Cl}_2$ was used as a standard when evaluating the dihalide pre-catalysts **2.7-210**. Similarly, $\text{CpTi}(\text{NP}^t\text{Bu}_3)\text{Me}_2$ was the standard when evaluating the dialkyl analogues **2.11-2.14**. Reasons behind the choice of the standard were twofold. Although metallocenes are commonly used for comparison for new Group IV transition metal catalysts, the tri-*tert*-butylphosphinimide complexes have comparable activity to Cp_2ZrCl_2 and CGC catalysts, and significantly higher activity in comparison to Cp_2TiCl_2 or CpTiCl_3 .³⁹ Secondly, the catalysts **2.7-2.14** (**Figure 3.4**) are structurally similar to the parent tri-*tert*-butylphosphinimide complexes, which make them a better benchmark for comparison in this study.

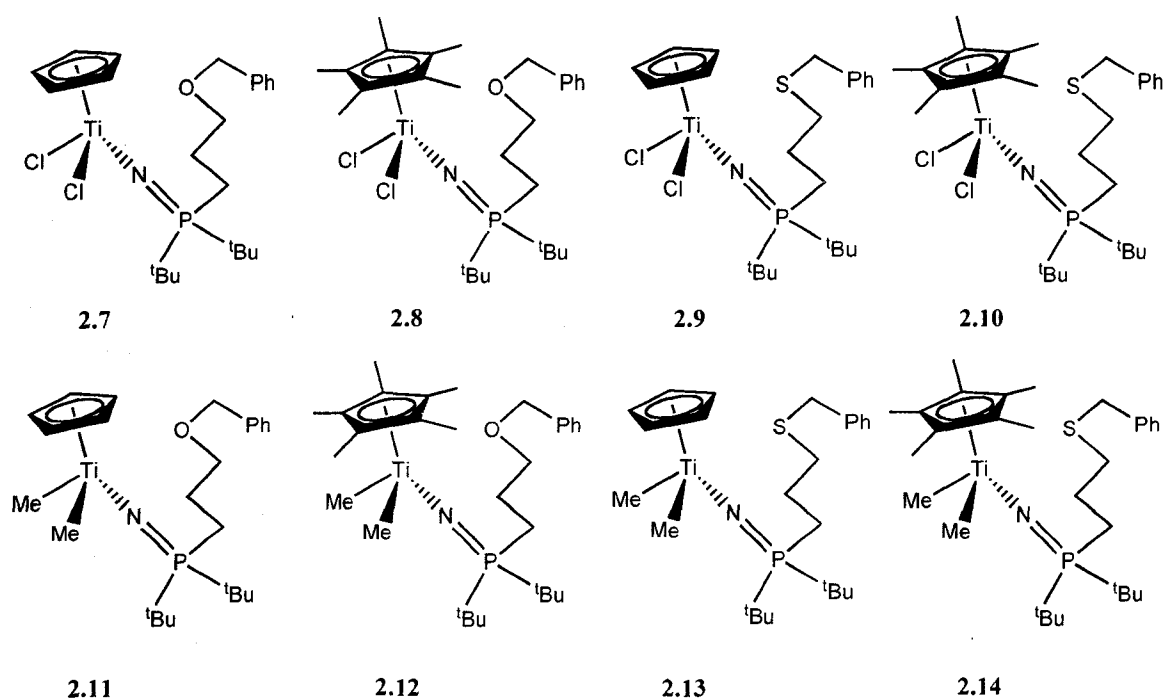


Figure 3.4 Catalysts tested for polymerization

The activities of pre-catalysts **2.7-2.15** were determined using three activation strategies. Dihalide precursors **2.7-2.10** were tested using MAO as the co-catalyst (Section 3.5.1). Dialkyl precursors **2.11-2.15** were tested with the activators $B(C_6F_5)_3$ (Section 3.5.2) and $[Ph_3C]^+[B(C_6F_5)_4]^-$ (Section 3.5.3). Polymerization testing was also done at 60 °C with 2 equivalents of $[Ph_3C]^+[B(C_6F_5)_4]^-$, and compared to analogous tests performed at 30 °C (Section 3.5.4). All polymerizations were tested in duplicate to test for reproducibility, and the percent difference was calculated using Equation 3.5:

$$\%Difference = \left(\frac{|Activity_{Trial\#1} - Activity_{Trial\#2}|}{Average\ Activity} \right) \times 100\% \quad (3.5)$$

3.5.1 Polymerizations with MAO as the Co-Catalyst

Polymerization tests using the Büchi polymerization reactor were first performed with 500 equivalents of MAO as the activator. Catalyst concentrations were kept constant at 10 $\mu\text{mol/L}$. Please refer to **Table 3.2** for the remaining polymerization conditions. The results of these polymerization tests are summarized in **Table 3.3**.

Table 3.3 Polymerization results with MAO as co-catalyst

Pre-Catalyst	Activity (Trial 1) (g mmol ⁻¹ h ⁻¹ atm ⁻¹)	Activity (Trial 2) (g mmol ⁻¹ h ⁻¹ atm ⁻¹)	Average Activity (g mmol ⁻¹ h ⁻¹ atm ⁻¹)	% Difference
CpTiCl ₂ [NP(^t Bu) ₃]	21915	20349	21132	7
2.7	465	336	401	32
2.8	896	621	759	36
2.9	127	83	105	42
2.10	169	162	166	4

The activity of the standard CpTi(NP^tBu₃)Cl₂ and excess MAO was found to be very high, whereas only moderate activities were found for complexes **2.7-2.10**. Stephan and coworkers reported that the pre-catalyst TiCl₂[NP(^tBu)₃]₂ had limited activity in combination with MAO, whereas activation of TiMe₂[NP(^tBu)₃]₂ with B(C₆F₅)₃ or [Ph₃C]⁺[B(C₆F₅)₄]⁻ led to much higher activities.³⁵ Reaction with excess AlMe₃ and TiMe₂[NP(^tBu)₃]₂ gave divergent decomposition pathways consisting of phosphinimide abstraction and C-H bond activation (**Figure 3.5**). This suggests that the aluminum centre can interact with the titanium-bound nitrogen atoms or the aluminum-bound methyl groups can interact with the titanium centre.

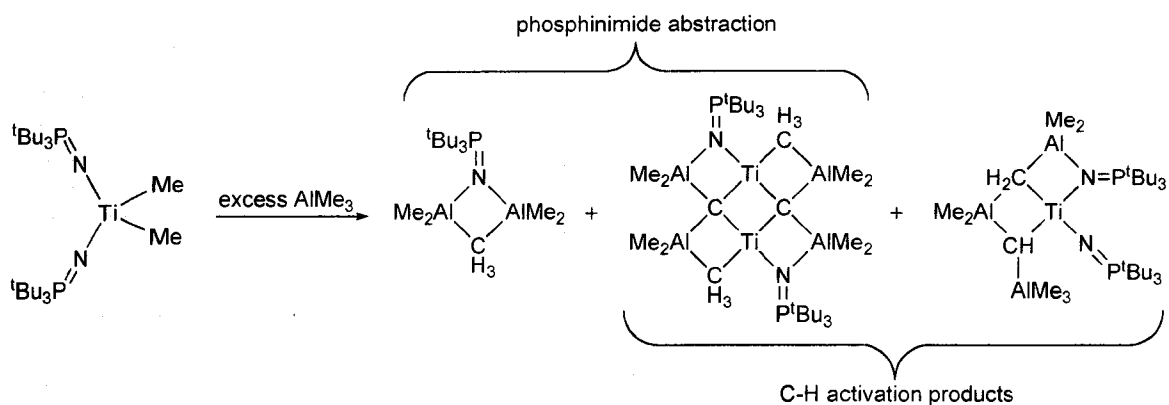
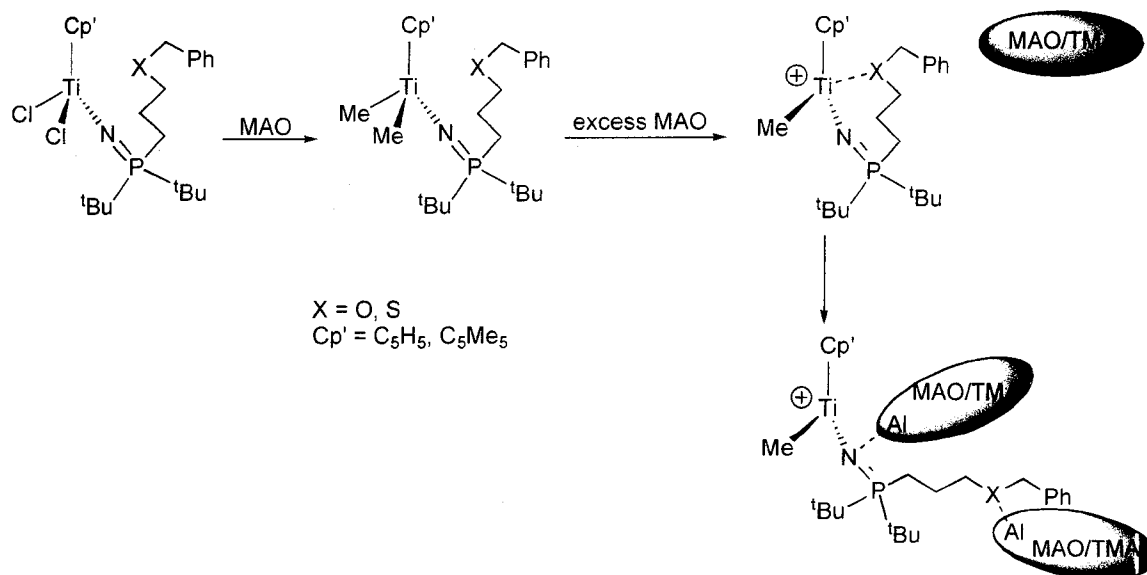


Figure 3.5 Decomposition pathways in the reaction of AlMe_3 and $\text{TiMe}_2[\text{NP}(\text{tBu})_2]_2$

One possible explanation for the lower activities seen with complexes **2.7-2.10** may be that Lewis acid-base interactions are also taking place between the aluminum centers of MAO and the pendant heteroatom donor (**Scheme 3.1**). Interaction between oxygen or sulfur with residual AlMe_3 or the Lewis acidic sites in MAO could potentially draw the pendant arm away from the electron-poor titanium centre, making the titanium-bound nitrogen more accessible for attack by the aluminum centers in MAO.



Scheme 3.1 Possible interaction between aluminum centers and the pendant donor

Although this explanation currently remains speculative, Do and coworkers have recently reported similar interactions between the amine nitrogen of the unbridged zirconocene [1-(*p*-Me₂NC₆H₄)-3,4-Me₂C₂H₂]₂ZrCl₂ and the aluminum centers in MAO.⁸³ In this system, the authors propose that aluminum-nitrogen interactions prevent the amine-functionalized ligands from freely rotating. This observation lends credence to the possibility of Lewis acid-base interactions between aluminum and a heteroatom donor with a free lone-pair, disrupting the titanium-heteroatom interaction. This would in turn lead to nitrogen-aluminum interactions, causing ligand degradation.

In comparing complexes **2.7-2.10**, the oxygen derivatives showed better activity. The distance between sulfur and the cationic titanium centre is expected to be greater when compared to oxygen. Hence it may be easier for the aluminum centre of MAO to destabilize the sulfur derivatives. The percent differences for the polymerizations were not particularly low, but were still under 50%. This speaks to the difficulty with percentage errors for systems with low activities; reported activities with MAO in the literature have been known to vary widely.⁷

3.5.2 Polymerizations with B(C₆F₅)₃ as the Co-Catalyst

The dialkyl titanium phosphinimides **2.11-2.14** were tested for ethylene polymerization with B(C₆F₅)₃ as the co-catalyst. Both 1 and 2 equivalents of the activator were used to determine if increasing the concentration increased the activity of the catalyst. Please refer to **Table 3.2** for the polymerization conditions. The results of polymerization screenings with B(C₆F₅)₃ are tabulated in **Table 3.4**.

Table 3.4 Polymerization results with B(C₆F₅)₃ as co-catalyst

Pre-Catalyst	Activity (Trial 1) (g mmol ⁻¹ h ⁻¹ atm ⁻¹)	Activity (Trial 2) (g mmol ⁻¹ h ⁻¹ atm ⁻¹)	Average Activity (g mmol ⁻¹ h ⁻¹ atm ⁻¹)	% Difference
CpTiMe ₂ [NP(^t Bu) ₃] ^a	8937	11313	10125	23
2.11^a	228	357	293	44
2.12^a	793	1422	1108	57
2.13^a	933	813	873	14
2.14^a	1952	1835	1894	6
CpTiMe ₂ [NP(^t Bu) ₃] ^b	6877	7981	7429	15
2.11^b	1438	1560	1499	8
2.12^b	3087	2637	2862	16
2.13^b	1200	1169	1185	3
2.14^b	4284	3900	4092	9

^aOne equivalent of B(C₆F₅)₃; ^b two equivalents of B(C₆F₅)₃

The percent difference for complexes **2.11** and **2.12** were quite high due to polymer swelling in the reactor. If the polymer tends to form near the top of the reactor vessel and becomes swollen with toluene, the ethylene inlet can become partially blocked, which disrupts the flow. The percent difference values for all other tests in this series indicate good to excellent reproducibility.

Polymerization results in **Table 3.4** indicate that the dimethyl precursors (**2.11-2.14**)/B(C₆F₅)₃ are much more active than the dichloride precursors (**2.7-2.10**)/MAO. Complexes **2.12** and **2.14**, which feature the bulkier Cp* ancillary ligand, have higher activities than the Cp complexes **2.11** and **2.13**, respectively. A similar trend was seen with the related pre-catalyst Cp'Ti(NPR₃)Me₂ (Cp' = C₅H₅, ^tBuC₅H₄; R = Cy, ⁱPr, ^tBu),

which showed a dramatic increase in polymerization activity with additional steric bulk on the cyclopentadienyl ligand.³⁹

Furthermore, the pre-catalysts **2.11-2.14** showed a significant increase in activity when two equivalents of the co-catalyst were used. Increasing the concentration of the active species may in turn increase the concentration of the catalytically active species. When one equivalent of $B(C_6F_5)_3$ is used, there may be competition for interaction with the Lewis acidic boron centre between the methyl group and the pendant sulfur or oxygen heteroatom. Interactions between $B(C_6F_5)_3$ and the pendant donor would reduce the concentration of the active cationic titanium complex for polymerization.

Interestingly, the standard $CpTiMe_2[NP(^tBu)_3]$ significantly dropped in activity by 26% when two equivalents of the activator was used, lying in stark contrast to the pendant donor systems. One possible explanation could be the formation of the dication $[(Cp)(^tBu_3NP)Ti(\mu-MeB(C_6F_5)_3)_2]^{2+}$ due to abstraction of both of the titanium-methyl groups (**Figure 3.6**). Guerin and coworkers⁶³ reported that the bisphosphinimide system $(^tBu_3NP)_2TiMe_2$ afforded similar reactivity with two equivalents of $B(C_6F_5)_3$ to give the dication $[(^tBu_3NP)_2Ti((\mu-MeB(C_6F_5)_3)_2)]^{2+}$. Similar attempts to affect double alkyl abstraction using $[Ph_3C]^+[B(C_6F_5)_4]^-$ led to decomposition. The possible partial formation of a dication $[(Cp)(^tBu_3NP)Ti(\mu-MeB(C_6F_5)_3)_2]^{2+}$, which would be an ineffective catalyst, would lower the activity as shown in **Table 3.4**.

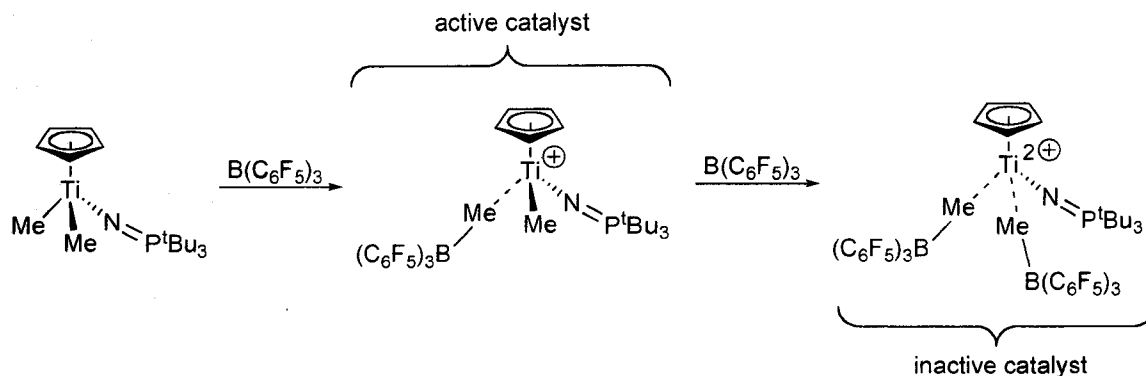


Figure 3.6 Suggested formation of the dication $[(\text{Cp})(^t\text{Bu}_3\text{NP})\text{Ti}(\mu\text{-MeB}(\text{C}_6\text{F}_5)_3)_2]^{2+}$

Thioether complex **2.14** showed the highest activity whether one or two equivalents of $\text{B}(\text{C}_6\text{F}_5)_3$ were used. The very high activity of **2.14** approaches 55% of the activity of the standard $\text{CpTiMe}_2[\text{NP}(^t\text{Bu})_3]$ when two equivalents of co-catalyst were used. The results indicate that the introduction of a soft donor gives markedly improved activities for α -olefin polymerization. Although this seemed surprising, there is literature precedent for this type of trend.^{84,85} For example, Gibson and coworkers⁸⁴ prepared a series of titanium complexes featuring tridentate ligands with pendant hard (O) or soft (S, P) donors (**Figure 3.7**).

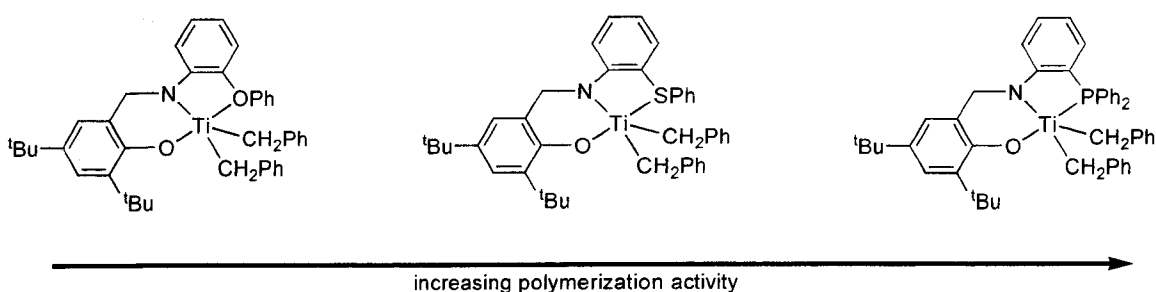


Figure 3.7 Order of polymerization activity of titanium complexes with a pendant hard or soft ligand

In the Gibson systems, the sulfur derivatives had a much higher activity (3530 g mmol⁻¹ hr⁻¹ bar⁻¹) than the analogous oxygen derivatives (88 g mmol⁻¹ hr⁻¹ bar⁻¹) upon activation with 2000 equivalents of MAO. The pendant phosphine pre-catalysts displayed the highest activity (19 500 g mmol⁻¹ h⁻¹ bar⁻¹). Although the titanium complexes shown in **Figure 3.7** are not structurally related to complexes **2.11-2.14**, this is an example of improved catalyst activity upon introduction of a pendant soft donor into the ligand framework.

3.5.3 Polymerizations with [Ph₃C]⁺[B(C₆F₅)₄]⁻ as the Co-Catalyst

The dialkyl pre-catalysts **2.11-2.14** were tested for polymerization activity with one and two equivalents of [Ph₃C]⁺[B(C₆F₅)₄]⁻ as the co-catalyst. Polymerization conditions can be found in **Table 3.2**. The polymerization screening results of these pre-catalysts are shown in **Table 3.5**.

Table 3.5 Polymerization results with $[\text{Ph}_3\text{C}]^+[\text{B}(\text{C}_6\text{F}_5)_4]^-$ as co-catalyst

Pre-Catalyst	Activity (Trial 1) (g mmol ⁻¹ h ⁻¹ atm ⁻¹)	Activity (Trial 2) (g mmol ⁻¹ h ⁻¹ atm ⁻¹)	Average Activity (g mmol ⁻¹ h ⁻¹ atm ⁻¹)	% Difference
$\text{CpTiMe}_2[\text{NP}(\text{tBu})_3]^a$	8329	8255	8292	1
2.11^a	43	40	42	7
2.12^a	2635	2094	2365	23
2.13^a	1914	1638	1776	16
2.14^a	4931	4761	4846	4
$\text{CpTiMe}_2[\text{NP}(\text{tBu})_3]^b$	9419	7457	8438	23
2.11^b	1814	1717	1766	5
2.12^b	3332	2675	3004	22
2.13^b	2495	2656	2575	6
2.14^b	4721	4903	4812	4

^a1 equivalent of $[\text{Ph}_3\text{C}]^+[\text{B}(\text{C}_6\text{F}_5)_4]^-$; ^b2 equivalents of $[\text{Ph}_3\text{C}]^+[\text{B}(\text{C}_6\text{F}_5)_4]^-$

The percent differences for the polymerization tests show much better reproducibility than the polymerization tests using MAO as the activator. Trends noted with the use of $\text{B}(\text{C}_6\text{F}_5)_3$ as the activator were also observed upon activation with $[\text{Ph}_3\text{C}]^+[\text{B}(\text{C}_6\text{F}_5)_4]^-$. For example, complex **2.14** was again found to have the highest activity, approaching 60% of the activity of $\text{CpTiMe}_2[\text{NP}(\text{tBu})_3]$. Additionally, the pendant thioether complexes had markedly better activities than the analogous pendant ether systems. Furthermore, increased steric bulk on the ancillary Cp ligand resulted in higher activities when comparing either the sulfur or oxygen complexes. Increasing the amount of co-catalyst to two equivalents resulted in improved activities for **2.11-2.13**. The activity of **2.14** was not significantly altered. Doubling the amount of co-catalyst may maximize the number of catalytically active species in solution.

Overall, pre-catalysts **2.11-2.14** were much more active upon activation with $[\text{Ph}_3\text{C}]^+[\text{B}(\text{C}_6\text{F}_5)_4]^-$ when compared to $\text{B}(\text{C}_6\text{F}_5)_3$ and MAO. Catalytic activity depending on the counterion employed was found to be $[\text{B}(\text{C}_6\text{F}_5)_4]^- > [\text{MeB}(\text{C}_6\text{F}_5)_3]^- > [\text{MeMAO}]^-$. This was not surprising since catalytic activities are highly dependent on the type of anion used and tend to increase as the anion becomes less coordinating.⁸ Theoretical studies with the aforementioned anions have shown that $[\text{B}(\text{C}_6\text{F}_5)_4]^-$ has the weakest interaction with $[\text{CpTi}(\text{NPM}_3)\text{Me}]^+$.⁴⁰ Stephan and coworkers³² have found dramatically improved activities when using $[\text{Ph}_3\text{C}]^+[\text{B}(\text{C}_6\text{F}_5)_4]^-$ to activate $\text{CpTi}(\text{NP}^t\text{Bu}_3)\text{Me}_2$. Thus, the initial polymerization screening results (**Tables 3.3-3.5**) fall in line with previous experimental and theoretical findings.

3.5.4 Polymerization Testing at Elevated Temperatures

To investigate the thermal stability of compounds **2.11-2.14**, polymerizations were performed at 60 °C. Two equivalents of $[\text{Ph}_3\text{C}]^+[\text{B}(\text{C}_6\text{F}_5)_4]^-$ were employed, as these conditions merited the highest activities at 30 °C. All other polymerization testing conditions can be found in **Table 3.2**. A comparison of catalyst activities at 30 °C and 60 °C are summarized in **Table 3.6**.

Table 3.6 Effect of temperature on catalyst activities

Pre-Catalyst	Activity (Trial 1)	Activity (Trial 2)	Average Activity	%
	(g mmol ⁻¹ h ⁻¹ atm ⁻¹)	(g mmol ⁻¹ h ⁻¹ atm ⁻¹)	(g mmol ⁻¹ h ⁻¹ atm ⁻¹)	Difference
CpTiMe ₂ [NP(^t Bu) ₃] ^a	8329	8255	8292	1
2.11 ^a	43	40	42	7
2.12 ^a	2635	2094	2365	23
2.13 ^a	1914	1638	1776	16
2.14 ^a	4931	4761	4846	4
CpTiMe ₂ [NP(^t Bu) ₃] ^b	12160	11388	11774	7
2.11 ^b	4766	5768	5267	19
2.12 ^b	5758	6030	5894	5
2.13 ^b	5462	6642	6052	19
2.14 ^b	7414	8046	7730	8

^aT = 30 °C; ^bT = 60 °C

The activities of complexes **2.11-2.14** increased dramatically at elevated temperatures. The standard CpTiMe₂[NP(^tBu)₃] also had an improved activity at 60 °C, however the increase in activity was more pronounced for species **2.11-2.14**. Complex **2.14**, which had the highest activity (7730 g mmol⁻¹ h⁻¹ atm⁻¹) was approximately 65% as active as CpTiMe₂[NP(^tBu)₃] (11774 g mmol⁻¹ h⁻¹ atm⁻¹). Although the results in **Table 3.6** are only preliminary, the markedly improved activities at elevated temperatures of these titanium-phosphinimide pendant ether and thioether systems points towards the possibility of commercial applications. The presence of a donor atom in the ligand framework could possibly stabilize the highly reactive cationic metal centre under industrial relevant conditions (70-160 °C).

3.6 Conclusions

New, highly active ethylene polymerization pre-catalysts, which feature a pendant hard or soft donor, have been prepared. A reliable polymerization testing protocol was used through control of variables such as temperature, pressure, stirring rate, solvent volume, reaction time, and concentration of pre-catalysts, co-catalyst, and solvent scrubber. The pre-catalysts were tested with the common activators MAO, $B(C_6F_5)_3$, and $[Ph_3C]^+[B(C_6F_5)_4]^-$. Due to lack of specialized equipment, analysis of the molecular weights of the polymer could not be obtained. As of this writing, polymer samples are being analyzed by Nova Chemicals Corp. However, the impact of these hemilabile systems on the molecular weight of the resulting polymers will be of particular interest. Aliquots of the reactor solution following each polymerization were taken and analyzed using gas chromatography (GC) analysis, which showed no evidence of lower oligomers in all polymerization trials.

The dichloride precursors **2.07-2.10** displayed moderate to good activity upon activation with MAO. Interaction between hard aluminum centers in MAO and the pendant donor may be a source of catalyst poisoning. The dimethyl precursors **2.11-2.14** showed substantially improved activities upon activation with either $B(C_6F_5)_3$ or $[Ph_3C]^+[B(C_6F_5)_4]^-$. With the choice of co-catalyst being a critical factor in terms of catalyst activities⁷, the order of polymerization activity depending on the counterion employed was found to be: $[B(C_6F_5)_4]^- > [MeB(C_6F_5)_3]^- > [MeMAO]^-$.

When comparing the dimethyl titanium systems, two major trends were found. First, added steric bulk on the ancillary cyclopentadienyl ligand resulted in markedly higher polymerization activities. Second, the choice of the pendant donor heteroatom in

the ligand framework was very influential. Remarkably, the choice of a soft thioether donor resulted in dramatically improved activities over the analogous ether systems. Overall, complex **2.14**, featuring both a bulky Cp* ancillary ligand and a pendant thioether donor, had the highest activity in all cases under the conditions employed. Previously synthesized derivatives of the highly active CpTiMe₂[NP(^tBu)₃] pre-catalyst where the groups on phosphorus were altered were orders of magnitude lower than the parent compound. Despite being unable to match the activity of CpTiMe₂[NP(^tBu)₃], the pendant donor systems **2.11-2.14** are the first phosphinimide derivatives to be on the *same* order of magnitude as CpTiMe₂[NP(^tBu)₃].

Complexes **2.11-2.14** were also tested under optimal reaction conditions (two equivalents of [Ph₃]⁺[B(C₆F₅)₄]⁻) at elevated temperatures (60 °C). These initial results were promising, as all pre-catalysts showed markedly improved activity at higher temperature. This leaves open the possibility for commercial applications, as the industrial standard of activity is limited to temperatures between 70 and 160 °C.³² The presence of a pendant heteroatom donor may stabilize the reactive metal centre at elevated temperatures. Indeed, these systems are the first variants of the simple titanium phosphinimide catalysts, CpTiMe₂[NP(^tBu)₃], to show good to excellent activities under laboratory conditions. The potential of the pendant donor derivatives has been demonstrated and evaluation for commercial trial is underway.

Chapter 4

Experimental

4.1 General Considerations

All preparations were performed in a dry, oxygen-free, nitrogen atmosphere employing either standard Schlenk line techniques or an Innovative Technologies glove box. All organic chemicals were purchased and used as received from Aldrich Chemical Co. All metal compounds were used as received from Strem Chemical Co. $B(C_6F_5)_3$ and $[Ph_3C]^+[B(C_6F_5)_4]^-$ was generously donated by Nova Chemical Corp. Hyflo Super Cel (Celite) was purchased from Aldrich Chemical Co. and dried overnight in a vacuum oven prior to use. Benzene, toluene, diethyl ether, hexanes and pentane were obtained directly from an Innovative Technologies solvent purification system. THF was freshly distilled from sodium-benzophenone ketyl. C_6D_5Br , C_6D_6 and C_7D_8 were purchased from Cambridge Isotopes Laboratories and were freshly distilled from sodium-benzophenone ketyl. 1H , $^{31}P\{^1H\}$ (121 MHz), $^{13}C\{^1H\}$ (75 MHz), $^{11}B\{^1H\}$ (96 MHz), and ^{19}F NMR (282 MHz) spectral data were acquired on Bruker Avance 300 or 500 MHz spectrometers. 1H and $^{13}C\{^1H\}$ NMR spectra were internally referenced to the residual proton or carbon peak of the solvent and chemical shifts are reported relative to $SiMe_4$. $^{31}P\{^1H\}$ spectra were referenced relative to 85% H_3PO_4 as an external standard. $^{11}B\{^1H\}$ and ^{19}F NMR spectra were referenced relative to the external standards $BF_3 \cdot Et_2O$ and 80% CCl_3F in $CDCl_3$, respectively.

4.2 Phosphines

(^tBu)₂P(CH₂)₃OCH₂Ph, 2.1. A solution of Br(CH₂)₃OBn (0.696 g, 3.04 mmol) in 10 mL THF was added dropwise at -35°C to a solution of (^tBu)₂PLi (0.462 g, 3.04 mmol) in 20 mL of THF. Following addition of the bromoether, there was an almost immediate color change from deep yellow to very pale yellow. The solution was stirred and allowed to warm to 25°C. The solvent was removed in vacuo to afford a white and yellow solid (due to LiBr). The yellow residue was redissolved in toluene to precipitate LiBr. The solution was filtered to remove LiBr and the solvent was removed in vacuo to afford a yellow oil. ³¹P{¹H} NMR (C₆D₆, 25 °C, δ): 27.0. ¹H NMR (C₆D₆, 25 °C, δ): 7.28 – 7.07 (C₆H₅); 4.35 (s, 2H, OCH₂); 3.46 (t, 2H, CH₂OCH₂, |*J*_{H-H}| = 6 Hz); 1.85 (m, 2H, CH₂-CH₂-CH₂); 1.42 (m, 2H, P-CH₂); 1.06 (d, 18H, ^tBu). ¹³C{¹H} NMR (C₆D₆, 25 °C, δ): 139.4 – 127.3 (C₆H₅); 73.1 (s, CH₂OCH₂); 71.1 (d, CH₂OCH₂, |*J*_{P-C}| = 14 Hz); 30.7 (d, P[C(CH₃)₃]₂, |*J*_{P-C}| = 8 Hz); 29.8 (s, P[C(CH₃)₃]₂); 25.7 (s, CH₂CH₂CH₂); 18.1 (d, P-CH₂, |*J*_{P-C}| = 22 Hz). Yield: 0.814 g, 91%.

Ph₂P(CH₂)₃OCH₂Ph, 2.2. A solution of Br(CH₂)₃OBn (0.656 g, 2.86 mmol) in 10 mL of THF was added dropwise at -35 °C to a solution of Ph₂PLi (0.5 g, 2.60 mmol) in 20 mL of THF. Following addition of the bromoether, there was an almost immediate color change from deep orange to pale yellow. The solution was stirred and allowed to warm to 25 °C. The solvent was removed in vacuo to afford a yellow oil. The oil was redissolved in toluene to precipitate LiBr. The solution was filtered to eliminate LiBr and solvent was removed in vacuo to afford a clear yellow oil.

$^{31}\text{P}\{^1\text{H}\}$ NMR (C_6D_6 , 25 °C, δ): -15.7 (s). ^1H NMR (C_6D_6 , 25 °C, δ): 7.55 – 7.18 (C_6H_5); 4.37 (s, 2H, CH_2OCH_2); 3.41 (t, CH_2OCH_2 , $|J_{\text{H-H}}| = 6$ Hz); 2.19 (m, 2H $\text{CH}_2\text{-CH}_2\text{-CH}_2$); 1.82 (m, 2H, P- CH_2). $^{13}\text{C}\{^1\text{H}\}$ NMR (C_6D_6 , 25 °C, δ): 139.5 – 127.3 (C_6H_5); 72.7 (s, CH_2OCH_2); 70.7 (d, CH_2OCH_2 , $|J_{\text{P-C}}| = 13$ Hz); 26.7 (d, $\text{CH}_2\text{-CH}_2\text{-CH}_2$, $|J_{\text{P-C}}| = 17$ Hz); 24.9 (d, P- CH_2 , $|J_{\text{P-C}}| = 12$ Hz). Yield: 0.703 g, 81%.

$^t\text{Bu}_2\text{P}(\text{CH}_2)_3\text{SCH}_2\text{Ph}$, 2.3. A solution of $\text{Br}(\text{CH}_2)_3\text{SCH}_2\text{Ph}$ (2.0 g, 8.16 mmol) in 20 mL of THF was added dropwise at -78 °C to a solution of $(^t\text{Bu})_2\text{PLi}$ (1.24 g, 8.16 mmol) in 40 mL of THF. The mixture was allowed to slowly warm to room temperature overnight. The solvent was removed in vacuo to afford a yellow oil. The oil was redissolved in toluene to precipitate LiBr. The solution was filtered to eliminate LiBr and solvent was removed in vacuo to afford a clear yellow oil. $^{31}\text{P}\{^1\text{H}\}$ NMR (C_6D_6 , 25 °C, δ): 27.4 (s). ^1H NMR (C_6D_6 , 25 °C, δ): 7.27 – 7.07 (C_6H_5); 3.53 (s, 2H, CH_2SCH_2); 2.46 (t, CH_2SCH_2 , $|J_{\text{H-H}}| = 7$ Hz); 1.79 (m, 2H $\text{CH}_2\text{-CH}_2\text{-CH}_2$); 1.36 (m, 2H, P- CH_2); 1.13 (d, ^tBu , $|J_{\text{H-H}}| = 12$ Hz). $^{13}\text{C}\{^1\text{H}\}$ NMR (C_6D_6 , 25 °C, δ): 129.1 – 126.8 (C_6H_5); 36.2 (s, CH_2SCH_2); 32.6 (d, CH_2SCH_2 , $|J_{\text{P-C}}| = 12$ Hz); 29.7 (d, $\text{P}[\text{C}(\text{CH}_3)_3]_2$, $|J_{\text{P-C}}| = 14$ Hz); 27.2 (s, $\text{P}[\text{C}(\text{CH}_3)_3]_2$); 26.4 (s, $\text{CH}_2\text{CH}_2\text{CH}_2$); 20.5 (d, P- CH_2 , $|J_{\text{P-C}}| = 22$ Hz). Yield: 2.33 g, 92%

4.3 Phosphinimines

$\text{Me}_3\text{SiNP}(^t\text{Bu})_2[(\text{CH}_2)_3\text{OCH}_2\text{Ph}]$, 2.4. Azidotrimethylsilane (5 eq., 6.49 g, 56.3 mmol) was added dropwise to a yellow solution of **2.1** (1.713 g, 3.315 mmol) in 20 mL of toluene. The mixture became off white and cloudy, and was refluxed overnight. The

solution was cooled and filtered to remove any impurities. Solvent was removed in vacuo to afford a yellow oil. $^{31}\text{P}\{^1\text{H}\}$ NMR (C_6D_6 , 25 °C, δ): 27.1 (s). ^1H NMR (C_6D_6 , 25 °C, δ): 7.28 – 7.05 (C_6H_5); 4.37 (s, 2H, CH_2OCH_2); 3.33 (t, 2H, CH_2OCH_2 , $|J_{\text{H-H}}| = 6$ Hz); 1.86 (m, 2H, $\text{CH}_2\text{-CH}_2\text{-CH}_2$); 1.51 (m, 2H, P- CH_2); 1.02 (d, 18H, ^tBu , $|J_{\text{H-H}}| = 13$ Hz); 0.31 (s, 9H, $\text{Si}(\text{CH}_3)_3$). $^{13}\text{C}\{^1\text{H}\}$ NMR (C_6D_6 , 25 °C, δ): 139.2 – 127.5 (C_6H_5); 72.9 (s, CH_2OCH_2); 71.1 (d, CH_2OCH_2 , $|J_{\text{P-C}}| = 11$ Hz); 36.7 (d, $\text{P}[\text{C}(\text{CH}_3)_3]_2$, $|J_{\text{P-C}}| = 63$ Hz); 27.0 (s, $\text{P}[\text{C}(\text{CH}_3)_3]_2$); 24.9 (s, $\text{CH}_2\text{-CH}_2\text{-CH}_2$); 19.2 (d, P- CH_2 , $|J_{\text{P-C}}| = 60$ Hz); 4.8 (s, $\text{Si}(\text{CH}_3)_3$). Yield: 1.11 g, 87.7%.

$\text{Me}_3\text{SiNP}(\text{Ph})_2[(\text{CH}_2)_3\text{OCH}_2\text{Ph}]$, 2.5. Azidotrimethylsilane (5 eq., 2.58 g, 22.4 mmol) was added dropwise to a yellow solution of **2.2** (1.50 g, 4.49 mmol) in 20 mL of toluene. The mixture became off white and cloudy, and was refluxed overnight. The solution was cooled and filtered to remove any impurities. Solvent was removed in vacuo to afford a viscous yellow oil. $^{31}\text{P}\{^1\text{H}\}$ NMR (C_6D_6 , 25 °C, δ): 1.56 (s). ^1H NMR (C_6D_6 , 25 °C, δ): 7.78 – 7.15 (C_6H_5); 4.56 (s, 2H, CH_2OCH_2); 3.29 (t, 2H, CH_2OCH_2 , $|J_{\text{H-H}}| = 8$ Hz); 2.27 (m, 2H, $\text{CH}_2\text{-CH}_2\text{-CH}_2$); 1.95 (m, 2H, P- CH_2); 0.49 (s, 9H, $\text{Si}(\text{CH}_3)_3$). $^{13}\text{C}\{^1\text{H}\}$ NMR (C_6D_6 , 25 °C, δ): 139.5 – 128.1 (C_6H_5); 73.2 (s, CH_2OCH_2); 70.9 (d, CH_2OCH_2 , $|J_{\text{P-C}}| = 15$ Hz); 29.2 (d, P- CH_2 , $|J_{\text{P-C}}| = 53$ Hz); 23.4 (s, $\text{CH}_2\text{-CH}_2\text{-CH}_2$); 5.1 (s, $\text{Si}(\text{CH}_3)_3$). Yield: 1.51 g, 79.9%.

$\text{Me}_3\text{SiNP}(^t\text{Bu})_2[(\text{CH}_2)_3\text{SCH}_2\text{Ph}]$, 2.6. Azidotrimethylsilane (5 eq., 4.70 g, 40.8 mmol) was added dropwise to a yellow solution of **2.3** (2.53 g, 8.16 mmol) in 30 mL of toluene. The mixture became off white and cloudy, and was refluxed overnight. The solution was

cooled and filtered to remove any impurities. Solvent was removed in vacuo to afford a yellow oil. $^{31}\text{P}\{^1\text{H}\}$ NMR (C_6D_6 , 25 °C, δ): 26.8 (s). ^1H NMR (C_6D_6 , 25 °C, δ): 7.28 – 7.07 (C_6H_5); 3.56 (s, 2H, CH_2SCH_2); 2.38 (t, 2H, CH_2SCH_2 , $|J_{\text{H-H}}| = 7$ Hz); 1.82 (m, 2H, $\text{CH}_2\text{-CH}_2\text{-CH}_2$); 1.42 (m, 2H, P- CH_2); 1.05 (d, 18H, ^tBu , $|J_{\text{H-H}}| = 13$ Hz); 0.32 (s, 9H, $\text{Si}(\text{CH}_3)_3$). $^{13}\text{C}\{^1\text{H}\}$ NMR (C_6D_6 , 25 °C, δ): 138.6 – 126.7 (C_6H_5); 35.6 (s, CH_2SCH_2); 32.9 (d, CH_2SCH_2 , $|J_{\text{P-C}}| = 13$ Hz); 29.6 (d, $\text{P}[\text{C}(\text{CH}_3)_3]_2$, $|J_{\text{P-C}}| = 13$ Hz); 27.1 (s, $\text{P}[\text{C}(\text{CH}_3)_3]_2$); 24.1 (s, $\text{CH}_2\text{-CH}_2\text{-CH}_2$); 20.4 (d, P- CH_2 , $|J_{\text{P-C}}| = 12$ Hz); 4.7 (s, $\text{Si}(\text{CH}_3)_3$). Yield: 3.24 g, 78.0%.

4.4 Titanium Complexes

$\text{CpTiCl}_2[\text{NP}(^t\text{Bu})_2\{(\text{CH}_2)_3\text{OCH}_2\text{Ph}\}]$, 2.7. A solution of **2.4** (0.30 g, 0.786 mmol) in 5 mL of toluene was added dropwise at room temperature to a solution of CpTiCl_3 (0.184 g, 0.825 mmol) in toluene. The yellow solution was then refluxed overnight to give a clear orange solution. The solvent was removed in vacuo to yield a dark orange oil. Treatment of the oil with hexanes, and subsequent decanting gave a yellow solid. $^{31}\text{P}\{^1\text{H}\}$ NMR (C_6D_6 , 25 °C, δ): 39.9 (s). ^1H NMR (C_6D_6 , 25 °C, δ): 7.30 – 7.09 (C_6H_5); 6.46 (s, 5H, C_5H_5); 4.35 (s, 2H, CH_2OCH_2); 3.34 (t, 2H, CH_2OCH_2 , $|J_{\text{H-H}}| = 7$ Hz); 2.12 (m, 2H, $\text{CH}_2\text{-CH}_2\text{-CH}_2$); 1.59 (m, 2H, P- CH_2); 0.99 (d, 18H, ^tBu , $|J_{\text{H-H}}| = 14$ Hz). $^{13}\text{C}\{^1\text{H}\}$ NMR (C_7D_8 , 25 °C, δ): 138.7 – 119.4 (C_6H_5); 118.2 (s, C_5H_5); 72.7 (s, CH_2OCH_2); 69.9 (d, CH_2OCH_2 , $|J_{\text{P-C}}| = 19$ Hz); 38.3 (d, $\text{P}[\text{C}(\text{CH}_3)_3]_2$, $|J_{\text{P-C}}| = 62$ Hz); 26.4 (s, $\text{P}[\text{C}(\text{CH}_3)_3]_2$); 24.5 (s, $\text{CH}_2\text{-CH}_2\text{-CH}_2$); 18.7 (d, P- CH_2 , $|J_{\text{P-C}}| = 64$ Hz). Yield: 0.289 g, 73.2%.

Cp*TiCl₂[NP(^tBu)₂{(CH₂)₃OCH₂Ph}], (Cp* = C₅Me₅), 2.8. A solution of **2.4** (0.50 g, 1.31 mmol) in 5 mL of toluene was added dropwise at room temperature to a solution of Cp*TiCl₃ (0.400 g, 1.38 mmol) in toluene. The yellow solution was then refluxed overnight to give a clear orange solution. The solvent was removed in vacuo to yield a dark orange oil. Treatment of the oil with hexanes, and subsequent decanting gave an orange solid. ³¹P{¹H} NMR (C₆D₆, 25 °C, δ): 38.5 (s). ¹H NMR (C₆D₆, 25 °C, δ): 7.42 – 7.18 (C₆H₅); 4.45 (s, 2H, CH₂OCH₂); 3.47 (t, 2H, CH₂OCH₂, |J_{H-H}| = 6 Hz); 2.40 (m, 2H, CH₂-CH₂-CH₂); 2.30 (s, 5H, C₅H₅); 1.92 (m, 2H, P-CH₂); 1.11 (d, 18H, ^tBu, |J_{H-H}| = 14 Hz). ¹³C{¹H} NMR (C₆D₆, 25 °C, δ): 139.5 – 128.1 (C₆H₅); 125.9 (s, C₅(CH₃)₅); 73.4 (s, CH₂OCH₂); 71.4 (d, CH₂OCH₂, |J_{P-C}| = 13 Hz); 38.9 (d, P[C(CH₃)₃]₂, |J_{P-C}| = 53 Hz); 27.9 (s, P[C(CH₃)₃]₂); 25.2 (d, CH₂-CH₂-CH₂, |J_{P-C}| = 15 Hz); 21.8 (d, P-CH₂, |J_{P-C}| = 53 Hz); 13.5 (s, C₅(CH₃)₅). Yield: 0.600 g, 81.3%.

CpTiCl₂[NP(^tBu)₂{(CH₂)₃SCH₂Ph}], 2.9. A solution of **2.6** (1.01 g, 2.54 mmol) in 5 mL of toluene was added dropwise at room temperature to a solution of CpTiCl₃ (0.559 g, 2.54 mmol) in toluene. The reaction mixture was then refluxed overnight to give a clear yellow solution. The solvent was removed in vacuo to yield a dark orange oil. Following addition of 30 mL of hexanes, the mixture was allowed to stir overnight. Removal of hexanes in vacuo gave a dull yellow waxy solid. ³¹P{¹H} NMR (C₆D₆, 25 °C, δ): 39.2 (s). ¹H NMR (C₆D₆, 25 °C, δ): 7.42 – 7.01 (C₆H₅); 6.52 (s, 5H, C₅H₅); 3.63 (s, 2H, CH₂SCH₂); 2.31 (t, 2H, CH₂SCH₂, |J_{H-H}| = 6 Hz); 2.09 (m, 2H, CH₂-CH₂-CH₂); 1.45 (m, 2H, P-CH₂); 0.98 (d, 18H, ^tBu, |J_{H-H}| = 14 Hz). ¹³C{¹H} NMR (C₆D₆, 25 °C, δ): 139.2 – 127.6 (C₆H₅); 119.9 (s, C₅H₅); 38.9 (d, P[C(CH₃)₃]₂, |J_{P-C}| = 52 Hz); 36.2 (s, CH₂SCH₂);

32.8 (d, P[C(CH₃)₃]₂, |J_{P-C}| = 13 Hz); 27.5 (s, CH₂SCH₂); 24.2 (d, CH₂-CH₂-CH₂, |J_{P-C}| = 4 Hz); 21.2 (d, P-CH₂, |J_{P-C}| = 53 Hz). Yield: 0.956 g, 76.7%.

Cp*TiCl₂[NP(^tBu)₂{(CH₂)₃SCH₂Ph}], (Cp* = C₅Me₅), 2.10. A solution of **2.6** (0.505 g, 1.27 mmol) in 5 mL of toluene was added dropwise at room temperature to a solution of Cp*TiCl₃ (0.387 g, 1.33 mmol) in 20 mL of toluene. The red solution was then refluxed overnight to give a clear orange solution. The solvent was removed in vacuo to yield a dark red solid. Washing the product with hexanes, and subsequent decanting gave a bright orange solid. ³¹P{¹H} NMR (C₆D₆, 25 °C, δ): 37.7 (s). ¹H NMR (C₆D₆, 25 °C, δ): 7.61 – 7.00 (C₆H₅); 3.65 (s, 2H, CH₂SCH₂); 2.40 (m, 2H, CH₂SCH₂); 2.25 (m, 2H, CH₂-CH₂-CH₂); 2.19 (s, 15H, C₅(CH₃)₅); 1.70 (m, 2H, P-CH₂); 1.07 (d, 18H, ^tBu, |J_{H-H}| = 14 Hz). ¹³C{¹H} NMR (C₆D₆, 25 °C, δ): 139.5 – 127.5 (C₆H₅); 126.0 (s, C₅(CH₃)₅); 38.8 (d, P[C(CH₃)₃]₂, |J_{P-C}| = 53 Hz); 36.5 (s, CH₂SCH₂); 33.4 (d, CH₂SCH₂, |J_{P-C}| = 15 Hz); 27.8 (s, P[C(CH₃)₃]₂); 24.4 (s, CH₂-CH₂-CH₂); 23.7 (d, P-CH₂, |J_{P-C}| = 52 Hz); 13.5 (s, C₅(CH₃)₅). Yield: 0.451 g, 61.3%.

CpTiMe₂[NP(^tBu)₂{(CH₂)₃OCH₂Ph}], 2.11. 0.405 mL (0.648 mmol) of a 1.6 M MeLi ether solution was added dropwise to a yellow benzene solution of 155 mg (0.314 mmol) of **2.7**. After stirring for 25 minutes, the mixture turned cloudy with a grey-yellow color. Removal of benzene in vacuo afforded a yellow oil. Treatment with hexanes precipitated LiCl, which was removed via filtration to afford a clear orange filtrate. Removal of hexanes in vacuo afforded a dark orange oil. ³¹P{¹H} NMR (C₆D₆, 25 °C, δ): 25.7 (s). ¹H NMR (C₆D₆, 25 °C, δ): 7.31 – 7.09 (C₆H₅); 6.19 (s, 5H, C₅H₅); 4.35 (s, 2H, OCH₂);

3.34 (t, 2H, CH₂OCH₂, |J_{H-H}| = 6 Hz); 2.08 (m, 2H, CH₂-CH₂-CH₂); 1.59 (m, 2H, P-CH₂); 1.04 (d, 18H, ^tBu, |J_{H-H}| = 14 Hz); 0.63 (s, 6H, Ti-(CH₃)₂). ¹³C{¹H} NMR (C₇D₈, 25 °C, δ): 138.9 – 124.5 (C₆H₅); 110.5 (s, C₅H₅); 72.7 (s, CH₂OCH₂); 70.4 (d, CH₂OCH₂, |J_{P-C}| = 11 Hz); 40.3 (s, Ti-CH₃); 37.8 (d, P[C(CH₃)₃], |J_{P-C}| = 55 Hz); 26.7 (s, P[C(CH₃)₃]); 24.7 (s, CH₂-CH₂-CH₂); 19.0 (d, P-CH₂, |J_{P-C}| = 54 Hz). Yield: 0.109 g, 77%.

Cp*TiMe₂[NP(^tBu)₂{(CH₂)₃OCH₂Ph}], (Cp* = C₅Me₅), **2.12**. 2.33 mL (3.73 mmol) of a 1.6 M MeLi ether solution was added dropwise to a yellow benzene solution of 1.0 g (1.77 mmol) of **2.8**. After stirring for 25 minutes, the mixture turned cloudy with a grey-yellow color. Removal of benzene in vacuo afforded an orange oil. Treatment with hexanes precipitated LiCl, which was removed via filtration to afford a clear orange filtrate. Removal of hexanes in vacuo afforded a dark orange oil. A concentrated hexanes solution was prepared and stored in a vial at -35°C overnight. The solvent was then removed in vacuo to give a yellow solid. ³¹P{¹H} NMR (C₆D₆, 25 °C, δ): 24.0 (s). ¹H NMR (C₆D₆, 25 °C, δ): 7.32 – 7.07 (C₆H₅); 4.35 (s, 2H, CH₂OCH₂); 3.35 (t, 2H, CH₂OCH₂, |J_{H-H}| = 6 Hz); 2.13 (m, 2H, CH₂-CH₂-CH₂); 2.06 (s, 15H, C₅(CH₃)₅); 1.78 (m, 2H, P-CH₂); 1.1 (d, 18H, ^tBu, |J_{H-H}| = 13 Hz); 0.41 (s, 6H, Ti-(CH₃)₂). ¹³C{¹H} NMR (C₆D₆, 25 °C, δ): 129.0 – 128.1 (C₆H₅); 118.7 (s, C₅(CH₃)₅); 73.4 (s, CH₂OCH₂); 71.8 (d, CH₂OCH₂, |J_{P-C}| = 13 Hz); 43.3 (s, Ti-(CH₃)₂); 38.8 (d, P[C(CH₃)₃], |J_{P-C}| = 55 Hz); 28.0 (s, P[C(CH₃)₃]); 25.5 (s, CH₂-CH₂-CH₂); 21.9 (d, P-CH₂, |J_{P-C}| = 54 Hz); 12.6 (s, C₅(CH₃)₅). Yield: 0.758 g, 81.7%.

CpTiMe₂[NP(^tBu)₂{(CH₂)₃SCH₂Ph}], 2.13. 1.88 mL (5.64 mmol) of a 3.0 M MeMgBr ether solution was added dropwise at -78 °C to a yellow ether solution of 840 mg (1.71 mmol) of **2.9**. The reaction mixture was allowed to warm slowly to room temperature. Following filtration over Celite, removal of solvent in vacuo afforded a brownish orange oil. The product was extracted with hexanes to give a clear orange filtrate. Subsequent removal of hexanes in vacuo afforded a viscous orange oil. ³¹P{¹H} NMR (C₆D₆, 25 °C, δ): 25.0 (s). ¹H NMR (C₆D₆, 25 °C, δ): 7.31 – 7.02 (C₆H₅); 6.23 (s, 5H, C₅H₅); 3.53 (s, 2H, CH₂SCH₂); 2.34 (t, 2H, CH₂SCH₂, |J_{H-H}| = 4 Hz); 2.02 (m, 2H, CH₂-CH₂-CH₂); 1.54 (m, 2H, P-CH₂); 1.07 (d, 18H, ^tBu, |J_{H-H}| = 12 Hz); 0.66 (s, 6H, Ti-(CH₃)₂). ¹³C{¹H} NMR (C₆D₆, 25 °C, δ): 139.3 – 127.6 (C₆H₅); 111.2 (s, C₅H₅); 41.0 (s, Ti-(CH₃)₂); 38.5 (d, P[C(CH₃)₃], |J_{P-C}| = 55 Hz); 36.6 (s, CH₂SCH₂); 33.4 (d, P[C(CH₃)₃], |J_{P-C}| = 13 Hz); 27.8 (s, CH₂SCH₂); 24.4 (d, CH₂-CH₂-CH₂, |J_{P-C}| = 4 Hz); 21.6 (d, P-CH₂, |J_{P-C}| = 54 Hz). Yield: 0.369 g, 46%.

Cp*TiMe₂[NP(^tBu)₂{(CH₂)₃SCH₂Ph}], (Cp* = C₅Me₅), 2.14. 0.39 mL (1.17 mmol) of a 3.0 M solution of MeMgBr was added dropwise at -78°C to an orange ether solution of 0.206 g (0.355 mmol) of **2.10**. The solution was allowed to warm slowly to room temperature overnight. Removal of ether in vacuo afforded a yellow oil. The product was extracted with hexanes and a concentrated 5 mL solution was cooled at -35°C overnight. Removal of hexanes in vacuo afforded a bright yellow waxy solid. ³¹P{¹H} NMR (C₆D₆, 25 °C, δ): 23.5 (s). ¹H NMR (C₆D₆, 25 °C, δ): 7.27 – 7.01 (C₆H₅); 3.54 (s, 2H, CH₂SCH₂); 2.37 (t, 2H, CH₂SCH₂, |J_{H-H}| = 7 Hz); 2.12 (m, 2H, CH₂-CH₂-CH₂); 2.06 (m, 15H, C₅(CH₃)₅); 1.60 (m, 2H, P-CH₂); 1.20 (d, 18H, ^tBu, |J_{H-H}| = 10 Hz); 0.40 (s, 6H, Ti-

(CH₃)₂). ¹³C{¹H} NMR (C₆D₆, 25 °C, δ): 139.4 – 127.6 (C₆H₅); 118.7 (s, C₅(CH₃)₅); 43.5 (s, Ti-(CH₃)₂); 38.9 (d, P[C(CH₃)₃], |J_{P-C}| = 55 Hz); 36.9 (s, CH₂SCH₂); 33.9 (d, CH₂SCH₂, |J_{P-C}| = 14 Hz); 28.0 (s, P[C(CH₃)₃]); 24.7 (s, CH₂CH₂CH₂); 24.0 (d, P-CH₂, |J_{P-C}| = 46 Hz); 12.6 (s, C₅(CH₃)₅). Yield: 0.176 g, 91.9%.

4.5 Activated Complexes

Synthesis of Cp'TiMe[NP(^tBu)₂{(CH₂)₃XCH₂Ph}][MeB(C₆F₅)₃] (Cp' = C₅H₅, X = O **2.15; Cp' = C₅Me₅, X = O **2.16**; Cp' = C₅H₅, X = S **2.17**; Cp' = C₅Me₅, X = S **2.18**), and Cp'TiMe[NP(^tBu)₂{(CH₂)₃XCH₂Ph}][B(C₆F₅)₄] (Cp' = C₅H₅, X = O **2.19**; Cp' = C₅Me₅, X = O **2.20**; Cp' = C₅H₅, X = S **2.21**; Cp' = C₅Me₅, X = S **2.22**).** These compounds were prepared in a similar fashion, and thus one preparation is detailed. Some methylene proton resonances were obscured, thus only a partial NMR of the product ion pair is reported. A 4 mL solution of B(C₆F₅)₃ (79 mg, 0.155 mmol) in deuterated bromobenzene was slowly added dropwise at -35 °C to a 4 mL deuterated bromobenzene solution of **2.11** (70 mg, 0.155 mmol). The reaction mixture was stored at -35 °C overnight. **2.15**: ³¹P{¹H} NMR (C₆D₅Br, 25 °C, δ): 45.4 (s). ¹H NMR (partial, C₆D₅Br, -30 °C, δ): 7.62 – 7.34 (C₆H₅); 6.72 (s, 5H, C₅H₅); 4.96 (d, 1H, OCHHPh, |J_{H-H}| = 12 Hz); 4.61 (d, 1H, OCHHPh, |J_{H-H}| = 12 Hz); 3.98 (m, 1H, CHHO); 3.82 (m, 1H, CHHO); 1.47 (br s, 3H, Ti-CH₃); 1.24 (d, 9H, ^tBu, |J_{H-H}| = 7 Hz); 1.19 (d, 9H, ^tBu, |J_{H-H}| = 7 Hz); 0.58 (br s, 3H, B-CH₃). ¹¹B NMR (C₆D₅Br, 25 °C, δ): -15.0 (s). ¹⁹F NMR (C₆D₅Br, 25 °C, δ): -132.0 (d, 6F, C₆F₅ (*o*-F), |J_{F-F}| = 23 Hz); -164.0 (t, 3F, C₆F₅ (*p*-F), |J_{F-F}| = 20 Hz); -166.4 (m, 6F, C₆F₅ (*m*-F)). **2.16**: ³¹P{¹H} NMR (C₆D₅Br, 25 °C, δ): 43.0 (s). ¹H NMR (partial, C₆D₅Br, -30 °C, δ): 7.23 – 6.82 (C₆H₅); 4.08 (d, 1H, OCHHPh, |J_{H-H}| = 7 Hz); 3.99 (d,

1H, OCHHPh, $|J_{H-H}| = 7$ Hz); 3.52 (m, 1H, CHHO); 3.34 (m, 1H, CHHO); 1.69 (s, 15H, C₅(CH₃)₅); 1.12 (br s, 3H, Ti-CH₃); 0.82 (br s, 3H, B-CH₃); 0.77 (d, 9H, ^tBu, $|J_{H-H}| = 9$ Hz); 0.74 (d, 9H, ^tBu, $|J_{H-H}| = 10$ Hz). ¹¹B NMR (C₆D₅Br, 25 °C, δ): -15.0 (s). ¹⁹F NMR (C₆D₅Br, 25 °C, δ): -132.3 (d, 6F, C₆F₅ (*o*-F), $|J_{F-F}| = 20$ Hz); -164.4 (t, 3F, C₆F₅ (*p*-F), $|J_{F-F}| = 11$ Hz); -166.9 (m, 6F, C₆F₅ (*m*-F)). **2.17**: ³¹P{¹H} NMR (C₆D₅Br, 25 °C, δ): 45.7 (s). ¹H NMR (partial, C₆D₅Br, -30 °C, δ): 7.11 – 6.81 (C₆H₅); 5.77 (s, 5H, C₅H₅); 3.18 (d, 1H, SCHHPh, $|J_{H-H}| = 12$ Hz); 2.99 (d, 1H, SCHHPh, $|J_{H-H}| = 12$ Hz); 2.70 (m, 1H, CHHS); 2.43 (m, 1H, CHHS); 1.12 (br s, 3H, Ti-CH₃); 0.87 (br s, 3H, B-CH₃); 0.82 (d, 9H, ^tBu, $|J_{H-H}| = 20$ Hz); 0.76 (d, 9H, ^tBu, $|J_{H-H}| = 17$ Hz). ¹¹B NMR (C₆D₅Br, 25 °C, δ): -14.7 (s). ¹⁹F NMR (C₆D₅Br, 25 °C, δ): -132.2 (d, 6F, C₆F₅ (*o*-F), $|J_{F-F}| = 20$ Hz); -164.3 (t, 3F, C₆F₅ (*p*-F), $|J_{F-F}| = 24$ Hz); -166.8 (m, 6F, C₆F₅ (*m*-F)). **2.18**: ³¹P{¹H} NMR (C₆D₅Br, 25 °C, δ): 44.4 (s). ¹H NMR (partial, C₆D₅Br, -30 °C, δ): 7.13 – 6.81 (C₆H₅); 3.22 (d, 1H, SCHHPh, $|J_{H-H}| = 14$ Hz); 2.77 (d, 1H, SCHHPh, $|J_{H-H}| = 14$ Hz); 1.67 (s, 15H, C₅(CH₃)₅); 1.13 (br s, 3H, Ti-CH₃); 0.83 (d, 9H, ^tBu, $|J_{H-H}| = 13$ Hz); 0.79 (d, 9H, ^tBu, $|J_{H-H}| = 14$ Hz); 0.42 (br s, 3H, B-CH₃). ¹¹B NMR (C₆D₅Br, 25 °C, δ): -14.6 (s). ¹⁹F NMR (C₆D₅Br, 25 °C, δ): -132.2 (d, 6F, C₆F₅ (*o*-F), $|J_{F-F}| = 22$ Hz); -164.4 (t, 3F, C₆F₅ (*p*-F), $|J_{F-F}| = 23$ Hz); -166.9 (m, 6F, C₆F₅ (*m*-F)). **2.19**: ³¹P{¹H} NMR (C₆D₅Br, 25 °C, δ): 45.1 (s). ¹H NMR (partial, C₆D₅Br, -30 °C, δ): 7.00 – 6.81 (C₆H₅); 6.04 (s, 5H, C₅H₅); 3.99 (br s, 1H, OCH₂Ph); 3.39 (m, 1H, CHHO); 3.26 (m, 1H, CHHO); 1.88 (br s, 3H, Ph₃C-CH₃); 1.02 (br s, 3H, Ti-CH₃); 0.80 (d, 9H, ^tBu, $|J_{H-H}| = 14$ Hz); 0.76 (d, 9H, ^tBu, $|J_{H-H}| = 9$ Hz). **2.20**: ³¹P{¹H} NMR (C₆D₅Br, 25 °C, δ): 43.0 (s). ¹H NMR (partial, C₆D₅Br, -30 °C, δ): 7.14 – 6.76 (C₆H₅); 4.08 (d, 1H, OCHHPh, $|J_{H-H}| = 7$ Hz); 4.02 (d, 1H, OCHHPh, $|J_{H-H}| = 7$ Hz); 3.47 (m, 1H, CHHO); 3.33 (m, 1H, CHHO); 1.88 (br s, 3H, Ph₃C-CH₃);

1.71 (s, 15H, C₅(CH₃)₅); 0.85 (br s, 3H, Ti-CH₃); 0.83 (d, 9H, ^tBu, |J_{H-H}| = 9 Hz); 0.77 (d, 9H, ^tBu, |J_{H-H}| = 9 Hz). **2.21**: ³¹P{¹H} NMR (C₆D₅Br, 25 °C, δ): 45.4 (s). ¹H NMR (partial, C₆D₅Br, -30 °C, δ): 7.26 – 6.81 (C₆H₅); 5.88 (s, 5H, C₅H₅); 3.28 (d, 1H, SCHHPh, |J_{H-H}| = 13 Hz); 3.13 (d, 1H, SCHHPh, |J_{H-H}| = 13 Hz); 2.53 (m, 1H, CHHS); 2.43 (m, 1H, CHHS); 1.98 (br s, 3H, Ph₃CCH₃); 0.99 (br s, 3H, Ti-CH₃); 0.94 (d, 9H, ^tBu, |J_{H-H}| = 23 Hz); 0.83 (d, 9H, ^tBu, |J_{H-H}| = 13 Hz). **2.22**: ³¹P{¹H} NMR (C₆D₅Br, 25 °C, δ): 44.3 (s). ¹H NMR (partial, C₆D₅Br, -30 °C, δ): 7.10 – 6.81 (C₆H₅); 3.24 (d, 1H, SCHHPh, |J_{H-H}| = 14 Hz); 2.77 (d, 1H, SCHHPh, |J_{H-H}| = 14 Hz); 1.87 (br s, 3H, Ph₃C-CH₃); 1.68 (s, 15H, C₅(CH₃)₅); 0.80 (d, 9H, ^tBu, |J_{H-H}| = 13 Hz); 0.76 (d, 9H, ^tBu, |J_{H-H}| = 11 Hz); 0.42 (br s, 3H, Ti-CH₃).

4.6 Ethylene Polymerization Technique

All polymerizations were performed in a similar fashion, and thus only one representative example is detailed. Any variations on the polymerization conditions have been explicitly mentioned in **Chapter 3**.

The reactor vessel and solvent storage unit were refilled with nitrogen with 4 refill/evacuation cycles over at least 90 minutes. Approximately 600 mL of toluene was transferred to the solvent storage container from a purification column. The solvent was purged with dry nitrogen for 20 minutes and then transferred to the reactor vessel by differential pressure. The solvent was stirred at 1500 ± 10 RPM and the temperature was kept constant at 30 ± 2 °C. The system was then exposed to ethylene via five vent/refill cycles. Once the ethylene flow meter read 0.000, the reactor was ready for injection of the Al(^tBu)₃ (TiBAI) solvent scrubber, pre-catalyst, and co-catalyst.

Stock solutions of the pre-catalyst, co-catalyst, and solvent scrubber were prepared in an inert atmosphere glove box. 6.0 μmol of the pre-catalyst in 2.0 mL of toluene was loaded into a syringe. 6.0 μmol of the co-catalyst $\text{B}(\text{C}_6\text{F}_5)_3$ in 1.5 mL of toluene was loaded into a separate syringe. 20 equivalents of $\text{Al}(\text{iBu})_3$ (TiBAI) solvent scrubber in 3.0 mL of toluene was also loaded into a syringe. The stock solutions were immediately transferred to the reactor for injection to avoid contamination or sample decomposition. The TiBAI solution was injected into the reactor via the catalyst injection inlet. The solvent scrubber was allowed to stir for 5 minutes. Next, the 2.0 mL pre-catalyst solution was injected. Immediately afterwards, the 1.5 mL solution of $\text{B}(\text{C}_6\text{F}_5)_3$ was injected (when testing the dichloride precursors, MAO was injected and the solution was allowed to stir for 5 minutes; the dichloride pre-catalyst was then injected). The reactor was allowed to stir (1500 ± 10 RPM) for 5 minutes at 30 ± 2 °C and 2 atm of ethylene.

Following the 5 minute reaction time, the polymerization was halted by closing off the ethylene inlet valve and venting the reactor. Stirring was stopped and the reactor was disassembled. The reactor contents were then transferred to a 4 L beaker containing approximately 100 mL of 10% HCl (v/v) in MeOH to help precipitate any polymer remaining in solution. The polymer was then collected via filtration, washed with toluene, and dried overnight for subsequent weighing.

References

- (1) Fried, J. R.; Editor *Polymer Science and Technology*, First Edition; Prentice-Hall: New Jersey, **1995**.
- (2) Ziegler, K.; Holzkamp, E.; Breil, H.; Martin, H. *Angew. Chem.* **1955**, *67*, 541-547.
- (3) Natta, G.; Pino, P.; Corradini, P.; Danusso, F.; Mantica, E.; Mazzanti, G.; Moraglio, G. *J. Am. Chem. Soc.* **1955**, *77*, 1708-1710.
- (4) Ziegler, K.; Martin, H. Application: DEDE, 1969, p 4.
- (5) Crabtree, R. H. *The Organometallic Chemistry of the Transition Metals*, Third Edition; Wiley-Interscience: New York, **2001**.
- (6) Kim, S. H.; Somorjai, G. A. *Surf. Interface Anal.* **2001**, *31*, 701-710.
- (7) Chen, E. Y.-X.; Marks, T. J. *Chem. Rev.* **2000**, *100*, 1391-1434.
- (8) LaPointe, R. E.; Roof, G. R.; Abboud, K. A.; Klosin, J. *J. Am. Chem. Soc.* **2000**, *122*, 9560-9561.
- (9) Breslow, D. S.; Newburg, N. R. *J. Am. Chem. Soc.* **1959**, *81*, 81-86.
- (10) Breslow, D. S.; Newburg, N. R. *J. Am. Chem. Soc.* **1957**, *79*, 5072-5073.
- (11) Sinn, H.; Kaminsky, W. *Adv. Organomet. Chem.* **1980**, *18*, 99-149.
- (12) Alt, H. G.; Milius, W.; Palackal, S. J. *J. Organomet. Chem.* **1994**, *472*, 113-118.
- (13) Alt, H. G.; Koepl, A. *Chem. Rev.* **2000**, *100*, 1205-1221.
- (14) Ewen, J. A. *J. Am. Chem. Soc.* **1984**, *106*, 6355-6364.
- (15) Kaminsky, W.; Kuelper, K.; Brintzinger, H. H.; Wild, F. R. W. P. *Angew. Chem.* **1985**, *97*, 507-508.
- (16) Gibson Vernon, C.; Spitzmesser Stefan, K. *Chem. Rev.* **2003**, *103*, 283-315.
- (17) Ittel, S. D.; Johnson, L. K.; Brookhart, M. *Chem. Rev.* **2000**, *100*, 1169-1203.
- (18) Shapiro, P. J.; Bunel, E.; Schaefer, W. P.; Bercaw, J. E. *Organometallics* **1990**, *9*, 867-869.
- (19) Stevens, J. C.; Neithamer, D. R. In *Eur. Pat. Appl.* (Dow Chemical Co., USA). Application: Ep, 1991, p 9 pp.
- (20) Stevens, J. C.; Timmers, F. J.; Wilson, D. R.; Schmidt, G. F.; Nickias, P. N.; Rosen, R. K.; Knight, G. W.; Lai, S. Y. In *Eur. Pat. Appl.* (Dow Chemical Co., USA). Application: Ep, 1991, p 58 pp.
- (21) Canich, J. A. M. In *Eur. Pat. Appl.* (Exxon Chemical Patents, Inc., USA). Application: Ep, 1991, p 30 pp.
- (22) Canich, J. A. M. In US.; (Exxon Chemical Patents, Inc., USA). Application: US, 1991, p 15 pp Cont -in-part of U S Ser No 533, 245.
- (23) Canich, J. A. M.; Licciardi, G. F. In US.; (Exxon Chemical Patents, Inc., USA). Application: US, 1991, p 15 pp Cont -in-part of U S Ser No 533,245.
- (24) McKnight, A. L.; Waymouth, R. M. *Chem. Rev.* **1998**, *98*, 2587-2598.
- (25) Scollard, J. D.; McConville, D. H. *J. Am. Chem. Soc.* **1996**, *118*, 10008-10009.
- (26) Scollard, J. D.; McConville, D. H.; Payne, N. C.; Vittal, J. J. *Macromolecules* **1996**, *29*, 5241-5243.

- (27) Scollard, J. D.; McConville, D. H.; Vittal, J. J. *Organometallics* **1997**, *16*, 4415-4420.
- (28) Matsui, S.; Fujita, T. *Catal. Today* **2001**, *66*, 63-73.
- (29) Matsui, S.; Mitani, M.; Saito, J.; Tohi, Y.; Makio, H.; Matsukawa, N.; Takagi, Y.; Tsuru, K.; Nitabaru, M.; Nakano, T.; Tanaka, H.; Kashiwa, N.; Fujita, T. *J. Am. Chem. Soc.* **2001**, *123*, 6847-6856.
- (30) Matsukawa, N.; Matsui, S.; Mitani, M.; Saito, J.; Tsuru, K.; Kashiwa, N.; Fujita, T. *J. Mol. Catal. A: Chem.* **2001**, *169*, 99-104.
- (31) Saito, J.; Mitani, M.; Mohri, J.-I.; Yoshida, Y.; Matsui, S.; Ishii, S.-I.; Kojoh, S.-I.; Kashiwa, N.; Fujita, T. *Angew. Chem., Int. Ed.* **2001**, *40*, 2918-2920.
- (32) Stephan, D. W. *Organometallics* **2005**, *24*, 2548-2560.
- (33) Lubben, T. V.; Wolczanski, P. T.; Van Duyne, G. D. *Organometallics* **1984**, *3*, 977-983.
- (34) Stephan, D. W.; Stewart, J. C.; Guerin, F.; Courtenay, S.; Kickham, J.; Hollink, E.; Beddie, C.; Hoskin, A.; Graham, T.; Wei, P.; Spence, R. E. v. H.; Xu, W.; Koch, L.; Gao, X.; Harrison, D. G. *Organometallics* **2003**, *22*, 1937-1947.
- (35) Stephan, D. W.; Guerin, F.; Spence, R. E. v. H.; Koch, L.; Gao, X.; Brown, S. J.; Swabey, J. W.; Wang, Q.; Xu, W.; Zoricak, P.; Harrison, D. G. *Organometallics* **1999**, *18*, 2046-2048.
- (36) Dehnicke, K.; Weller, F. *Coord. Chem. Rev.* **1997**, *158*, 103-169.
- (37) Dehnicke, K.; Krieger, M.; Massa, W. *Coord. Chem. Rev.* **1999**, *182*, 19-65.
- (38) Guerin, F.; Beddie, C. L.; Stephan, D. W.; Spence, R. E. v. H.; Wurz, R. *Organometallics* **2001**, *20*, 3466-3471.
- (39) Stephan, D. W.; Stewart, J. C.; Guerin, F.; Spence, R. E. v. H.; Xu, W.; Harrison, D. G. *Organometallics* **1999**, *18*, 1116-1118.
- (40) Xu, Z.; Vanka, K.; Firman, T.; Michalak, A.; Zurek, E.; Zhu, C.; Ziegler, T. *Organometallics* **2002**, *21*, 2444-2453.
- (41) Yue, N.; Hollink, E.; Guerin, F.; Stephan, D. W. *Organometallics* **2001**, *20*, 4424-4433.
- (42) Yue, N. L. S.; Stephan, D. W. *Organometallics* **2001**, *20*, 2303-2308.
- (43) Graham, T. W.; Kickham, J.; Courtenay, S.; Wei, P.; Stephan, D. W. *Organometallics* **2004**, *23*, 3309-3318.
- (44) Ghesner, I.; Fenwick, A.; Stephan, D. W. *Organometallics* **2006**, *25*, 4985-4995.
- (45) Slone, C. S.; Weinberger, D. A.; Mirkin, C. A. *Prog. Inorg. Chem.* **1999**, *48*, 233-350.
- (46) Jeffrey, J. C.; Rauchfuss, T. B. *Inorg. Chem.* **1979**, *18*, 2658-2666.
- (47) Orrell, K. G.; Osborne, A. G.; Sik, V.; Da Silva, M. W. *Polyhedron* **1995**, *14*, 2797-2802.
- (48) Chadwell, S. J.; Coles, S. J.; Edwards, P. G.; Hursthouse, M. B. *J. Chem. Soc., Dalton Trans.* **1996**, 1105-1112.
- (49) Jutzi, P.; Siemeling, U. *J. Organomet. Chem.* **1995**, *500*, 175-185.
- (50) Bader, A.; Lindner, E. *Coord. Chem. Rev.* **1991**, *108*, 27-110.
- (51) Dixon, J. T.; Green, M. J.; Hess, F. M.; Morgan, D. H. *J. Organomet. Chem.* **2004**, *689*, 3641-3668.

- (52) Peuckert, M.; Keim, W. *Organometallics* **1983**, *2*, 594-597.
- (53) Deckers, P. J. W.; Hessen, B.; Teuben, J. H. *Angew. Chem., Int. Ed.* **2001**, *40*, 2516-2519.
- (54) Deckers, P. J. W.; Hessen, B.; Teuben, J. H. *Organometallics* **2002**, *21*, 5122-5135.
- (55) Hessen, B. *J. Mol. Catal. A: Chem.* **2004**, *213*, 129-135.
- (56) Pellecchia, C.; Pappalardo, D.; Gruter, G.-J. *Macromolecules* **1999**, *32*, 4491-4493.
- (57) Blok, A. N. J.; Budzelaar, P. H. M.; Gal, A. W. *Organometallics* **2003**, *22*, 2564-2570.
- (58) Braunstein, P.; Naud, F. *Angew. Chem., Int. Ed.* **2001**, *40*, 680-699.
- (59) Wu, T.; Qian, Y.; Huang, J. *J. Mol. Catal. A: Chem.* **2004**, *214*, 227-229.
- (60) Palmer, D. C.; Taylor, E. C. *J. Org. Chem.* **1986**, *51*, 846-850.
- (61) Staudinger, H.; Meyer, J. *Helv. Chim. Acta* **1919**, *2*, 635-646.
- (62) Latham, I. A.; Leigh, G. J. *J. Chem. Soc., Dalton Trans.* **1986**, 399-401.
- (63) Guerin, F.; Stewart, J. C.; Beddie, C.; Stephan, D. W. *Organometallics* **2000**, *19*, 2994-3000.
- (64) Zhou, J.; Lancaster, S. J.; Walker, D. A.; Beck, S.; Thornton-Pett, M.; Bochmann, M. *J. Am. Chem. Soc.* **2001**, *123*, 223-237.
- (65) Yang, X.; Stern, C. L.; Marks, T. J. *J. Am. Chem. Soc.* **1991**, *113*, 3623-3625.
- (66) Yang, X.; Stern, C. L.; Marks, T. J. *J. Am. Chem. Soc.* **1994**, *116*, 10015-10031.
- (67) Ewen, J. A.; Elder, M. J. *Eur. Pat. Appl.* (Fina Technology, Inc., USA). Application: Ep, 1991, p 9 pp.
- (68) Krossing, I.; Raabe, I. *Angew. Chem., Int. Ed.* **2004**, *43*, 2066-2090.
- (69) Chien, J. C. W.; Tsai, W. M.; Rausch, M. D. *J. Am. Chem. Soc.* **1991**, *113*, 8570-8571.
- (70) Jia, L.; Yang, X.; Ishihara, A.; Marks, T. J. *Organometallics* **1995**, *14*, 3135-3137.
- (71) Kickham James, E.; Guerin, F.; Stephan Douglas, W. *J. Am. Chem. Soc.* **2002**, *124*, 11486-11494.
- (72) Horton, A. D.; de With, J.; van der Linden, A. J.; van de Weg, H. *Organometallics* **1996**, *15*, 2672-2674.
- (73) Horton, A. D.; de With, J. *Chem. Comm.* **1996**, 1375-1376.
- (74) Ma, K.; Piers, W. E.; Gao, Y.; Parvez, M. *J. Am. Chem. Soc.* **2004**, *126*, 5668-5669.
- (75) Cabrera, L.; Hollink, E.; Stewart, J. C.; Wei, P.; Stephan, D. W. *Organometallics* **2005**, *24*, 1091-1098.
- (76) Rappe, A. K.; Skiff, W. M.; Casewit, C. J. *Chem. Rev.* **2000**, *100*, 1435-1456.
- (77) Cossee, P. *J. Catal.* **1964**, *3*, 80-88.
- (78) Arlman, E. J.; Cossee, P. *J. Catal.* **1964**, *3*, 99-104.
- (79) Lanza, G.; Fragala, I. L.; Marks, T. J. *J. Am. Chem. Soc.* **1998**, *120*, 8257-8258.
- (80) Chan, M. S. W.; Ziegler, T. *Organometallics* **2000**, *19*, 5182-5189.

- (81) Britovsek, G. J. P.; Gibson, V. C.; Wass, D. F. *Angew. Chem., Int. Ed.* **1999**, *38*, 428-447.
- (82) Younkin, T. R.; Connor, E. F.; Henderson, J. I.; Friedrich, S. K.; Grubbs, R. H.; Bansleben, D. A. *Science* **2000**, *287*, 460-462.
- (83) Kim Seong, K.; Kim Hwa, K.; Lee Min, H.; Yoon Seung, W.; Do, Y. *Angew. Chem., Int. Ed.* **2006**, *45*, 6163-6166.
- (84) Oakes, D. C. H.; Kimberley, B. S.; Gibson, V. C.; Jones, D. J.; White, A. J. P.; Williams, D. J. *Chem. Comm.* **2004**, 2174-2175.
- (85) Long, R. J.; Gibson, V. C.; White, A. J. P.; Williams, D. J. *Inorg. Chem.* **2006**, *45*, 511-513.

Appendix A

Supplementary X-Ray Data

Table A.1. Crystallographic parameters for CpTiCl₂[NP(^tBu)₂(CH₂)₃OCH₂Ph] (**2.7**) and Cp*TiCl₂[NP(^tBu)₂(CH₂)₃OCH₂Ph] (**2.8**).

Crystal	2.7	2.8
Molecular Formula	C ₂₃ H ₃₇ Cl ₂ NOPTi	C ₂₈ H ₄₇ Cl ₂ NOPTi
Formula Weight	492.29	563.43
A (Å)	9.020(3)	10.6707(12)
B (Å)	20.667(7)	11.1671(12)
C (Å)	14.585(5)	25.8174(28)
α (°)	90.00	90.00
β (°)	106.219(1)	94.268(1)
γ (°)	90.00	90.00
Crystal System	Monoclinic	Monoclinic
Space Group	P2(1)/n	P2(1)/n
Volume (Å ³)	2610.52(35)	3067.89(6)
D _{calc} (gcm ⁻³)	1.25	1.22
Z	4	4
Abs coeff, μ, mm ⁻¹	0.608	0.525
θ range (°)	1.8-24.2	1.6-25.0
Reflections Collected	9175	5420
F ₀₀₀	1040	1204
Parameters	224	307
Goodness of Fit	0.990	1.052

Vita Auctoris

Date and Place of Birth: April 17, 1983, High Wycombe, England.

Education

M.Sc. Candidate, Chemistry, 2005-Present.

University of Windsor, Windsor, Ontario

B.Sc. Biochemistry, Graduated 2005.

University of Windsor, Windsor, Ontario

Honors and Awards

- University of Windsor Postgraduate Tuition Scholarship (December 2005-Present)
- William A. Redmond Bursary (December 2005)

Chemistry Work Experience

- *University of Windsor, Windsor, ON (2005-Present)*
Graduate Student with *Dr. Douglas Stephan*: Synthesis and reactivity of early transition metal pre-catalysts for olefin polymerization.

- *University of Windsor, Windsor, ON (2005-Present)*
Teaching Assistant: Instructed and evaluated students in 1st year chemistry

Conference Presentations

Yadav, K., Stephan, D.W. Ligand Design in Transition Metal Chemistry. Poster Presentation. Abstracts of Papers, 89th CSC Conference and Exhibition, Halifax, NS, Canada, May 27-31, 2006.

Yadav, K., Stephan, D.W. Design of Early Transition Metal Hemilabile Systems. Poster Presentation. Abstracts of Papers, 233rd ACS National Meeting, Chicago, IL, United States, March 25-29, 2007.